Effects of the Pion Detector Shielding for the Moller Experiment

Neven Simicevic*
Center for Applied Physics Studies
Louisiana Tech University, PO Box 10348, Ruston, LA 71272

Abstract

In this report detailed studies of the shielding properties and the physical consequences of the shielding of the pion detector are performed for the 8.8 GeV electrons and pions energies in the Moller experiment. Effects of the shielding on both, pion detector and the main detector system, are calculated for the lead shielding thicknesses of 5 cm, 10 cm, 20 cm, and 50 cm. The type, the energy distributions and the rates of the secondary particles are computed. In addition to help optimize the thickness of the shielding, the results will help to understand the consequences of the background produced by the shielding on both, pion detector and the main detector system, and, therefore, help in the design of the detectors. The result can be also used to estimate the secondary particles effects on the main detector system if one decides to put the shielding in front of main detectors.

* Address correspondence at Louisiana Tech University, PO Box 10348, Ruston, LA 71272
Tel: 1.318.257.3591
Fax: 1.318.257.4228
E-mail: neven@phys.latech.edu

I. Introduction

Moller experiment proposes to measure the parity-violating asymmetry in the scattering of longitudinally polarized 11 GeV electrons from the atomic electrons in a liquid hydrogen target [MOLLER 2012].

Nominal design parameters for the proposed measurement are shown in Table 1. While some of the design parameters could change in the future at the few percentage level as the design is further optimized, possible changes are not important for the scope of this report.

Parameter	Value
E [GeV]	≈ 11.0
E' [GeV]	1.8 - 8.8
θ_{cm}	46°-127°
θ_{lab}	0.23°-1.1°
$< Q^2 >$ [GeV^2]	0.0056
Maximum Current [μA]	85
Target Length (cm)	150
ρ_{tgt} [g/cm^3] (T= 20K, P = 35 psia)	0.0715
Max. Luminosity [cm^{-2} sec^{-1}]	$3.4 \cdot 10^{39}$
σ [μBarn]	≈ 40
Møller Rate [GHz]	≈ 135
Statistical Width(2 kHz flip) [ppm/pair]	≈ 83
Target Raster Size [mm]	5 x 5
ΔA_{raw} [ppb]	≈ 0.6
Background Fraction	≈ 0.08
P_{beam}	$\approx 85\%$
$< A_{pv} >$ [ppb]	≈ 35
$\Delta A_{stat} / < A_{expt} >$	2.1%
$\delta(\sin^2 \theta_W)_{stat}$	0.00026

Table 1. Nominal design parameters for the proposed Moller measurement [MOLLER 2012].

The scope of this report is to estimate the effects of the pion detector shielding on the pion detector itself and on the surrounding detectors. Any desired or undesired effects are function of the background rates produced at the shielding. They are reported here as a function of shielding thickness. Studying the shielding properties as a separate problem reduces the amount of the simulation needed to optimize the whole Moller experiment. This report could be used as the initial step for the Moller experiment's pion detector design. Finally, parts of this report could be of help in the process designing other subparts of the Moller experiment or, generally, for other experiments using 12 GeV electron beam at Jefferson Lab.

Detectors overview, including pion detector shielding positioned in front of the pion detector, is shown in Figure 1.

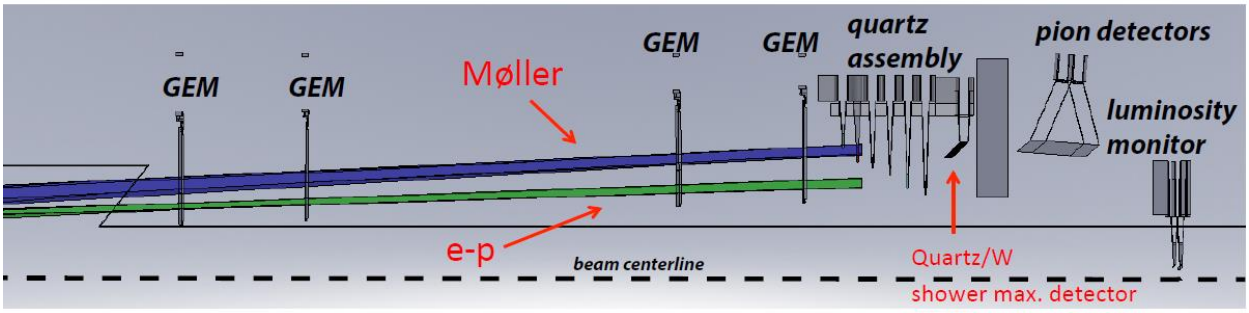

Figure 1. Schematics of the pion detectors shielding and the position of the surrounding detectors.

Propagation of particles through the shielding material, their range, the associate production of secondary particles and energy deposition was obtained using a simulation tool called FLUKA [FERRARI 2005, BATTISTONI 2007], a fully integrated particle physics Monte Carlo simulation package with many applications in high energy experimental physics and engineering, shielding, detectors and telescopes design, cosmic ray studies, dosimetry, medical physics and radio-biology. Once the incoming particles are generated and the properties of the material are known, it is straight forward to simulate the shielding capabilities. The physical mechanisms implemented in today's simulation software are very accurate and the differences between the simulated and measured results are in the most cases negligible.

In this report detailed study of the shielding properties are done for pion and electron energy of 8.8 GeV, the highest energy in Table 1. Effects of the shielding are calculated for the lead shielding thicknesses of 5 cm, 10 cm, 20 cm, and 50 cm.

II. Results for 5 cm thick lead shielding

In this section we study the effects of pions and electrons impinging on a 20 cm x 20 cm x 5 cm lead block. In addition to total deposited energy in the block, the fluences of pions, muons, neutrons, protons, electrons, photons, lambdas and sigma- are also calculated in units of number of particles per cm^2 normalized to number of incoming particles per cm^2. With such a choice of units one only needs to multiply shown fluences with primary particles rates (which can be calculated separately) to get the fluences expected in the Moller experiment. In the simulation the cutoff energy threshold for all the particles was 10^{-5} GeV, except for the neutrons where the cutoff threshold was 10^{-8} GeV.

In the case of pions, total deposited energy is shown in Figure 2 in units of MeV/cm^3. The average deposited energy in the entire 5 cm thick lead block was 450 MeV per incoming pion. The fluences integrated over all secondary particles energies are shown in Figures 3-10 and Figures 11-18.

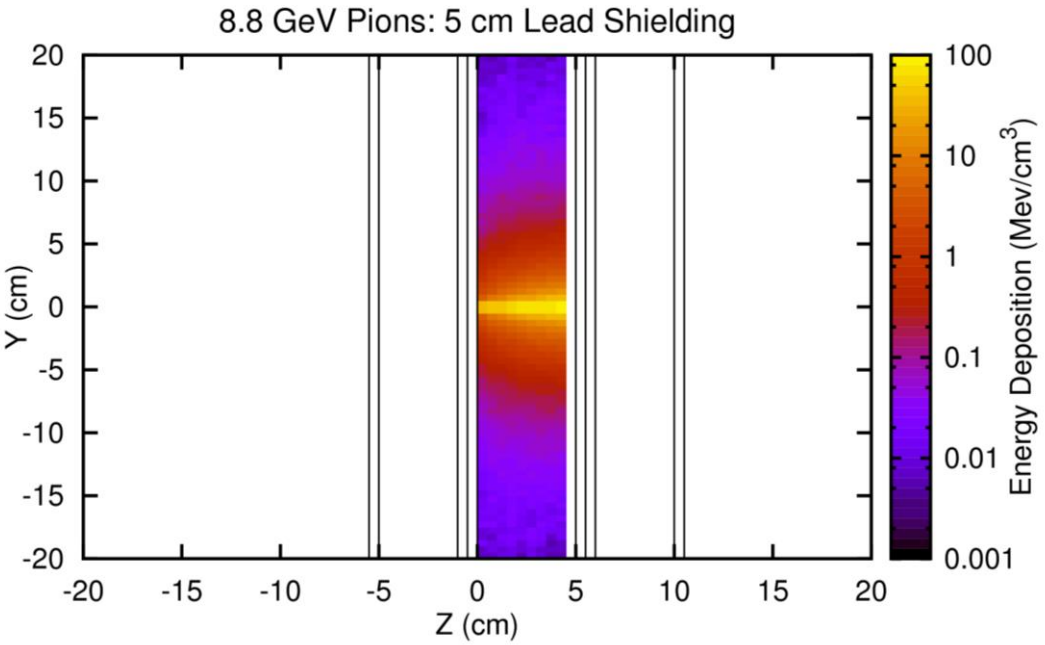

Figure 2. Total deposited energy in the 5 cm thick lead block per incoming 8.8 GeV pion.

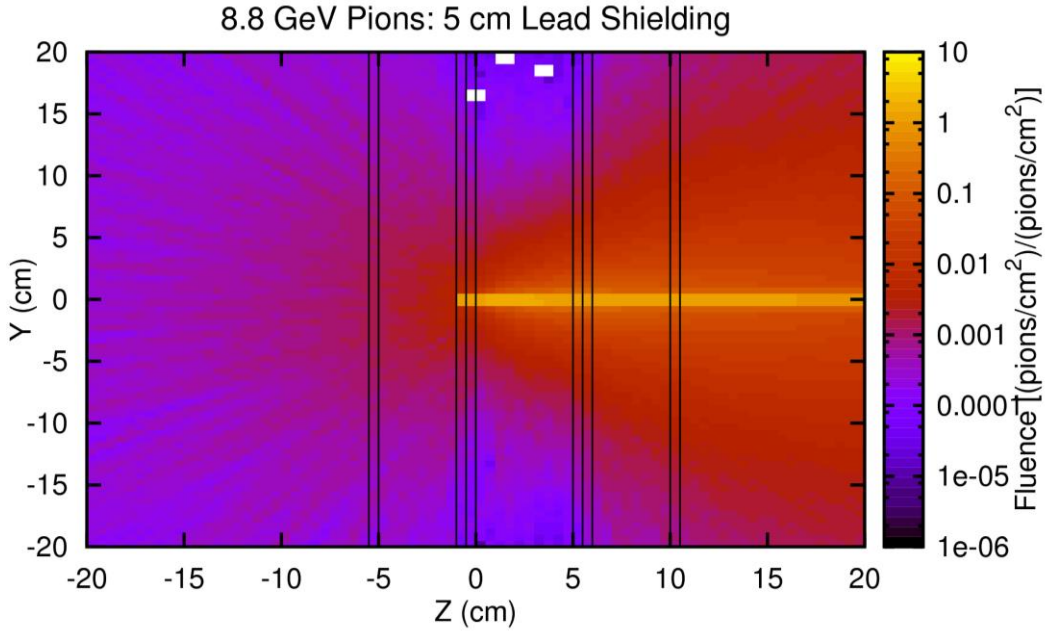

Figure 3. Pion fluence in the case of the 5 cm thick lead block per incoming 8.8 GeV pion.

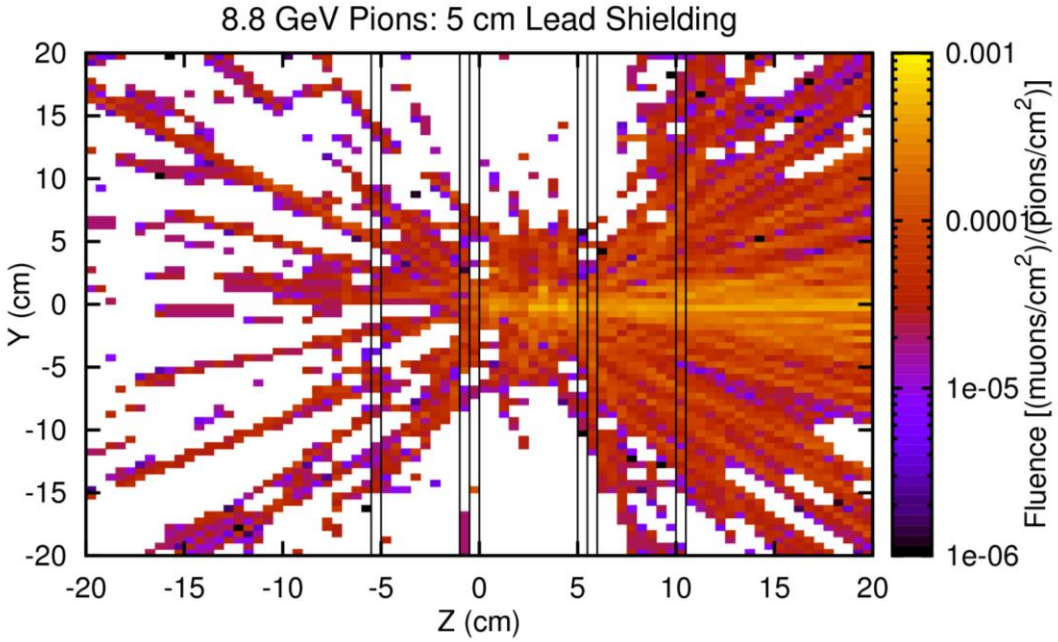

Figure 4. Muon fluence in the case of the 5 cm thick lead block per incoming 8.8 GeV pion.

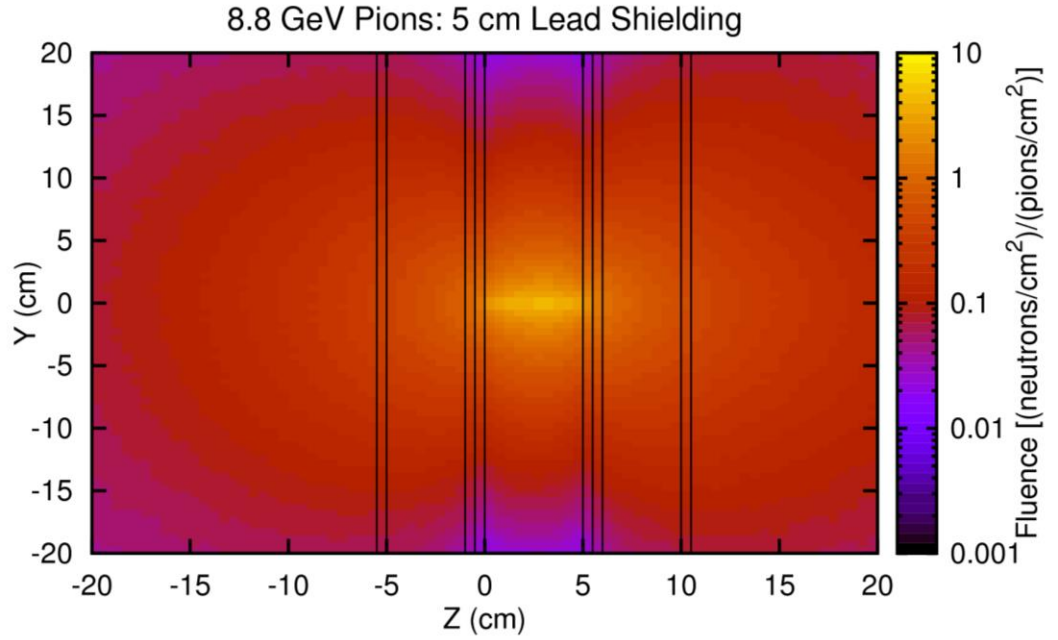

Figure 5. Neutron fluence in the case of the 5 cm thick lead block per incoming 8.8 GeV pion.

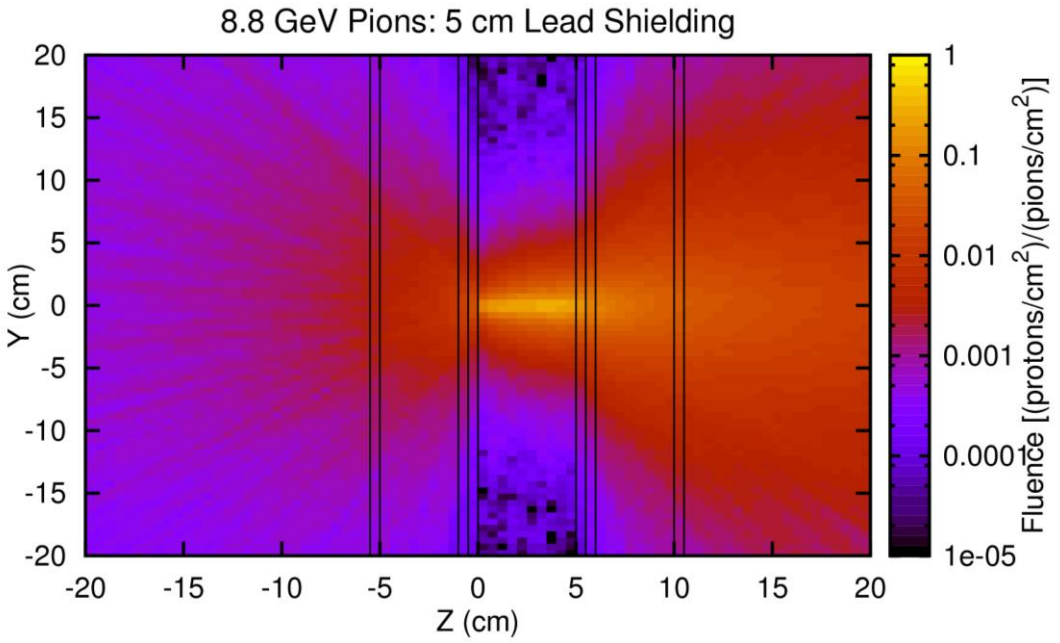

Figure 6. Proton fluence in the case of the 5 cm thick lead block per incoming 8.8 GeV pion.

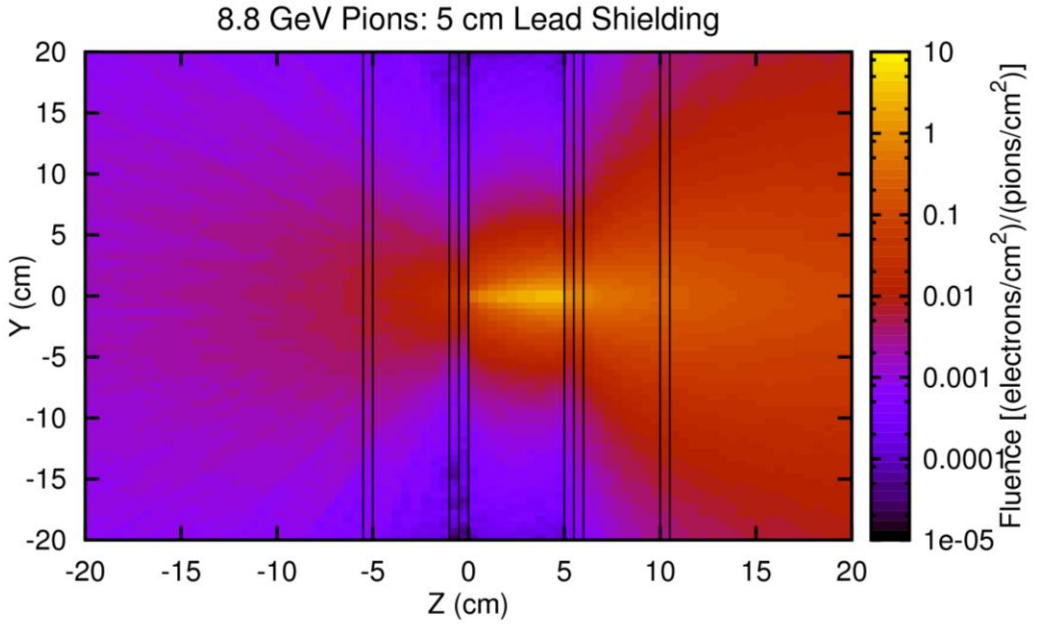

Figure 7. Electron fluence in the case of the 5 cm thick lead block per incoming 8.8 GeV pion.

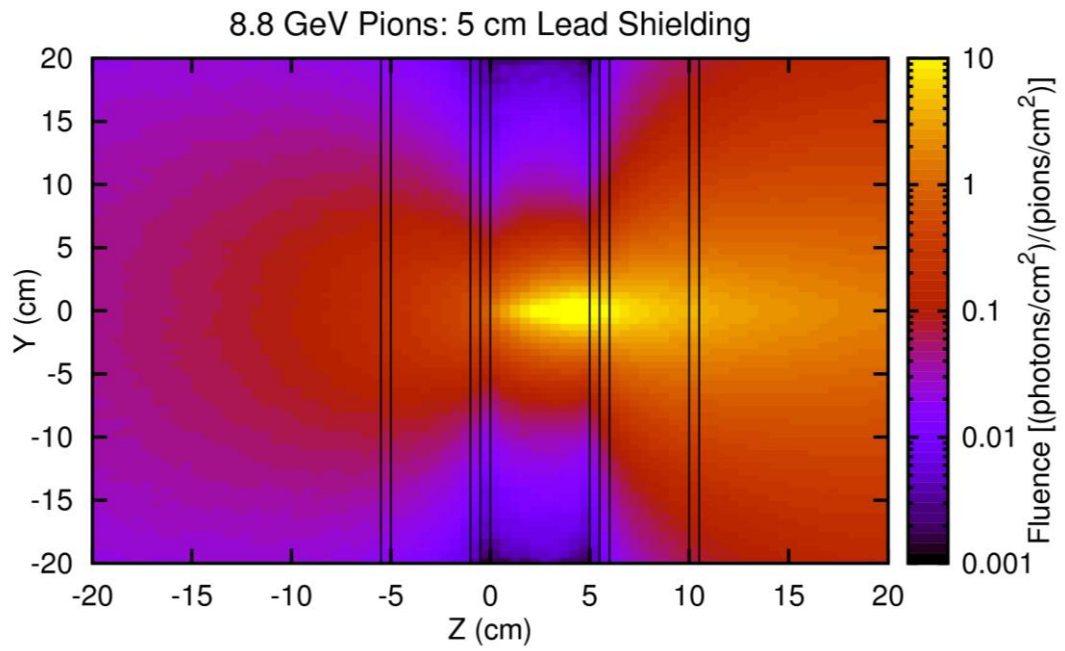

Figure 8. Photon fluence in the case of the 5 cm thick lead block per incoming 8.8 GeV pion.

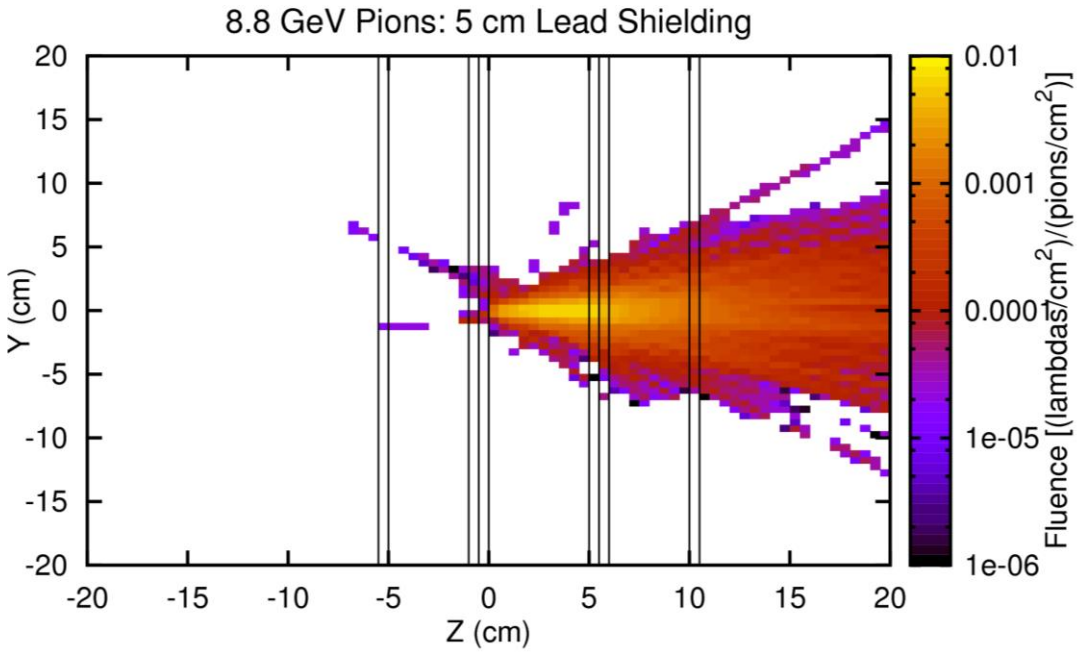

Figure 9. Lambda fluence in the case of the 5 cm thick lead block per incoming 8.8 GeV pion.

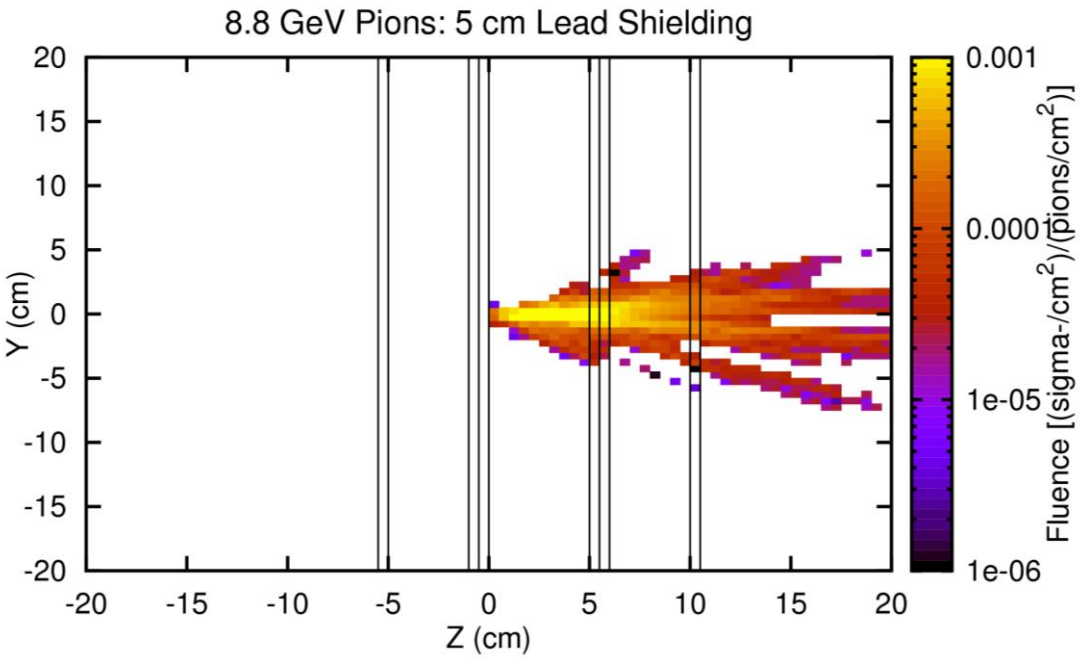

Figure 10. Sigma- fluence in the case of the 5 cm thick lead block per incoming 8.8 GeV pion.

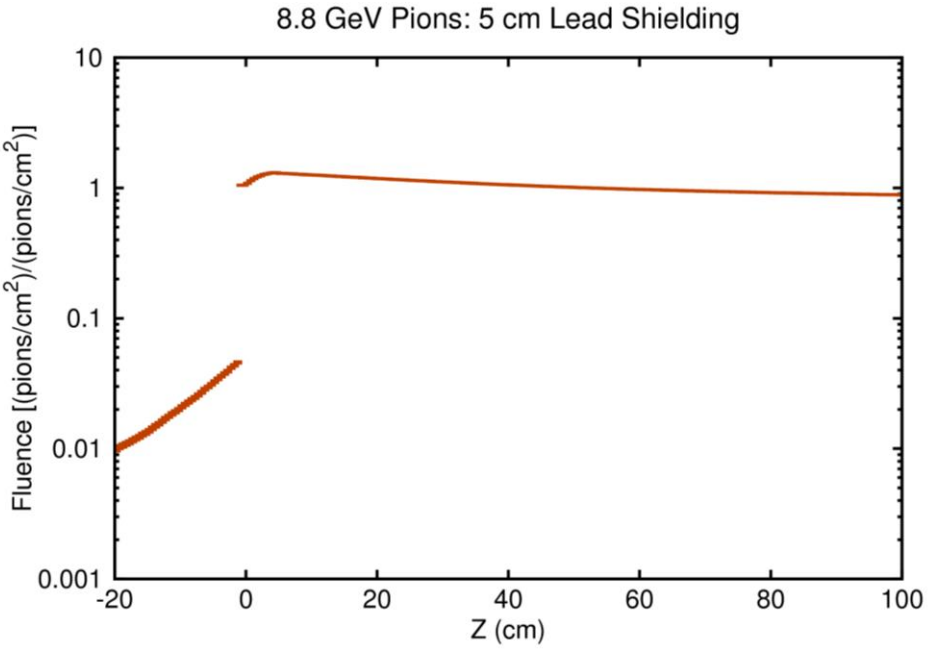

Figure 11. Energy integrated pion fluence as a function of position.

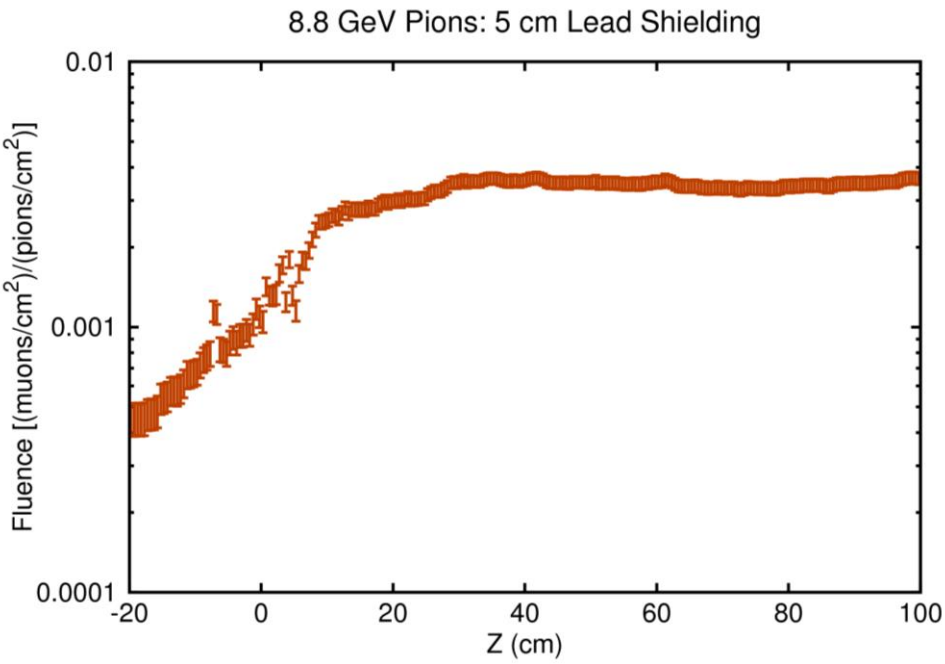

Figure 12. Energy integrated muon fluence as a function of position.

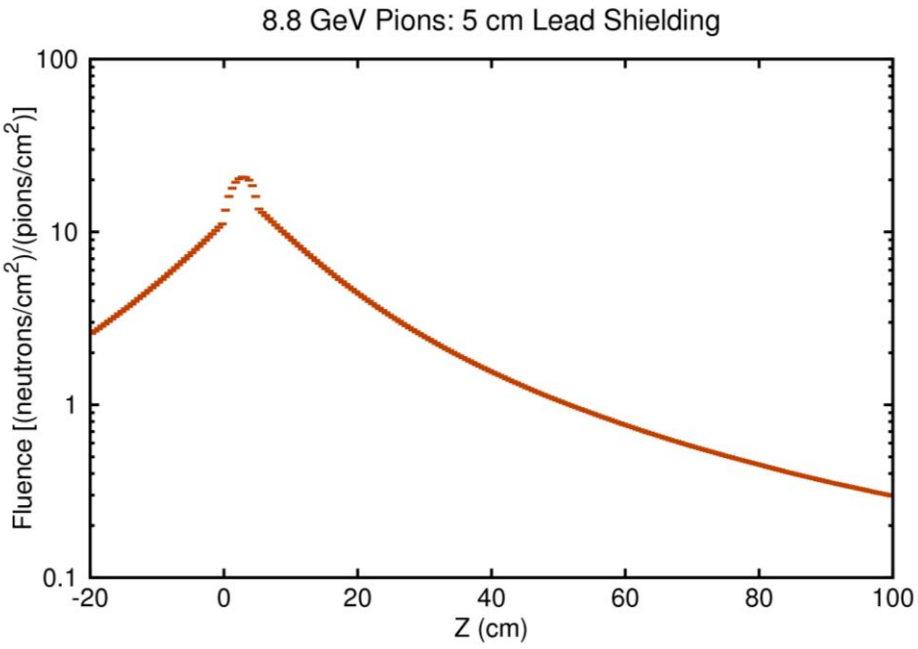

Figure 13. Energy integrated neutron fluence as a function of position.

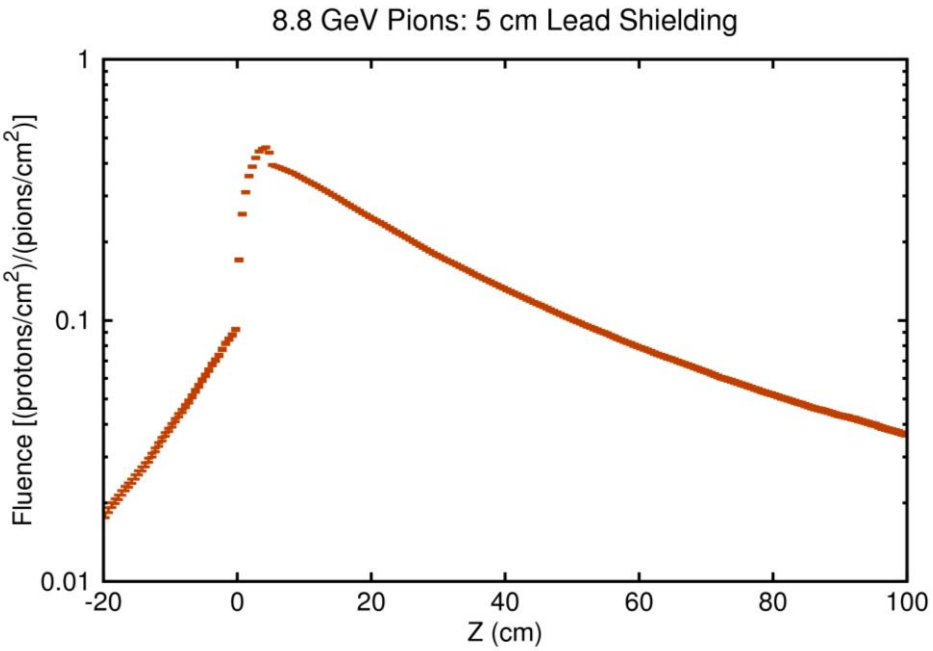

Figure 14. Energy integrated proton fluence as a function of position.

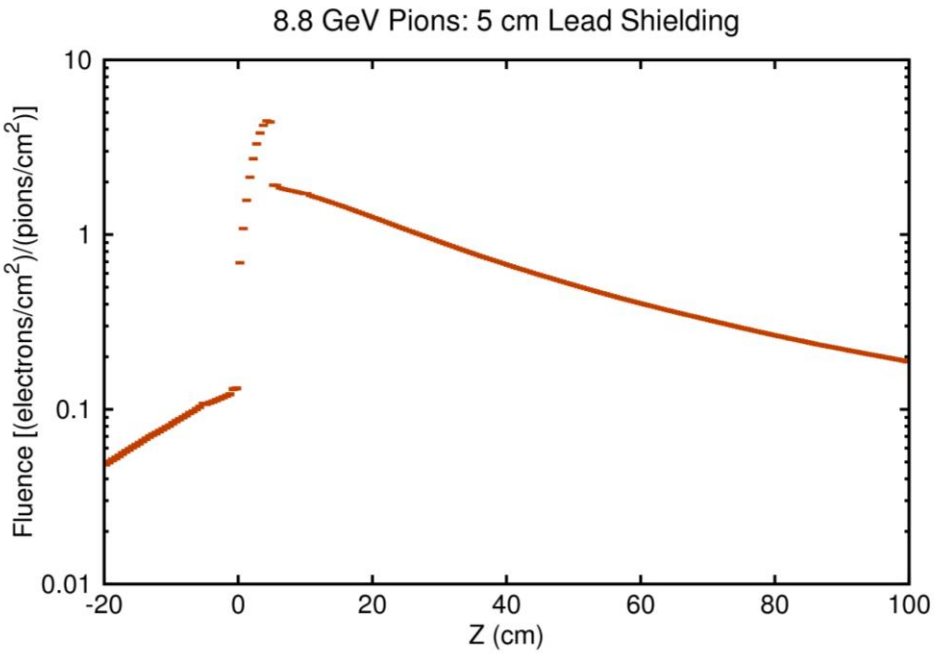

Figure 15. Energy integrated electron fluence as a function of position.

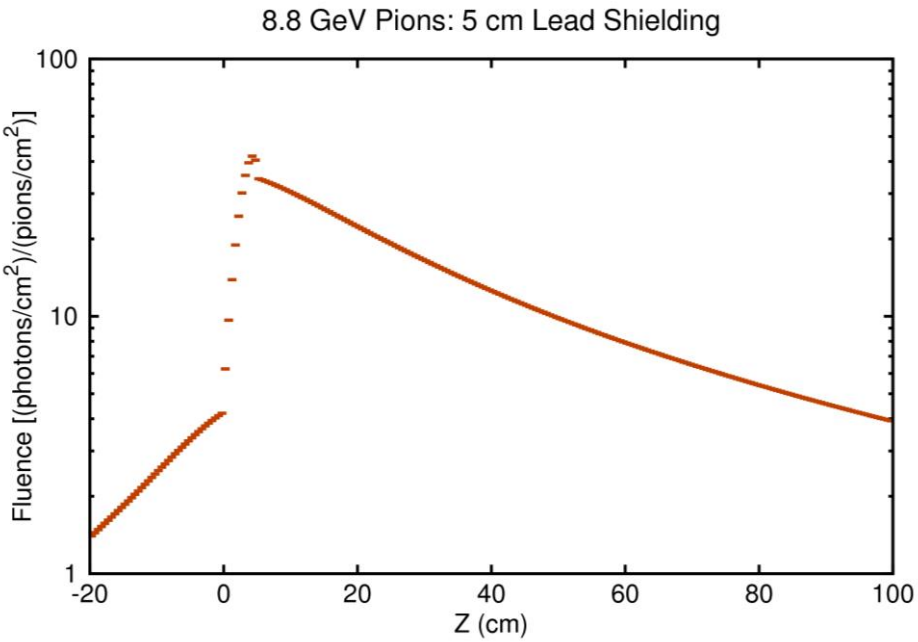

Figure 16. Energy integrated photon fluence as a function of position.

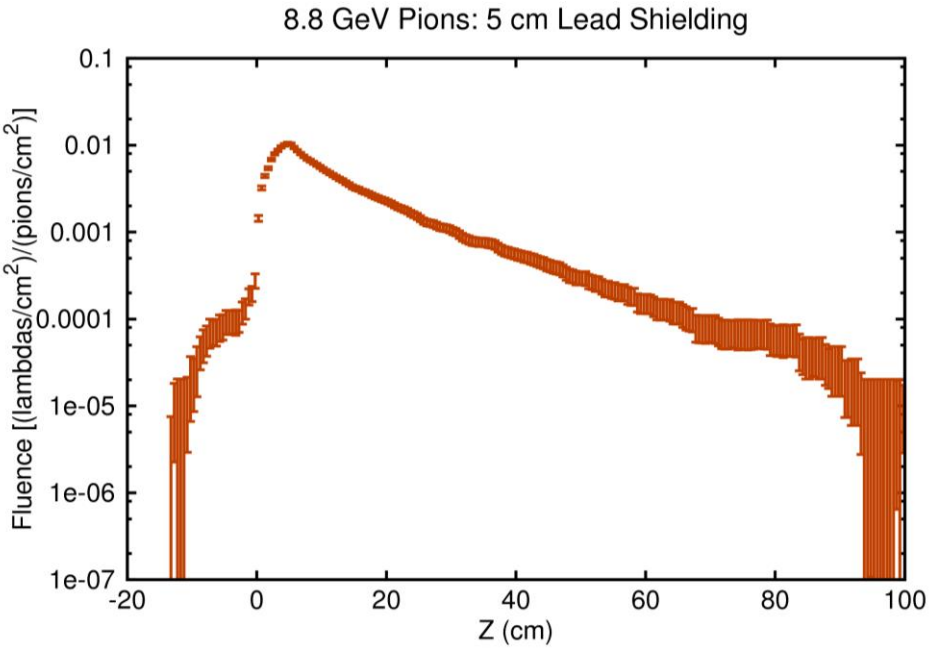

Figure 17. Energy integrated lambda fluence as a function of position.

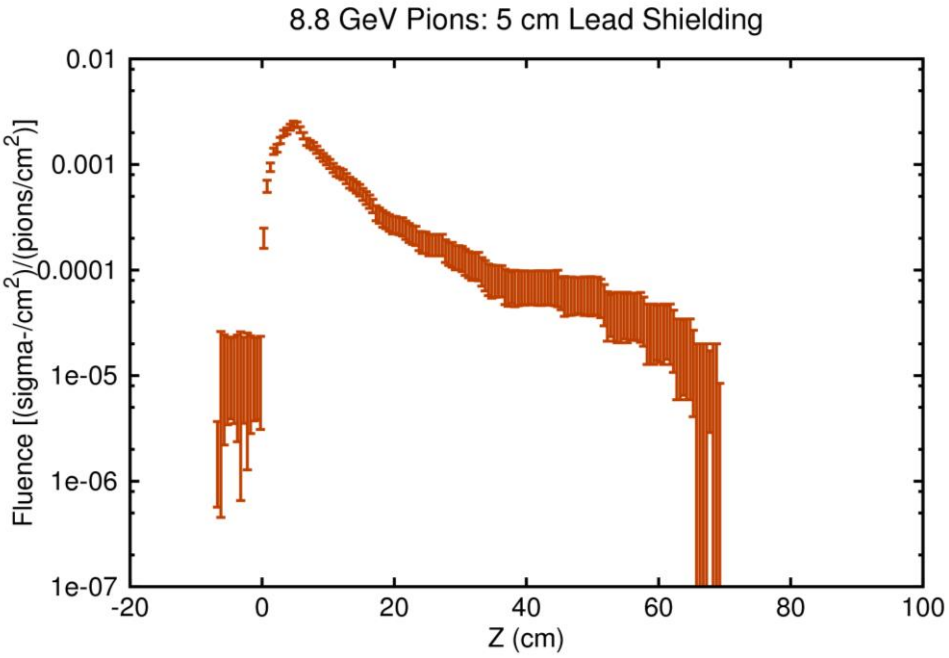

Figure 18. Energy integrated sigma- fluence as a function of position.

The fluences shown in Figures 11-18 are integrated over all the secondary particles energies and can be used to calculate the background rates, but, to fully understand the background, it is also important to know the secondary particles energy spectra. In Figures 19-26 the isolethargic spectra are shown for the secondary particles produced by the shielding in forward and backward directions. The reason for using isolethatrgic spectra is that the dynamic range of the secondary particles energies requires a logarithmic energy scale. For such a scale the area under the isolethargic spectrum curve is proportional to number of particles in a particular energy interval.

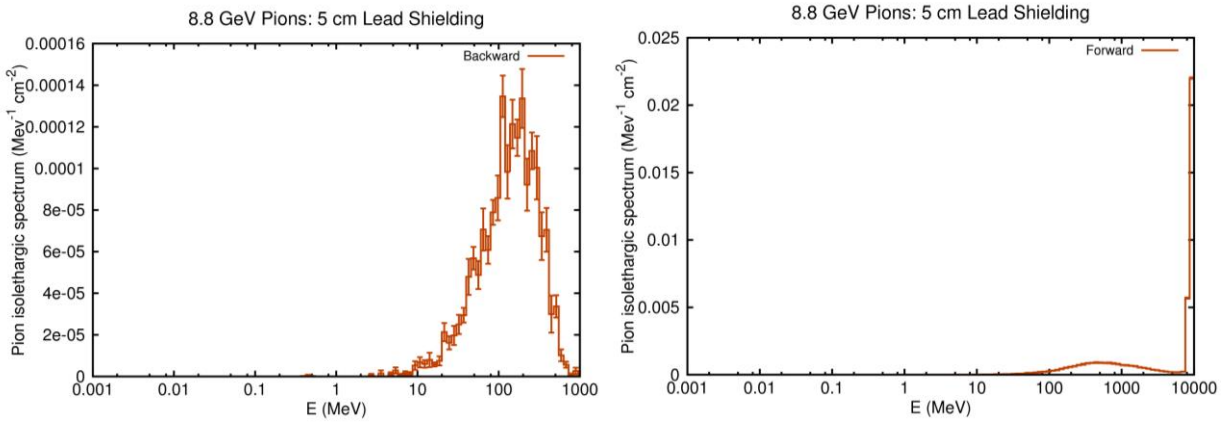

Figure 19. Pion isolethargic spectrum for backward and forward produced pions in a 5 cm thick lead shielding.

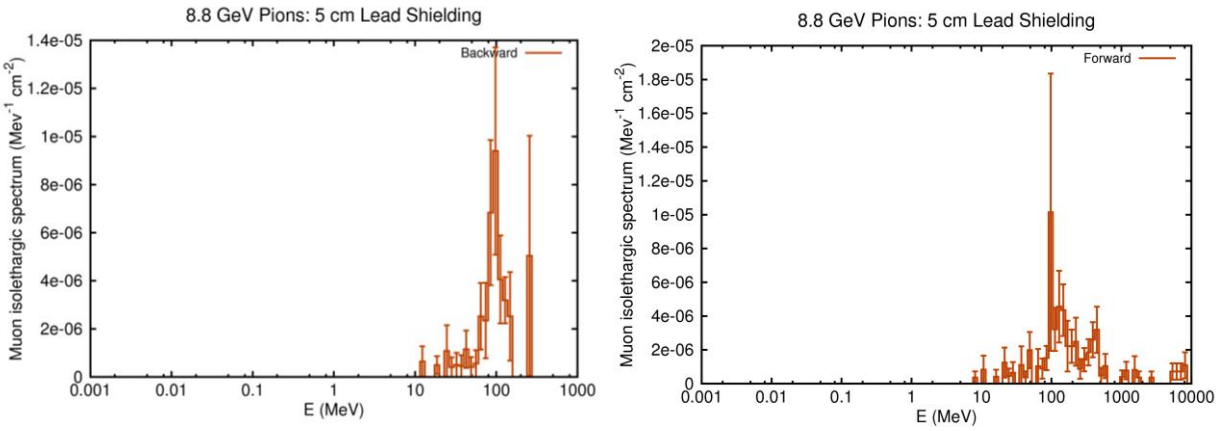

Figure 20. Muon isolethargic spectrum for backward and forward produced muons in a 5 cm thick lead shielding.

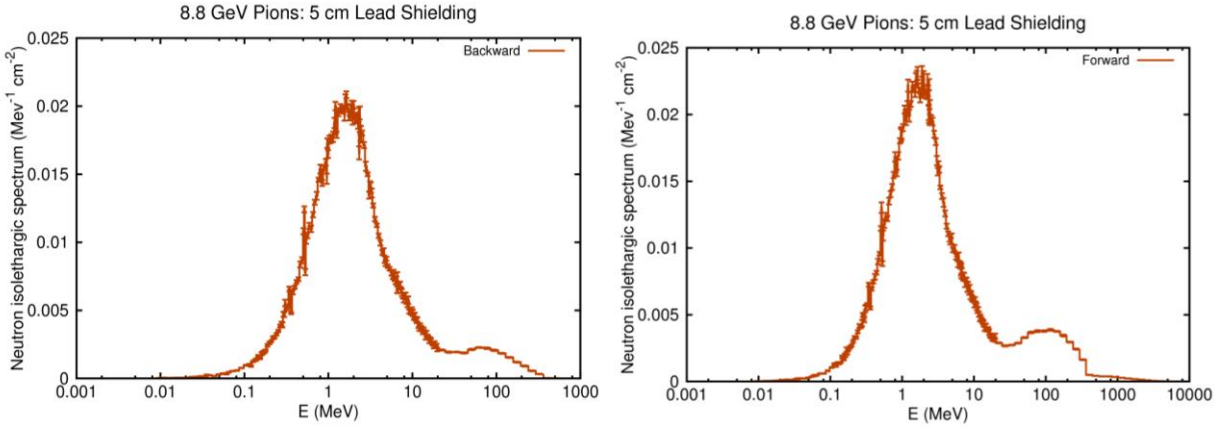

Figure 21. Neutron isolethargic spectrum for backward and forward produced neutrons in a 5 cm thick lead shielding.

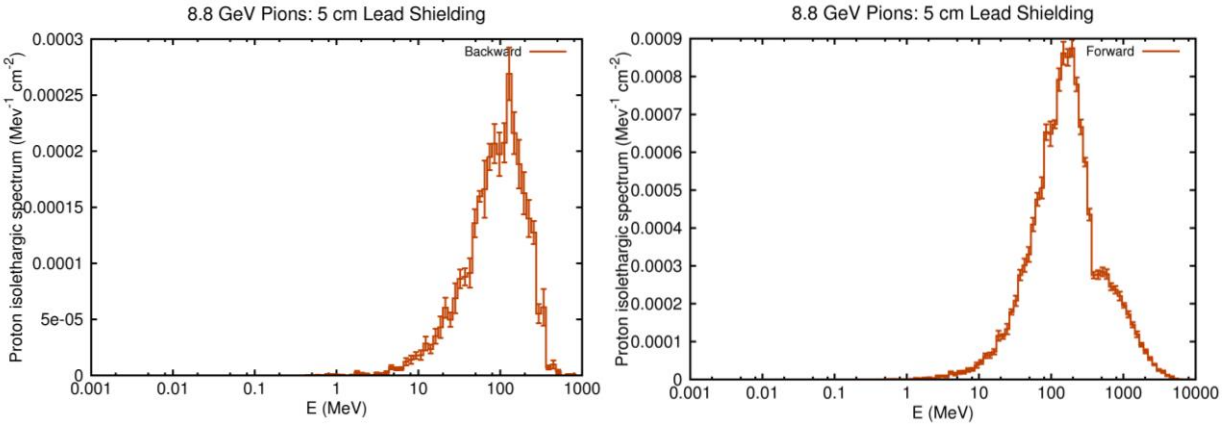

Figure 22. Proton isolethargic spectrum for backward and forward produced protons in a 5 cm thick lead shielding.

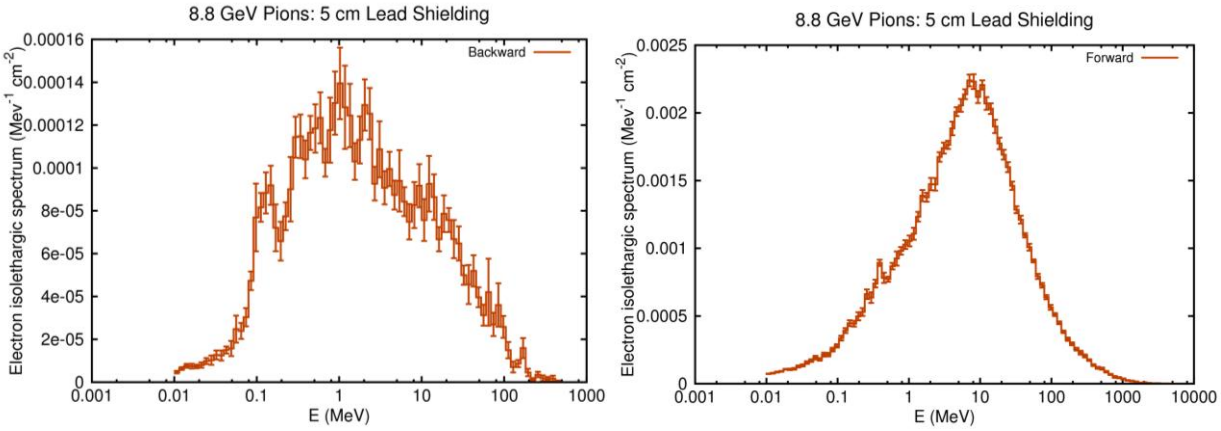

Figure 23. Electron isolethargic spectrum for backward and forward produced electrons in a 5 cm thick lead shielding.

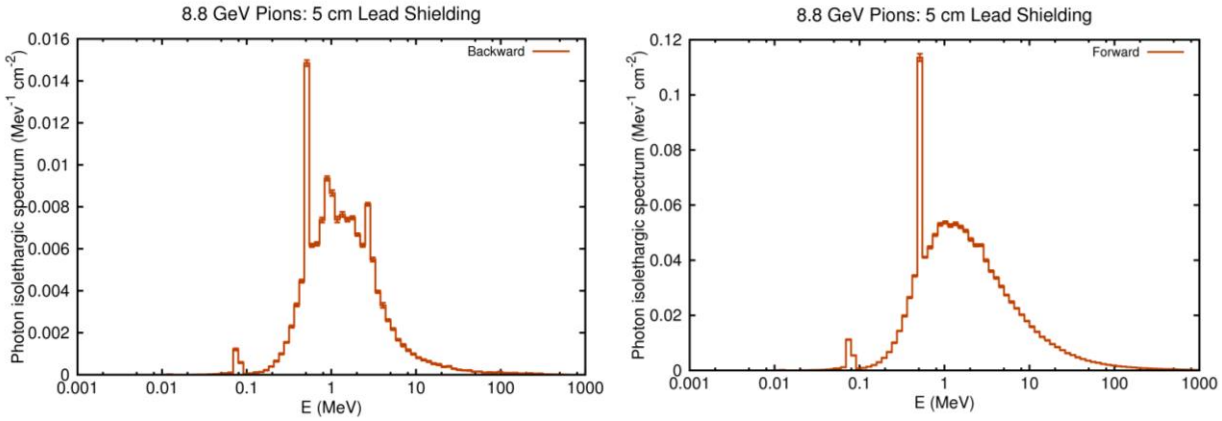

Figure 24. Photon isolethargic spectrum for backward and forward produced photons in a 5 cm thick lead shielding.

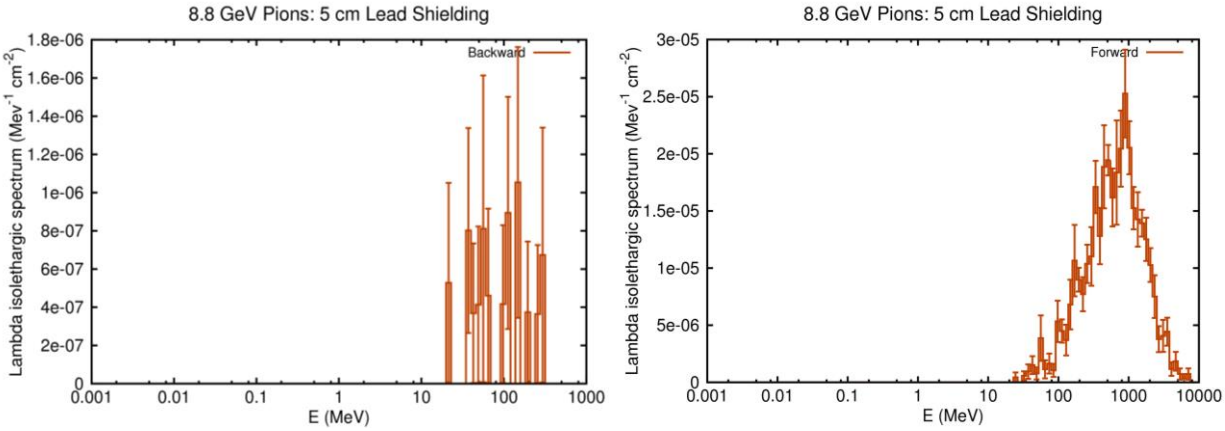

Figure 25. Lambda isolethargic spectrum for backward and forward produced lambdas in a 5 cm thick lead shielding.

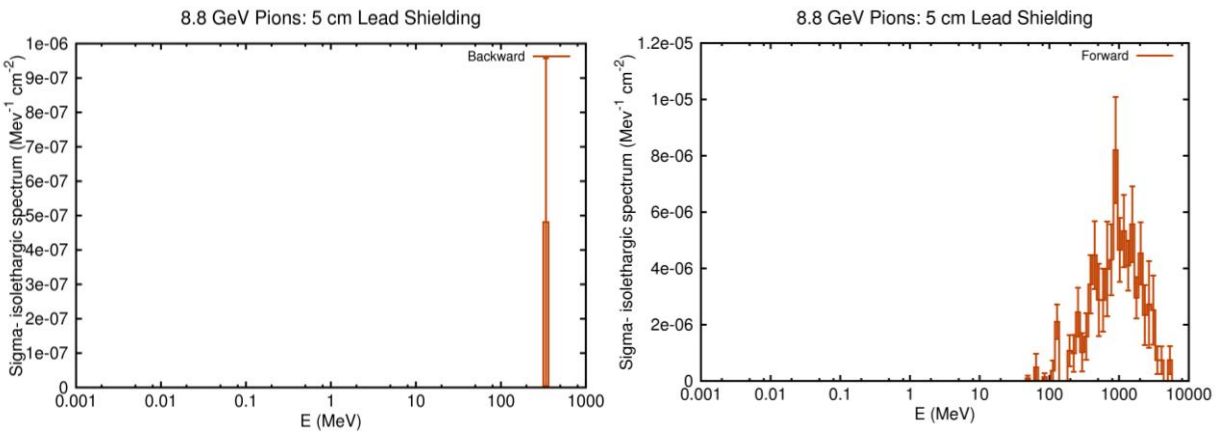

Figure 26. Sigma- isolethargic spectrum for backward and forward produced sigma- in a 5 cm thick lead shielding.

In the case of electrons, total deposited energy is shown in Figure 27 in units of MeV/cm^3. The average deposited energy in the entire 5 cm thick lead block was 5260 MeV per incoming electron. The fluences integrated over all secondary particles energies are shown in Figures 28-32 and Figures 33-39.

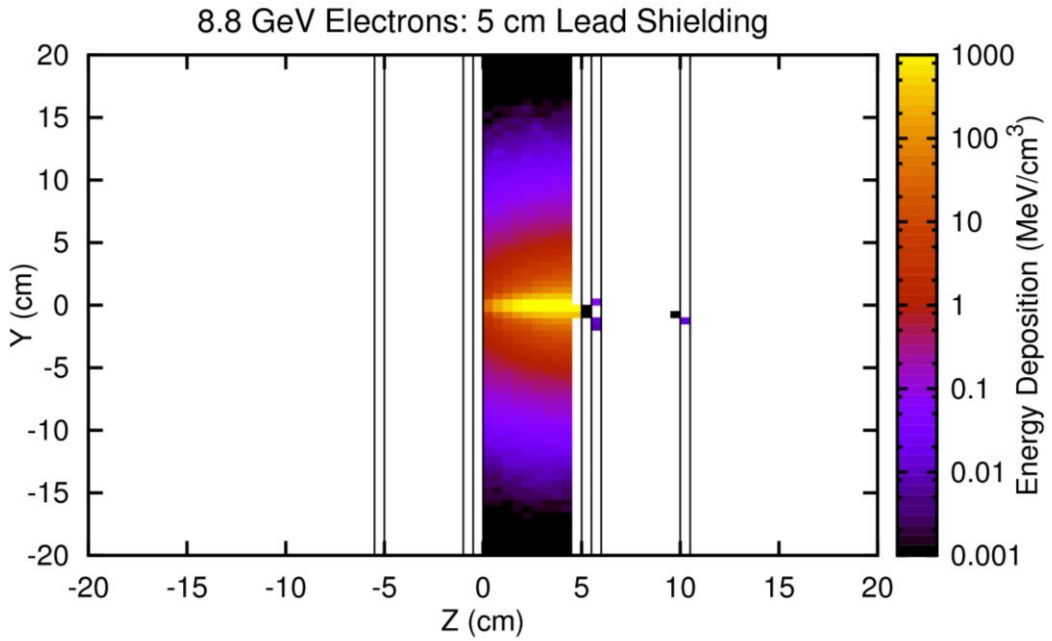

Figure 37. Total deposited energy in the 5 cm thick lead block per incoming 8.8 GeV electron.

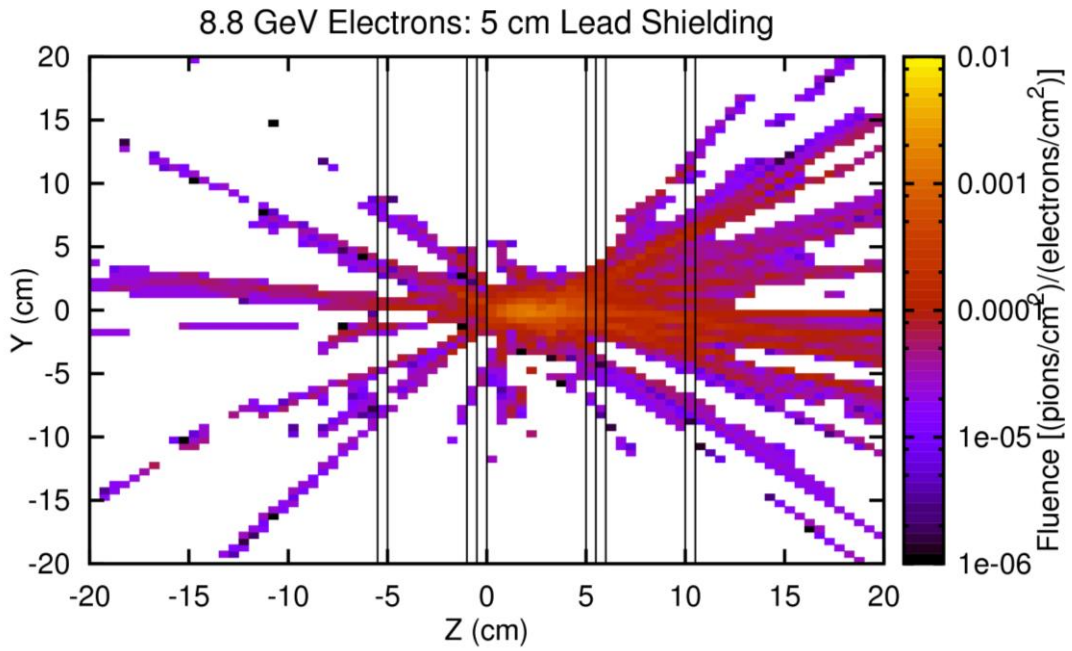

Figure 28. Pion fluence in the case of the 5 cm thick lead block per incoming 8.8 GeV electron.

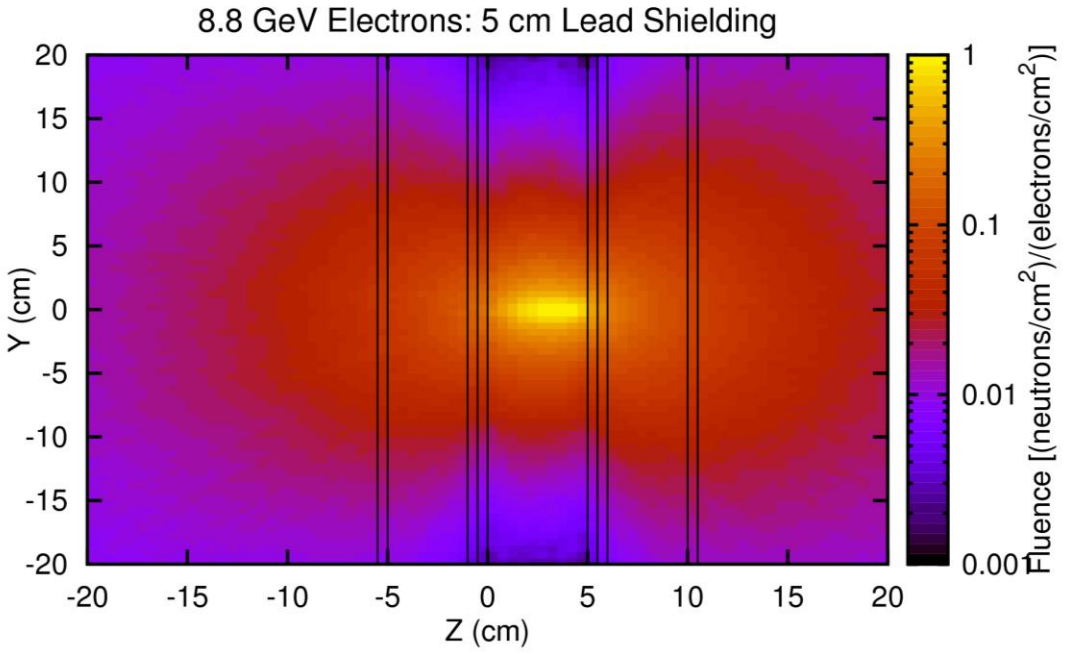

Figure 29. Neutron fluence in the case of the 5 cm thick lead block per incoming 8.8 GeV electron.

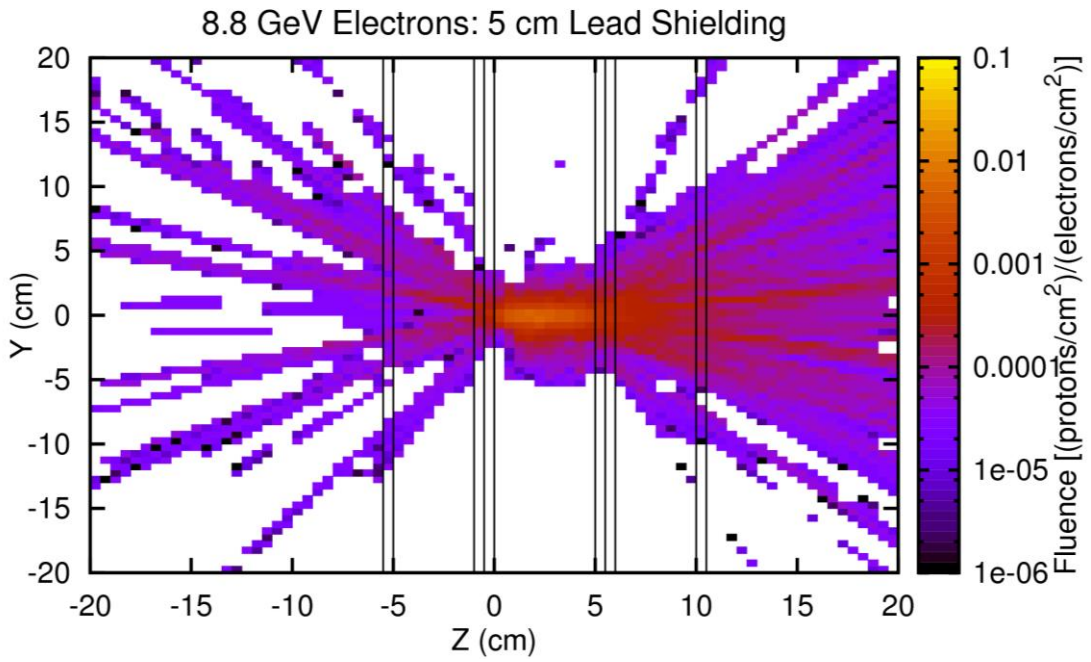

Figure 30. Proton fluence in the case of the 5 cm thick lead block per incoming 8.8 GeV electron.

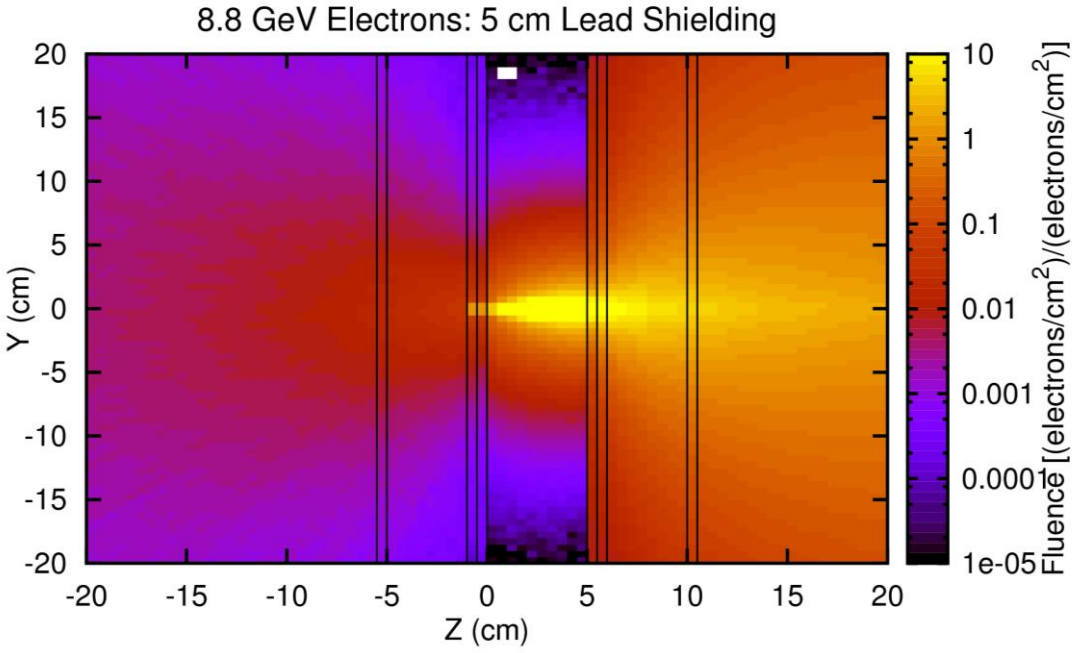

Figure 31. Electron fluence in the case of the 5 cm thick lead block per incoming 8.8 GeV electron.

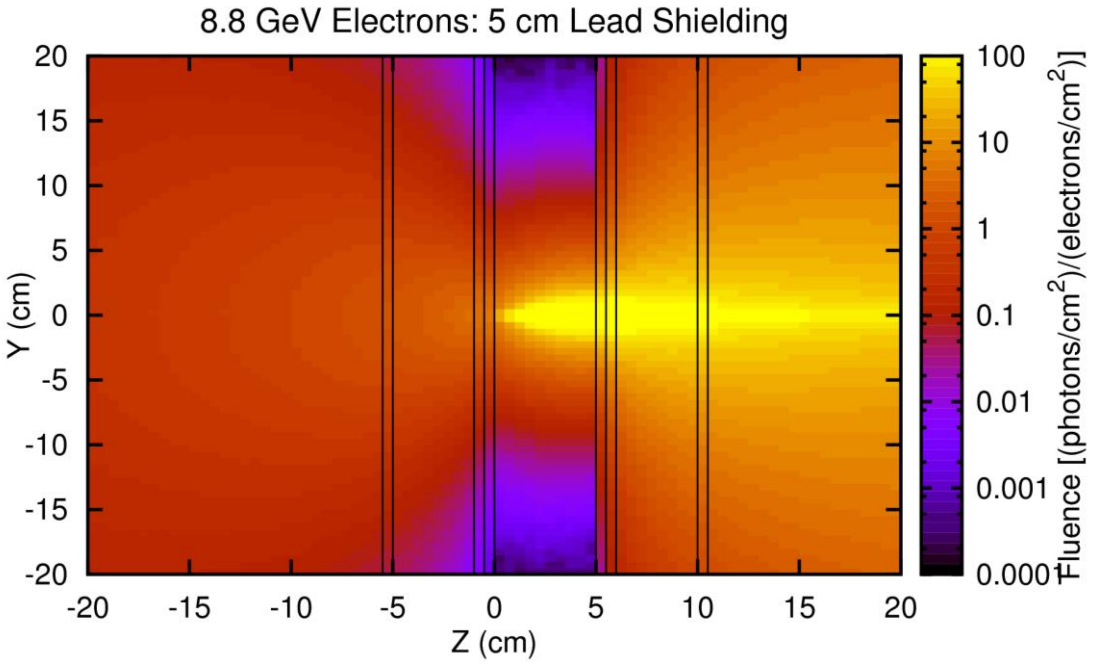

Figure 32. Photon fluence in the case of the 5 cm thick lead block per incoming 8.8 GeV electron.

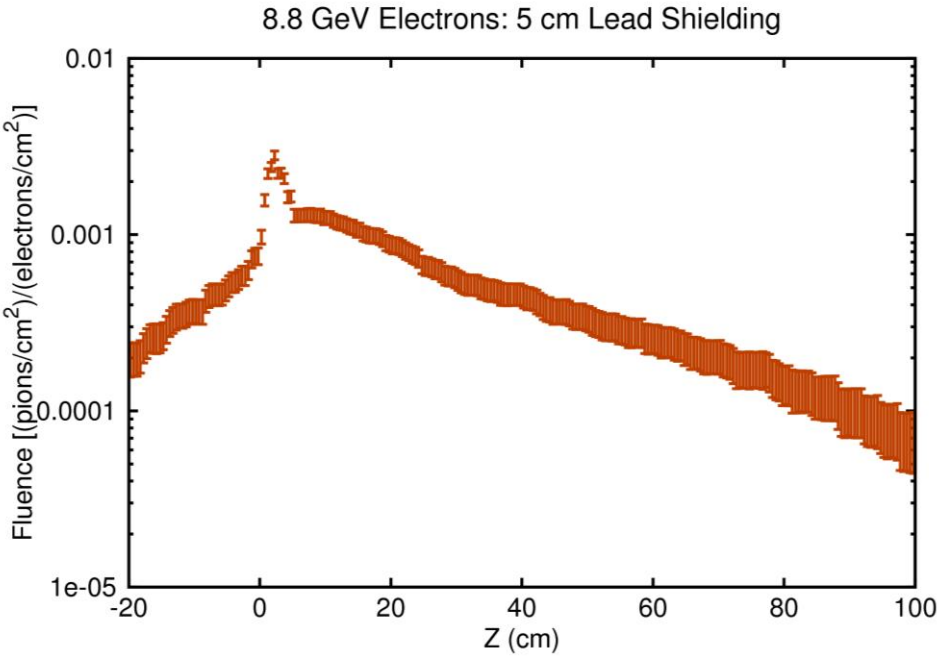

Figure 33. Energy integrated pion fluence as a function of position.

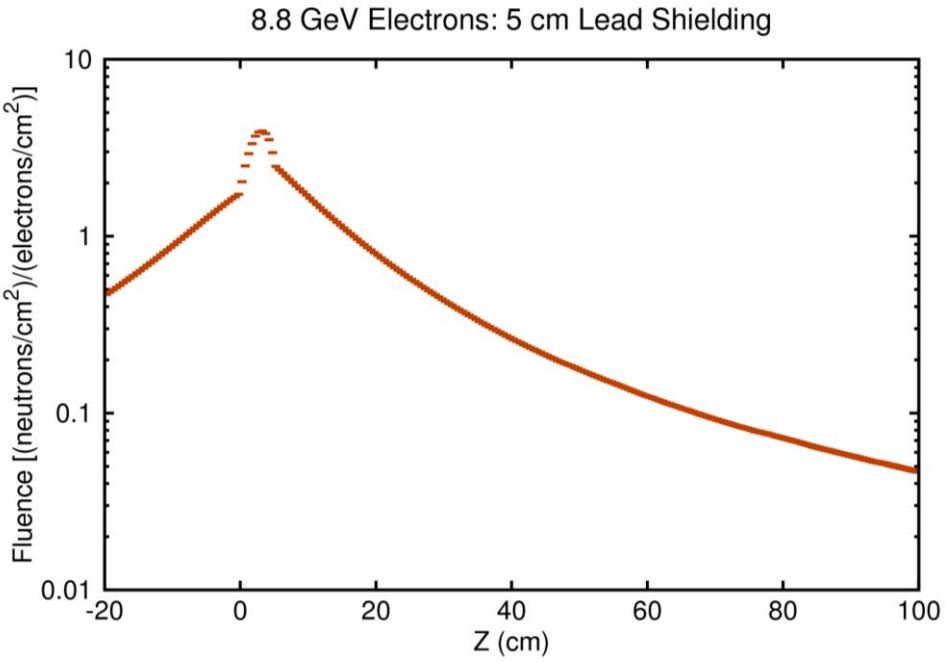

Figure 34. Energy integrated neutron fluence as a function of position.

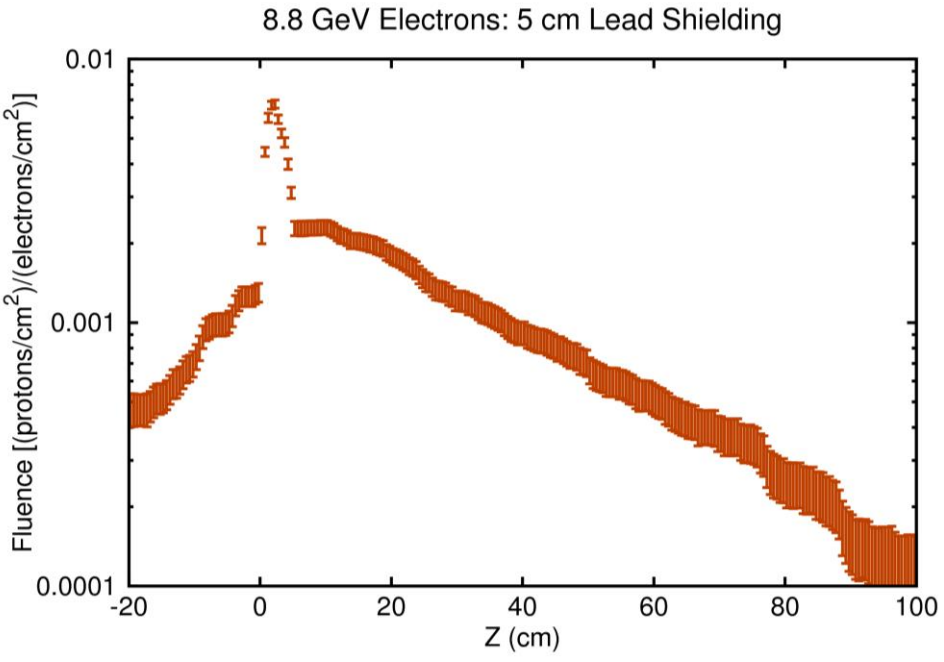

Figure 35. Energy integrated proton fluence as a function of position.

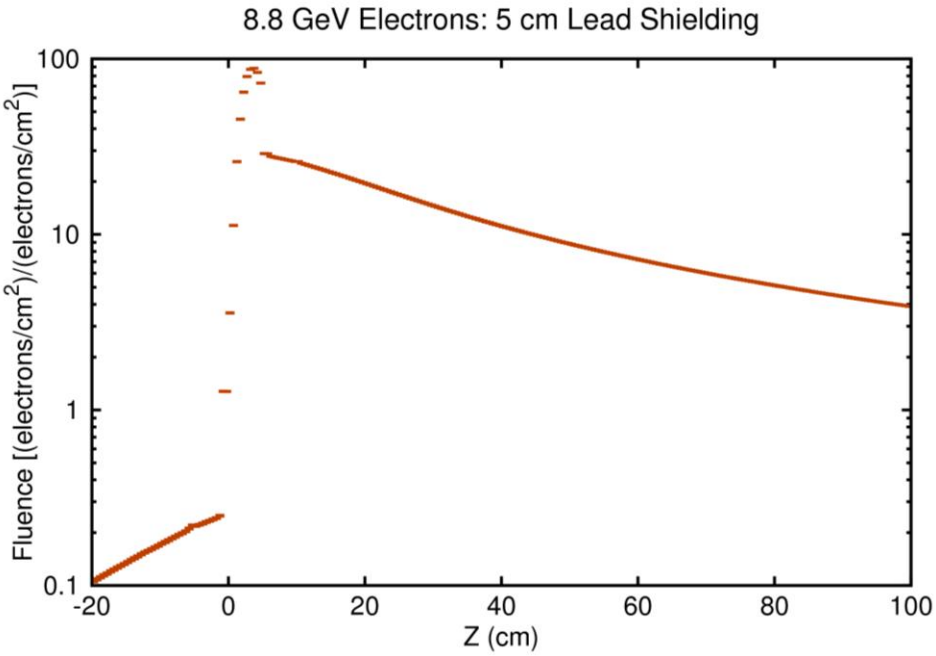

Figure 36. Energy integrated electron fluence as a function of position.

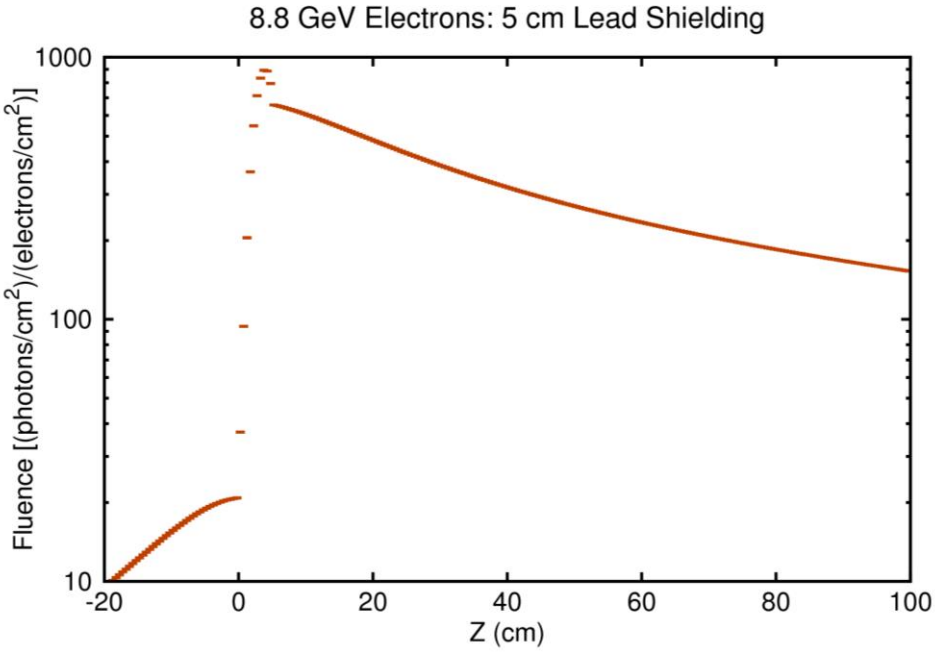

Figure 37. Energy integrated photon fluence as a function of position.

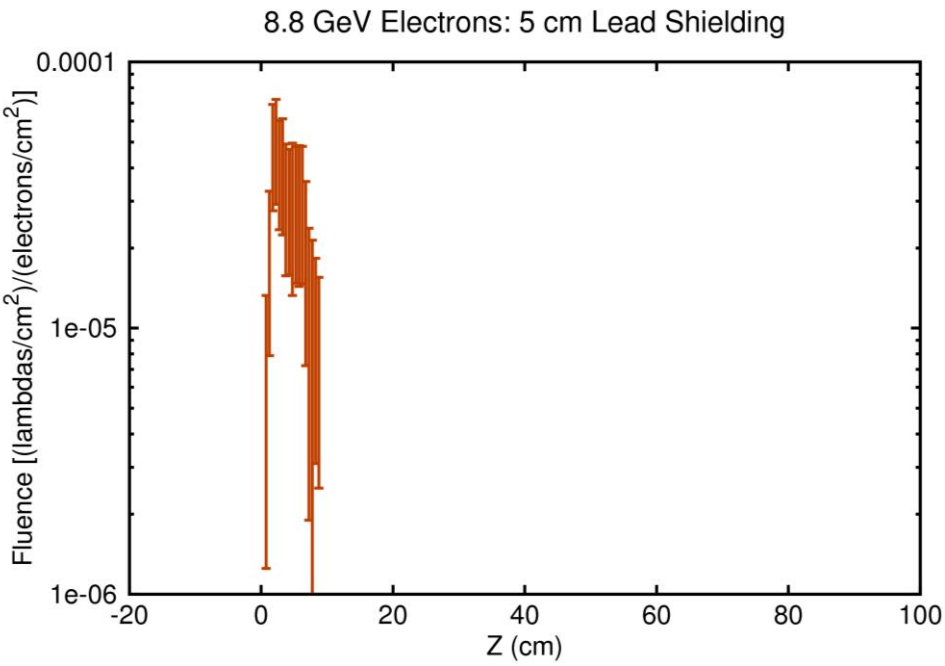

Figure 38. Energy integrated lambda fluence as a function of position.

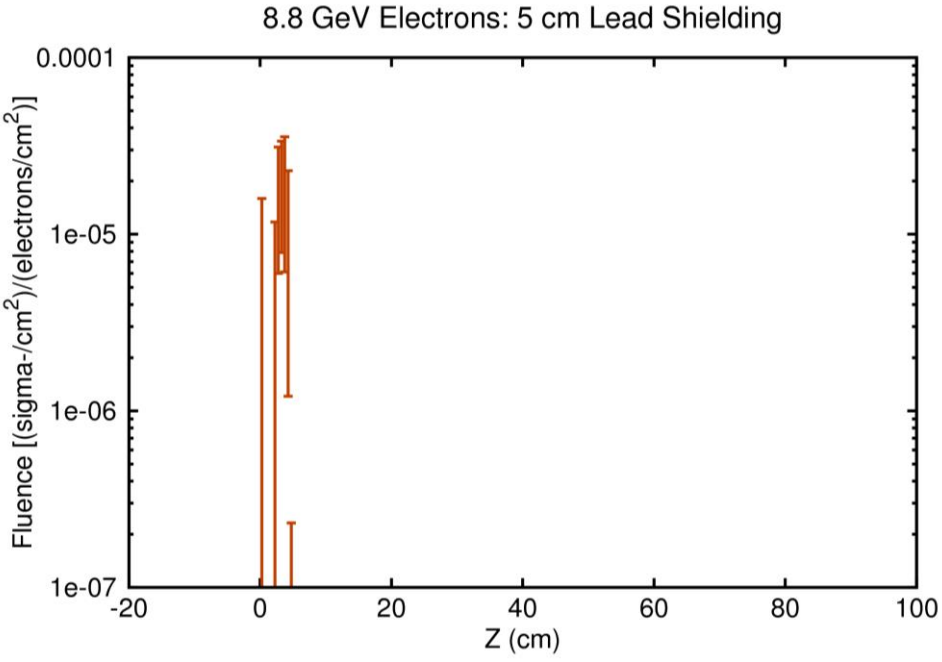

Figure 39. Energy integrated sigma- fluence as a function of position.

The fluences shown in Figures 33-39 are integrated over all the secondary particles energies and can be used to calculate the background rates, but, to fully understand the background, it is also important to know the secondary particles energy spectra. In Figures 40-44 the isolethargic spectra are shown for the secondary particles produced by the shielding in forward and backward directions. The reason for using isolethatrgic spectrum is that the dynamic range of the secondary particles energies requires a logarithmic energy scale. For such a scale the area under the isolethargic spectrum curve is proportional to number of particles in a particular energy interval.

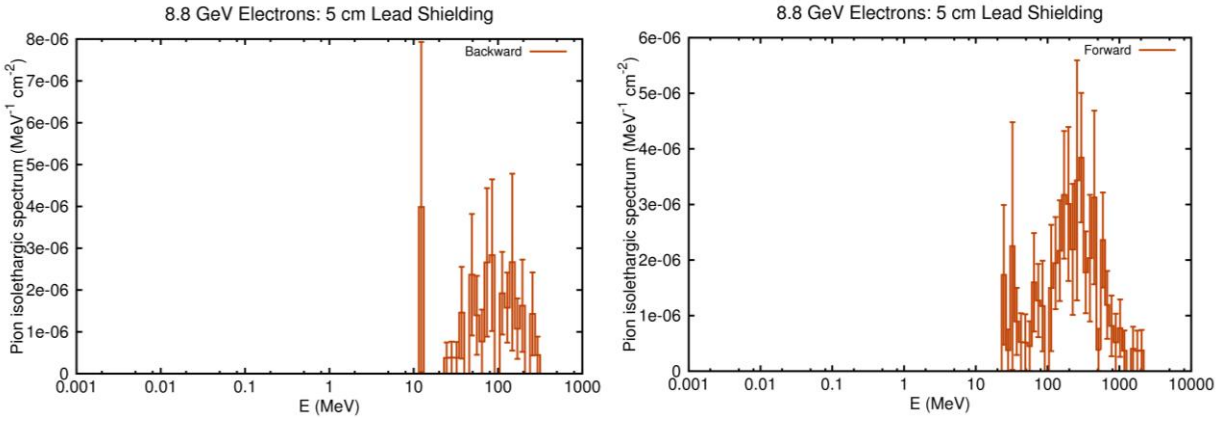

Figure 40. Pion isolethargic spectrum for backward and forward produced pions in a 5 cm thick lead shielding.

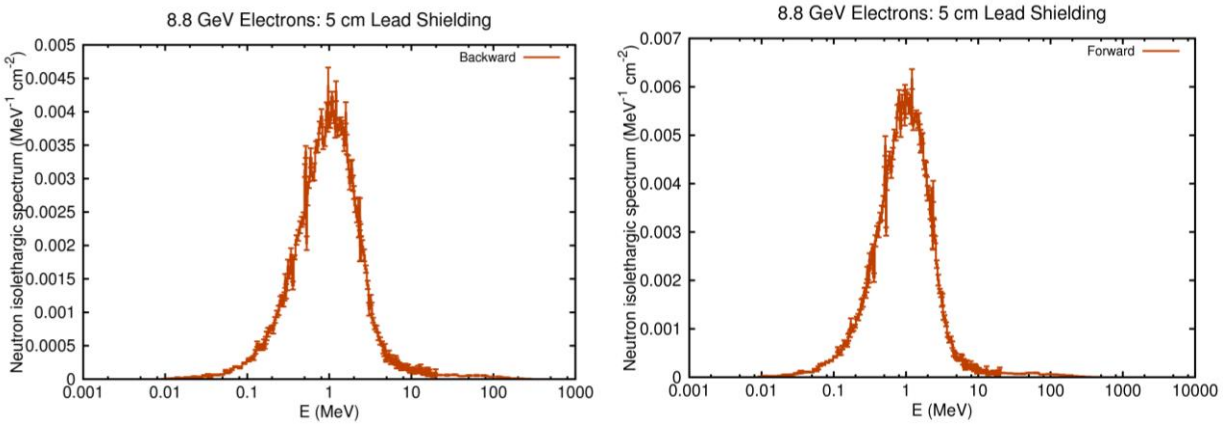

Figure 41. Neutron isolethargic spectrum for backward and forward produced neutrons in a 5 cm thick lead shielding.

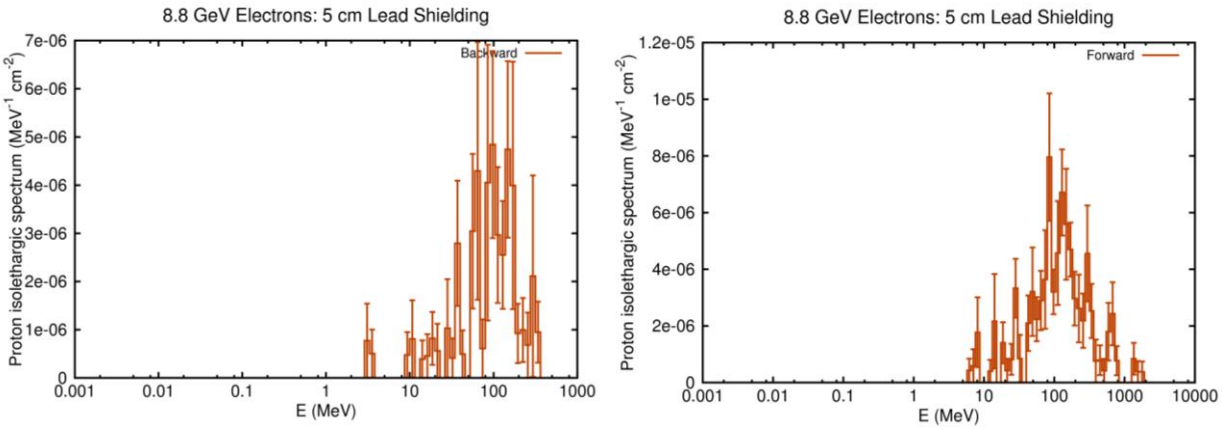

Figure 42. Proton isolethargic spectrum for backward and forward produced protons in a 5 cm thick lead shielding.

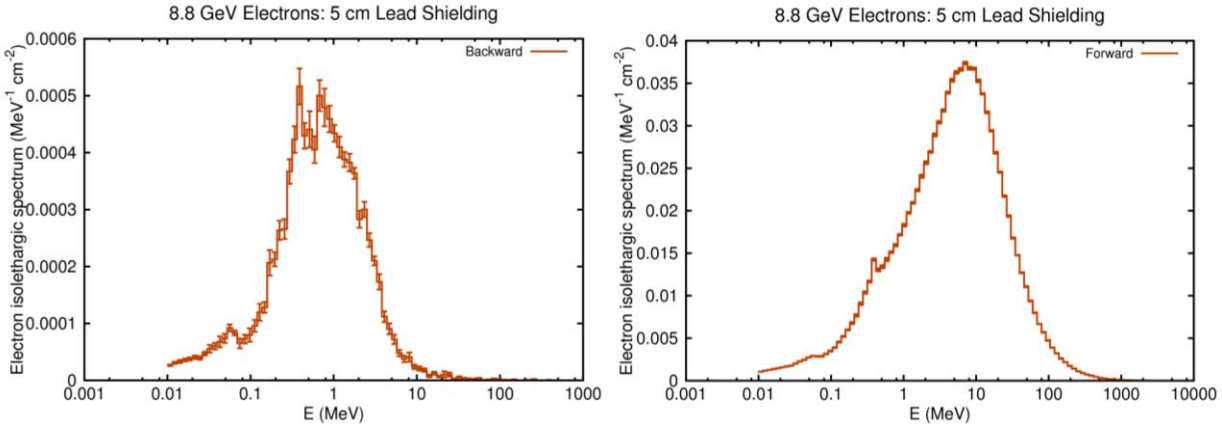

Figure 43. Electron isolethargic spectrum for backward and forward produced electrons in a 5 cm thick lead shielding.

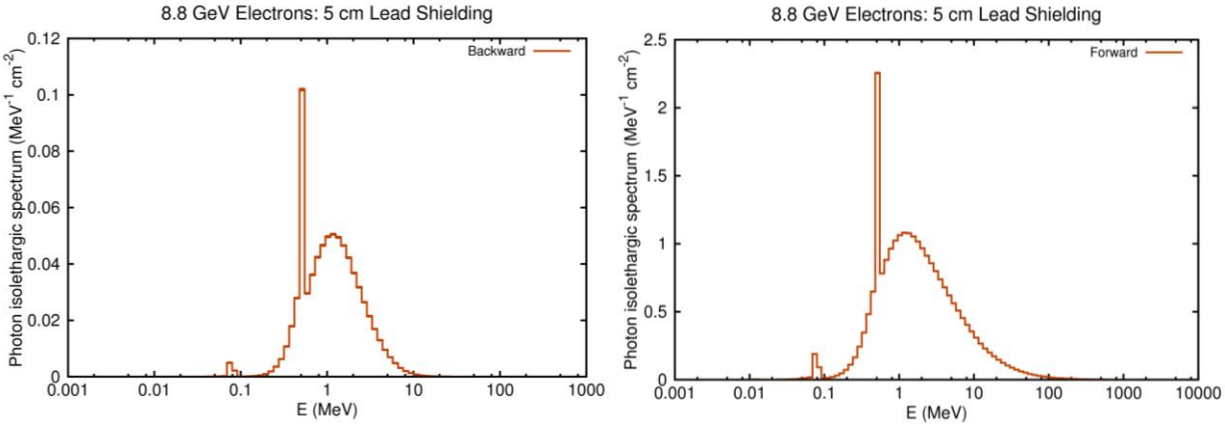

Figure 44. Photon isolethargic spectrum for backward and forward produced photons in a 5 cm thick lead shielding.

III. Results for 10 cm thick lead shielding

In this section we study the effects of pions and electrons impinging on a 20 cm x 20 cm x 10 cm lead block. In addition to the total deposited energy in the block, the fluences of pions, muons, neutrons, protons, electrons, photons, lambdas and sigma- are also calculated in units of number of particles per cm^2 normalized to number of incoming particles per cm^2. With such a choice of units one only needs to multiply shown fluences with primary particles rates (which can be calculated separately) to get the fluences expected in Moller experiment. In the simulation the cutoff energy threshold for all the particles was 10^{-5} GeV, except for the neutrons where the cutoff threshold was 10^{-8} GeV.

In the case of pions, the total deposited energy is shown in Figure 45 in units of MeV/cm^3. The average deposited energy in the entire lead block was 1250 MeV per incoming pion. The fluences integrated over all secondary particles energies are shown in Figures 46-53 and Figures 54-61.

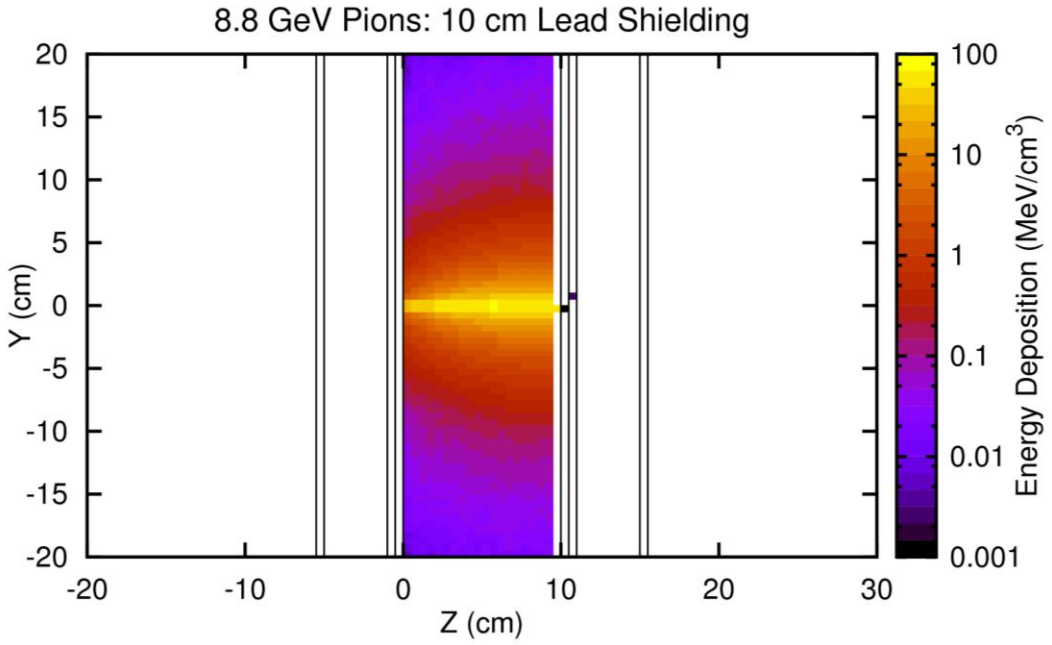

Figure 45. Total deposited energy in the 10 cm thick lead block per incoming 8.8 GeV pion.

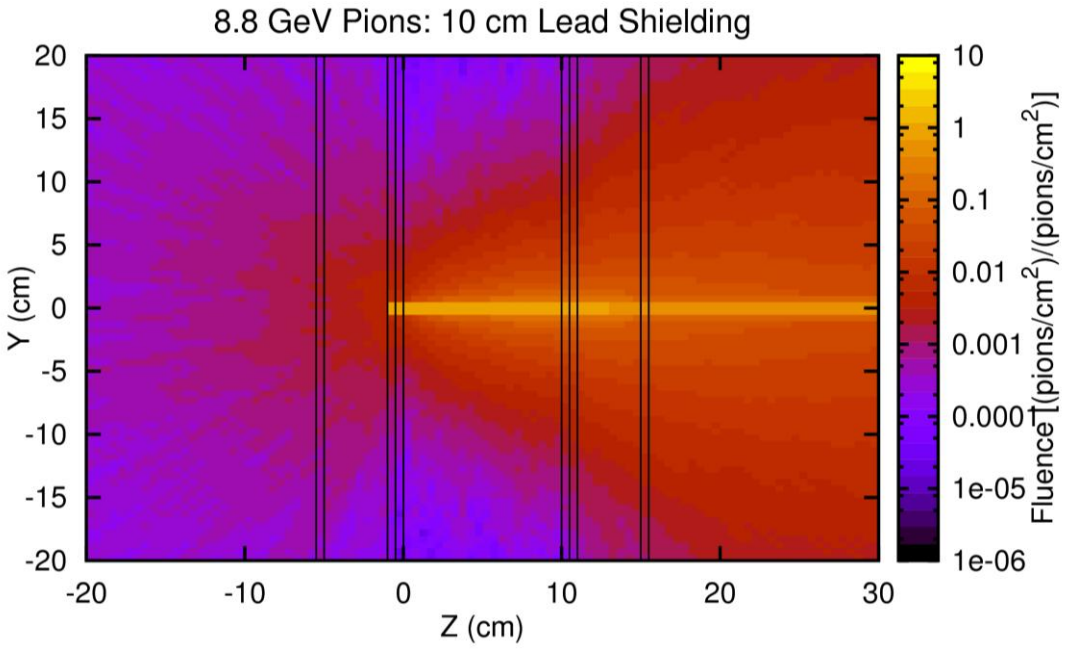

Figure 46. Pion fluence in the case of the 10 cm thick lead block per incoming 8.8 GeV pion.

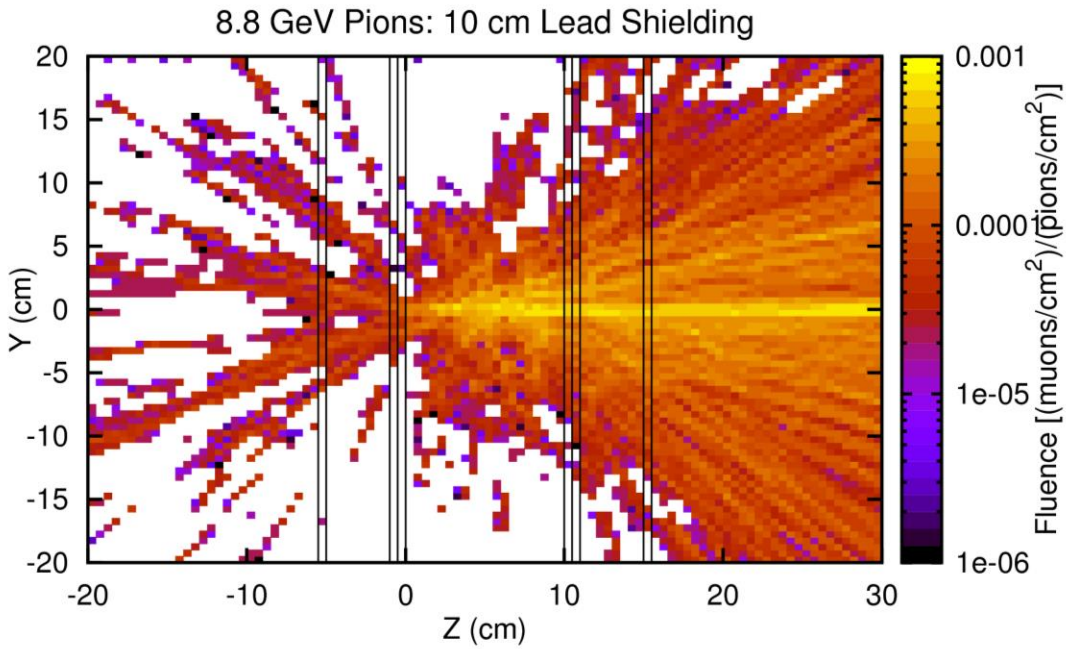

Figure 47. Muon fluence in the case of the 10 cm thick lead block per incoming 8.8 GeV pion.

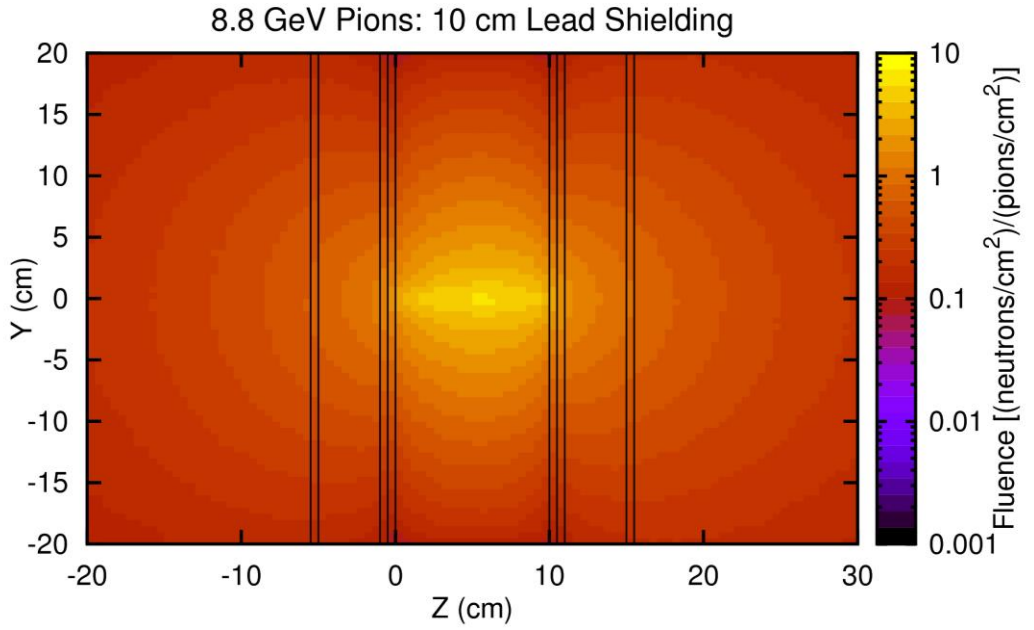

Figure 48. Neutron fluence in the case of the 10 cm thick lead block per incoming 8.8 GeV pion.

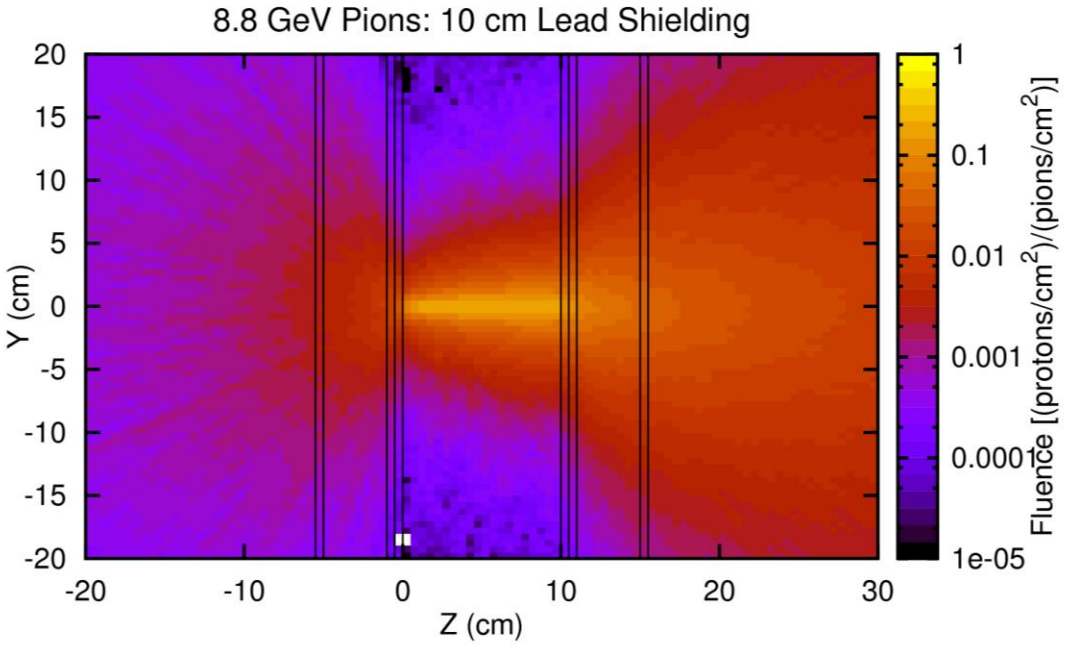

Figure 49. Proton fluence in the case of the 10 cm thick lead block per incoming 8.8 GeV pion.

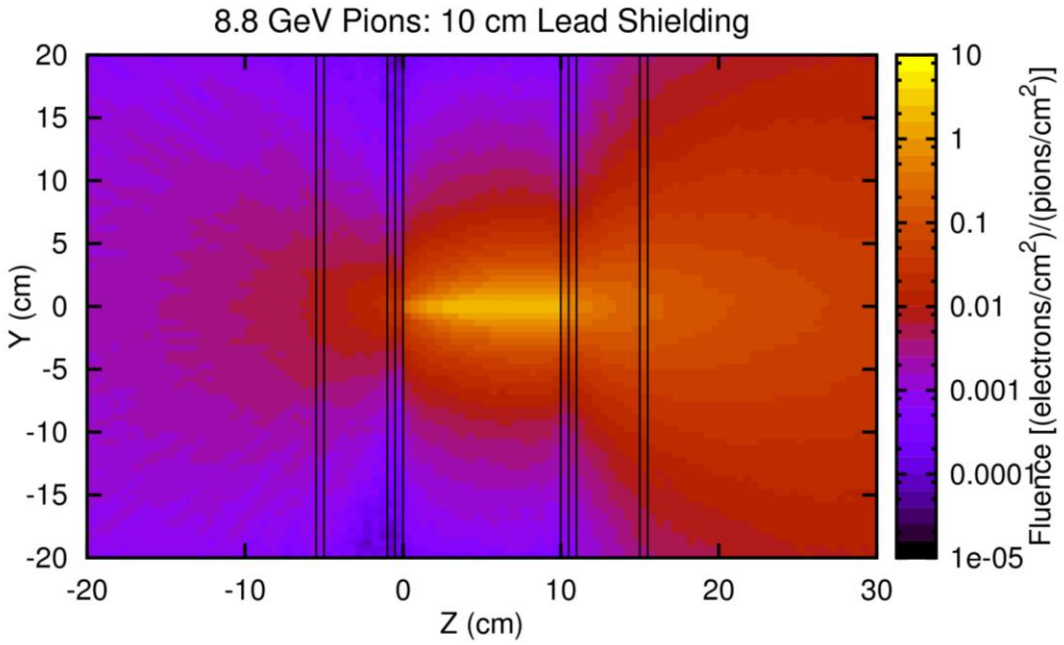

Figure 50. Electron fluence in the case of the 10 cm thick lead block per incoming 8.8 GeV pion.

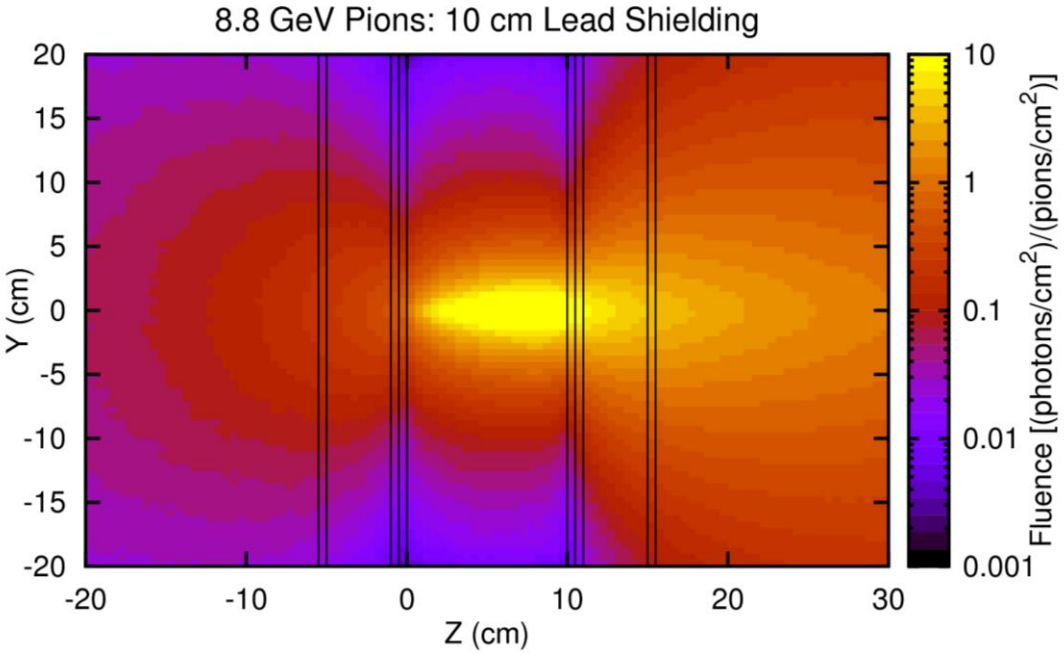

Figure 51. Photon fluence in the case of the 10 cm thick lead block per incoming 8.8 GeV pion.

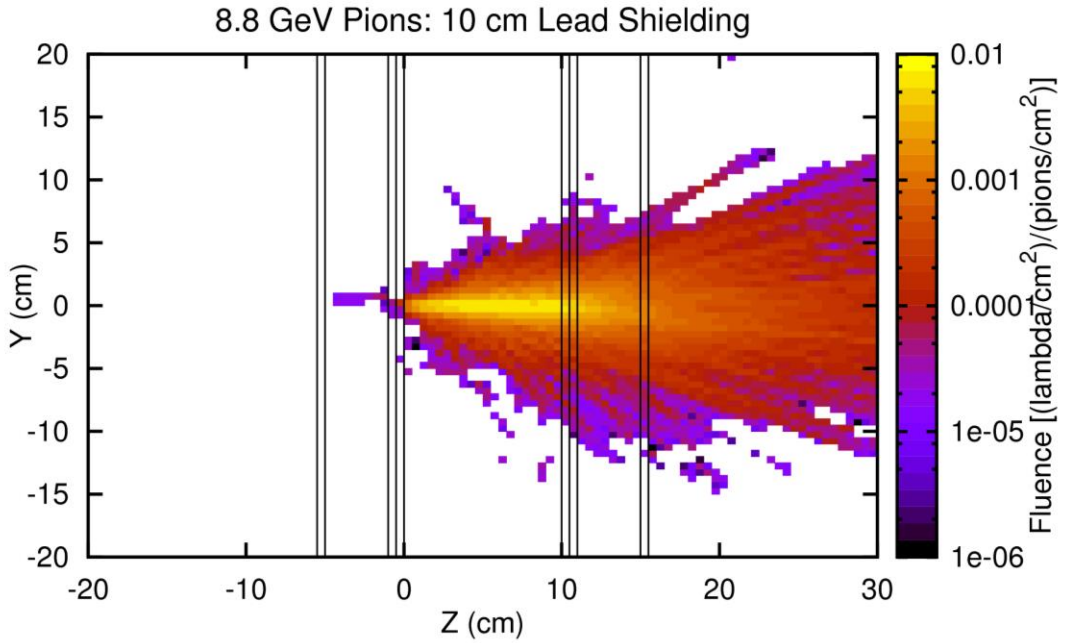

Figure 52. Lambda fluence in the case of the 10 cm thick lead block per incoming 8.8 GeV pion.

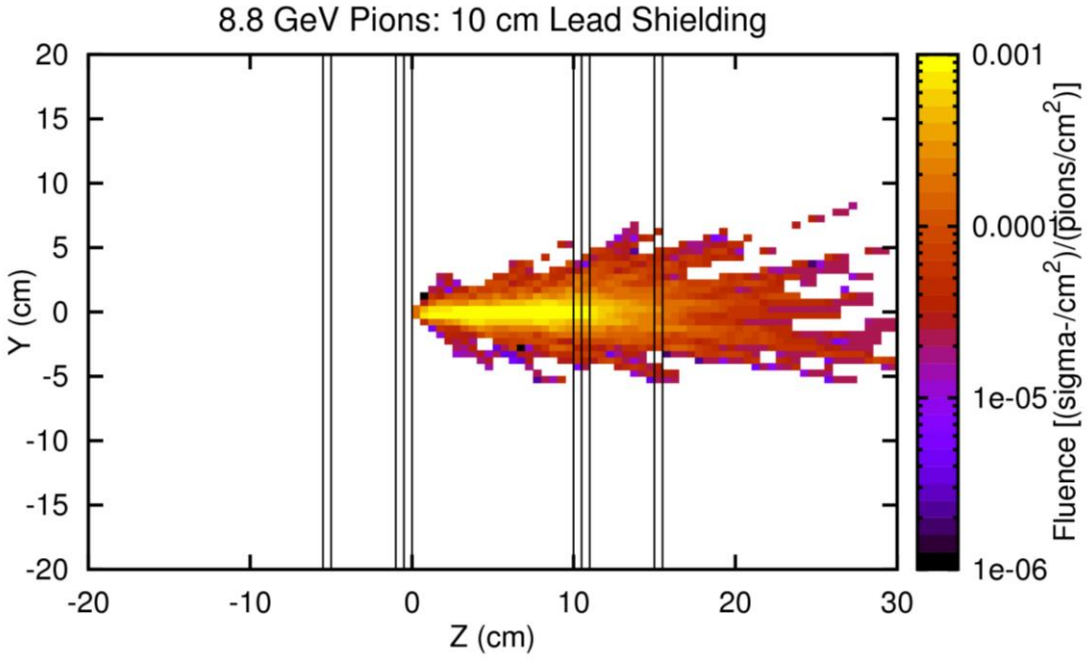

Figure 53. Sigma- fluence in the case of the 10 cm thick lead block per incoming 8.8 GeV pion.

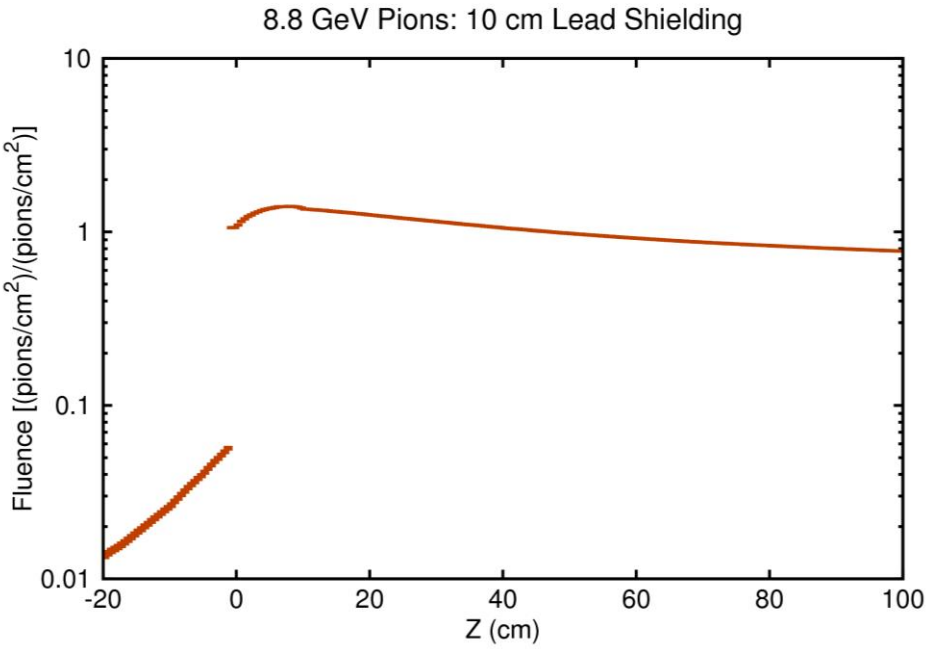

Figure 54. Energy integrated pion fluence as a function of position.

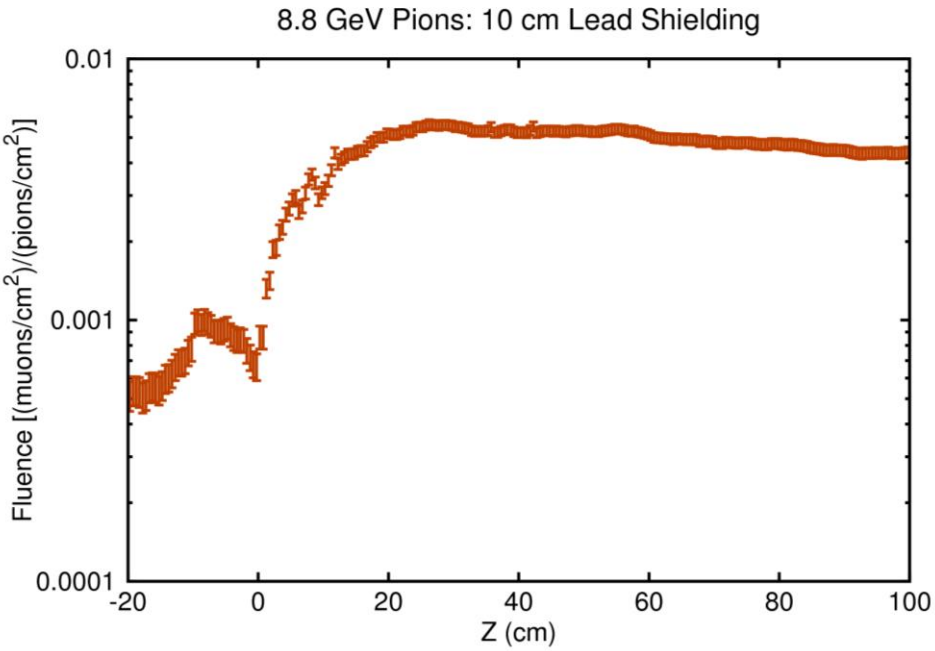

Figure 55. Energy integrated muon fluence as a function of position.

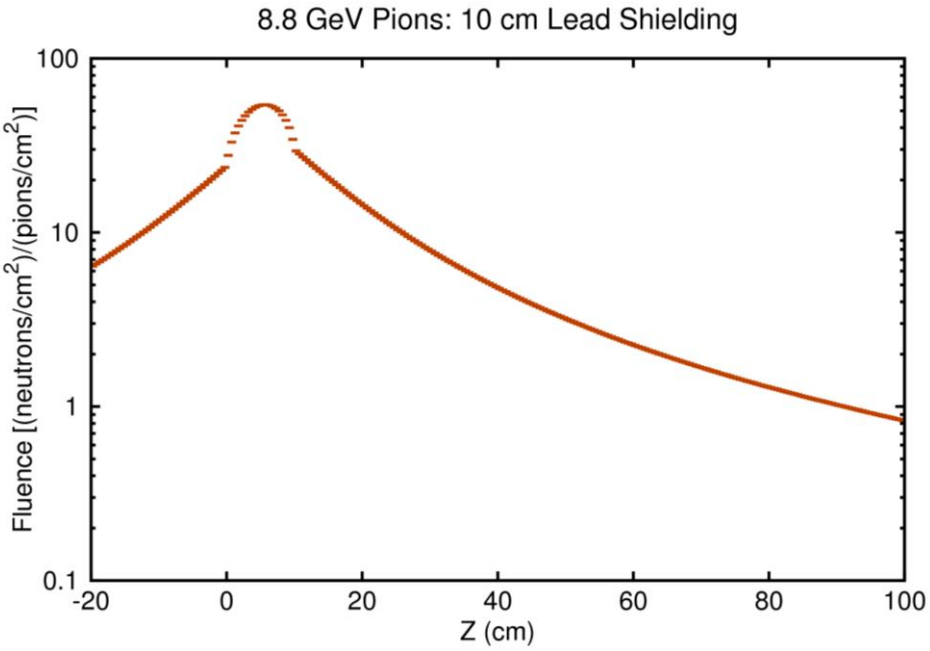

Figure 56. Energy integrated neutron fluence as a function of position.

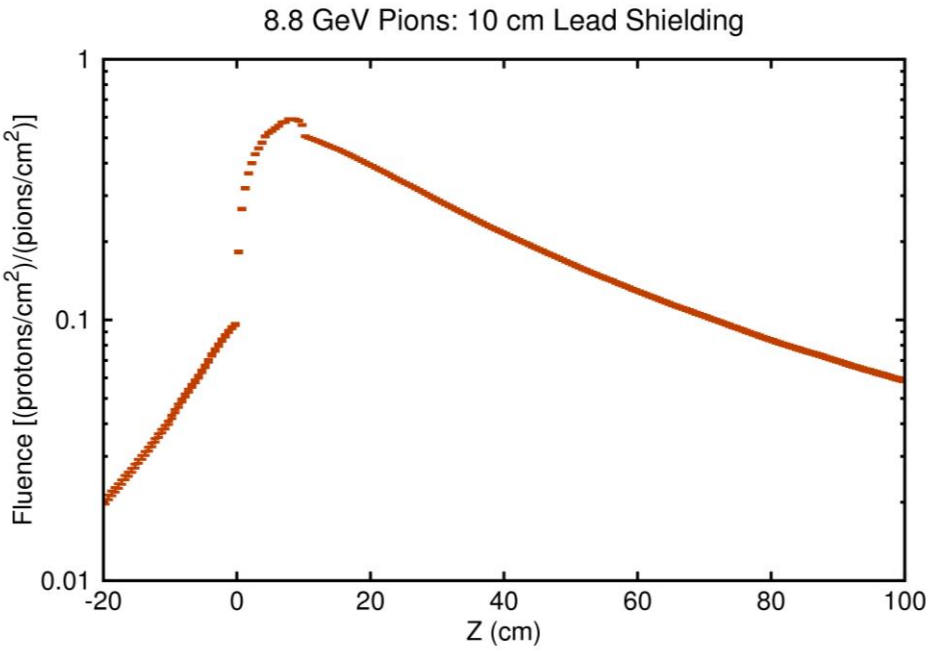

Figure 57. Energy integrated proton fluence as a function of position.

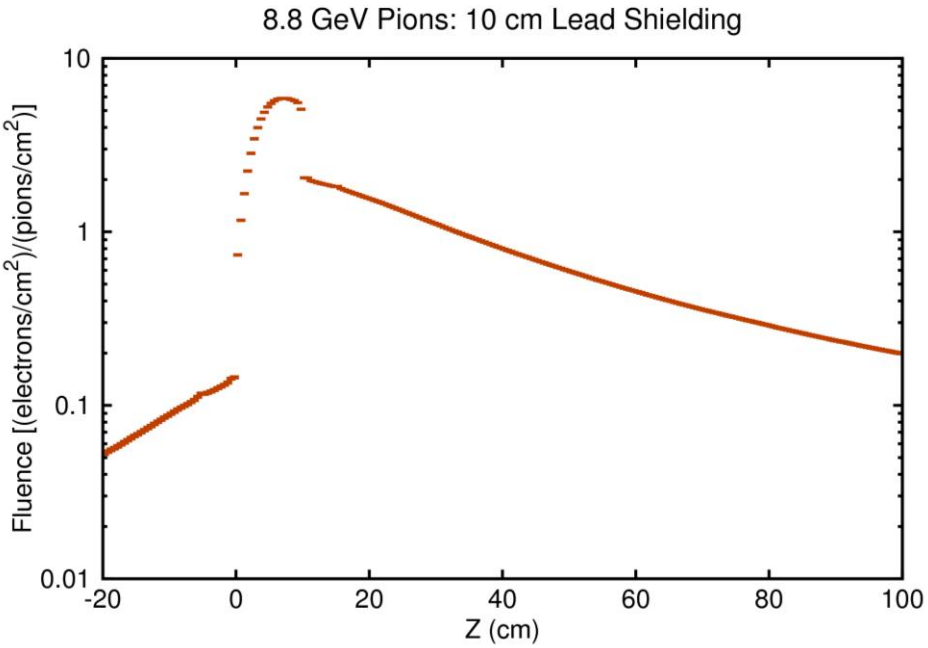

Figure 58. Energy integrated electron fluence as a function of position.

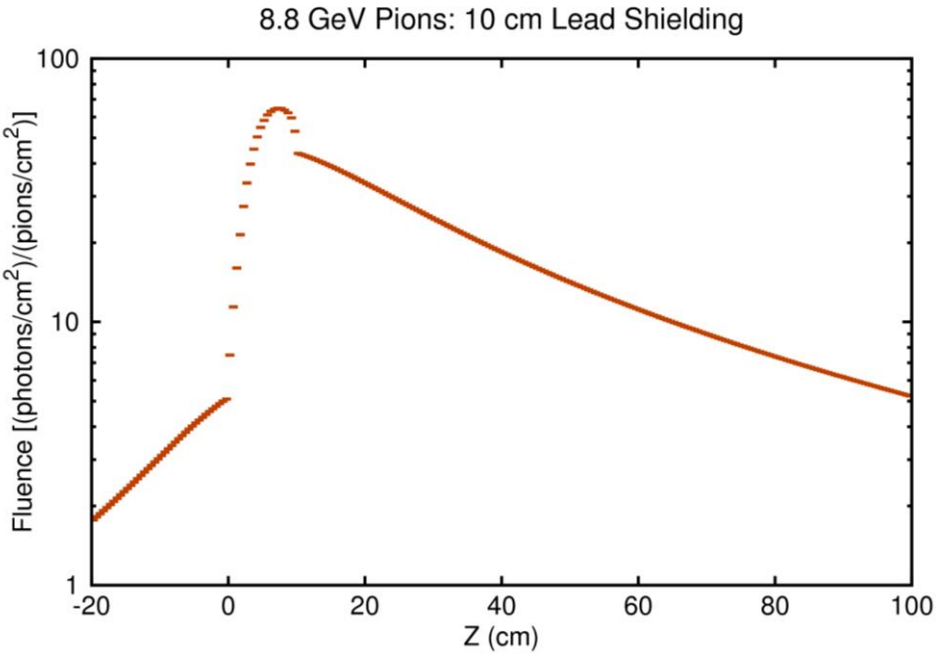

Figure 59. Energy integrated photon fluence as a function of position.

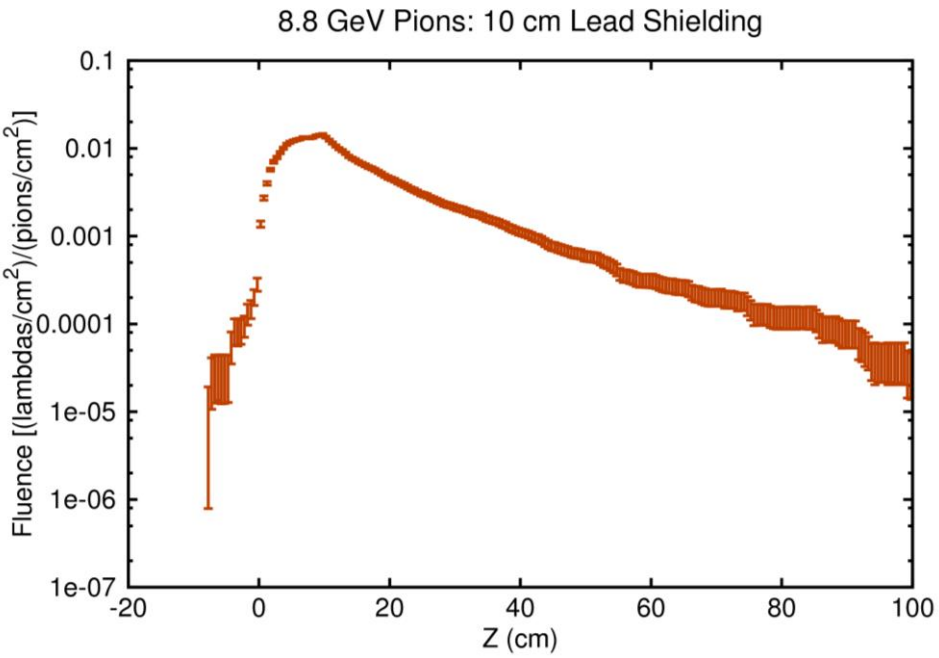

Figure 60. Energy integrated lambda fluence as a function of position.

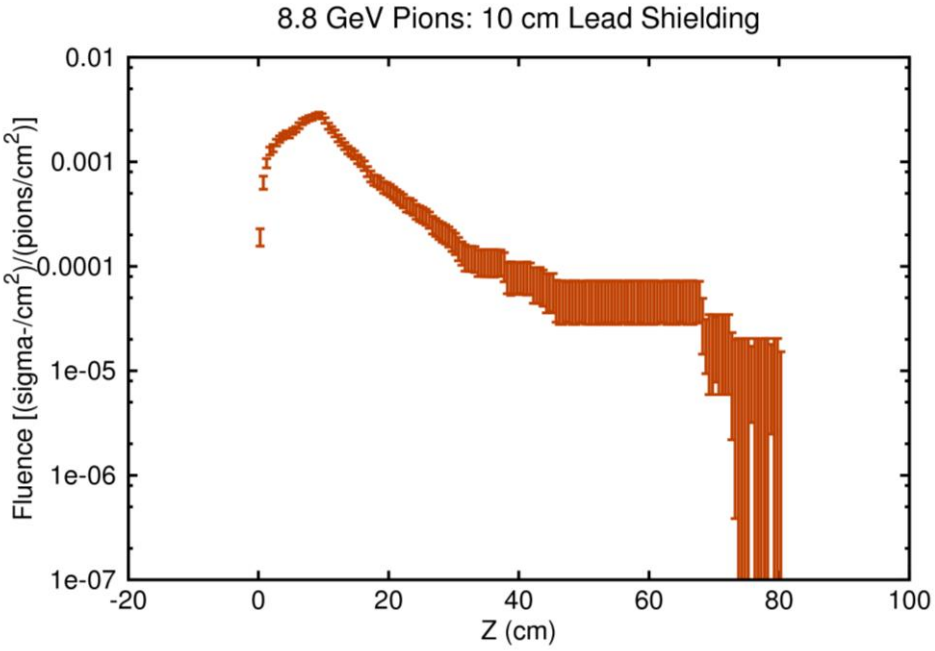

Figure 61. Energy integrated sigma- fluence as a function of position.

The fluences shown in Figures 54-61 are integrated over all the secondary particles energies and can be used to calculate the background rates, but, to fully understand the background, it is also important to know the secondary particles energy spectra. In Figures 62-69 the isolethargic spectra are shown for the secondary particles produced by the shielding in forward and backward directions. The reason for using isolethatrgic spectra is that the dynamic range of the energies of the secondary particles requires a logarithmic energy scale. For such a scale the area under the isolethargic spectrum curve is proportional to number of particles in a particular energy interval.

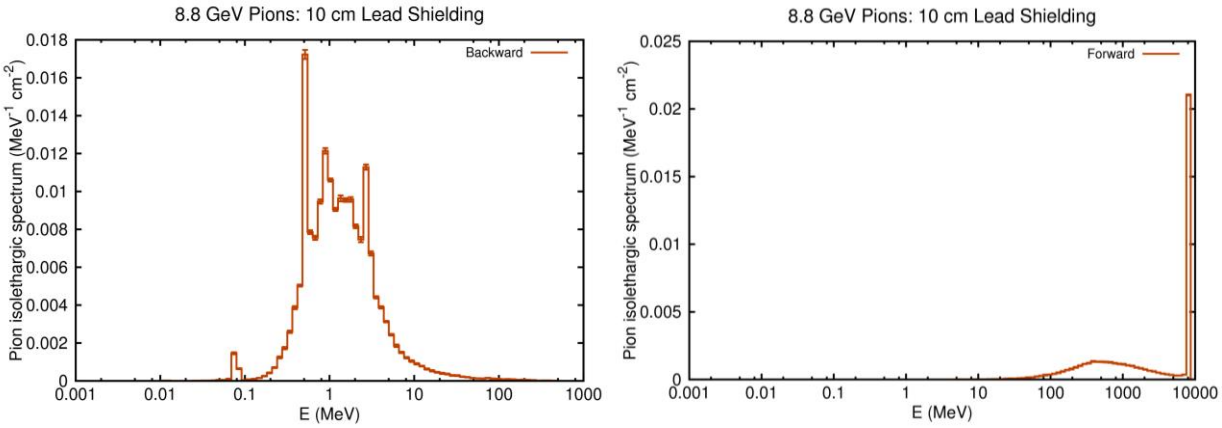

Figure 62. Pion isolethargic spectrum for backward and forward produced pions in a 10 cm thick lead shielding.

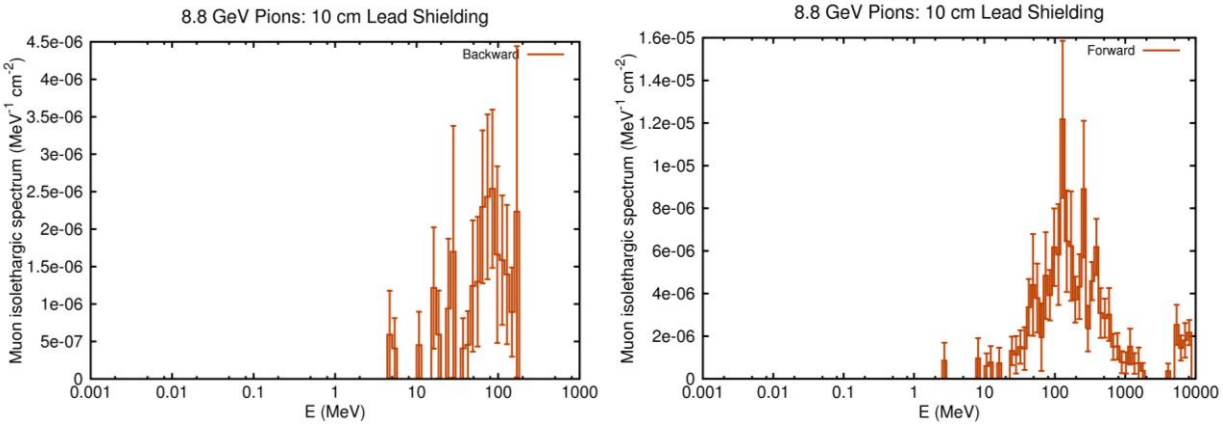

Figure 63. Muon isolethargic spectrum for backward and forward produced muons in a 10 cm thick lead shielding.

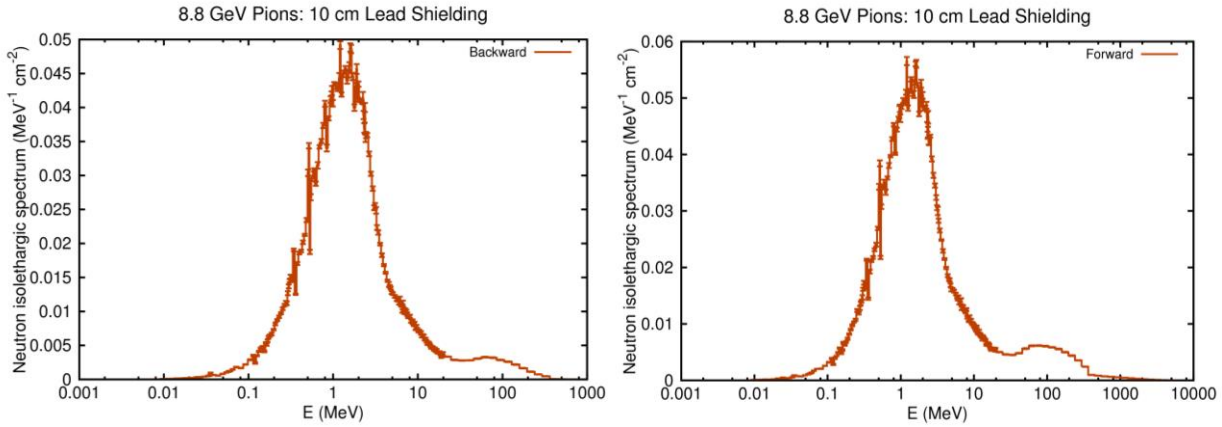

Figure 64. Neutron isolethargic spectrum for backward and forward produced neutrons in a 10 cm thick lead shielding.

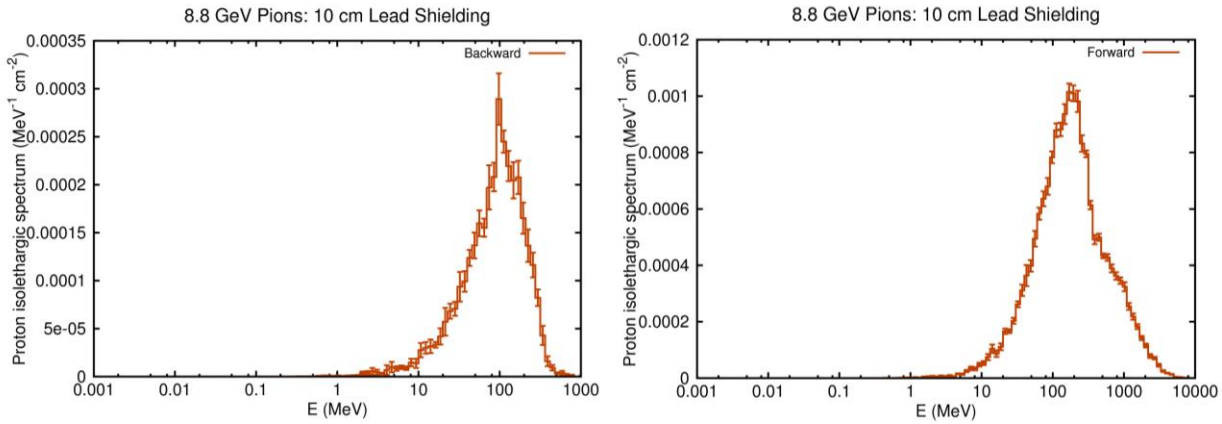

Figure 65. Proton isolethargic spectrum for backward and forward produced protons in a 10 cm thick lead shielding.

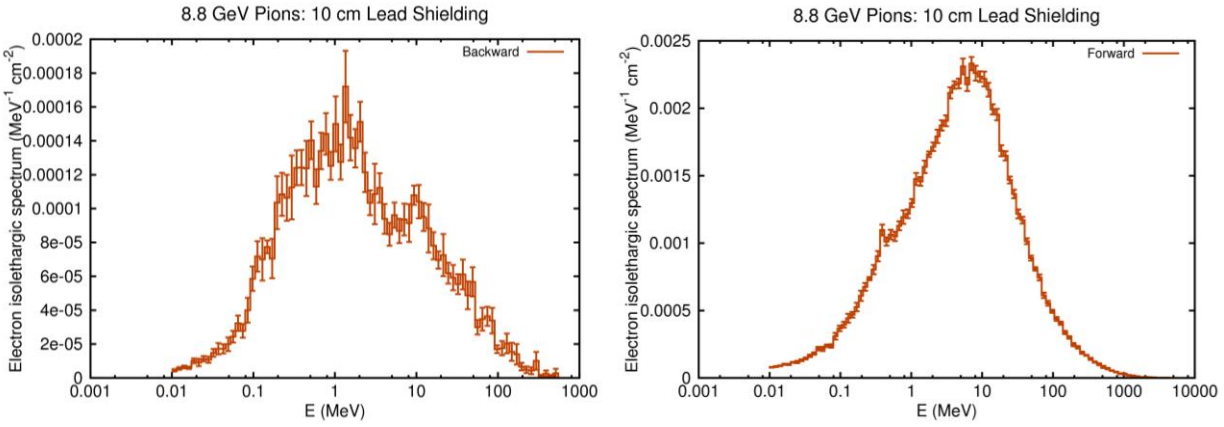

Figure 66. Electron isolethargic spectrum for backward and forward produced electrons in a 10 cm thick lead shielding.

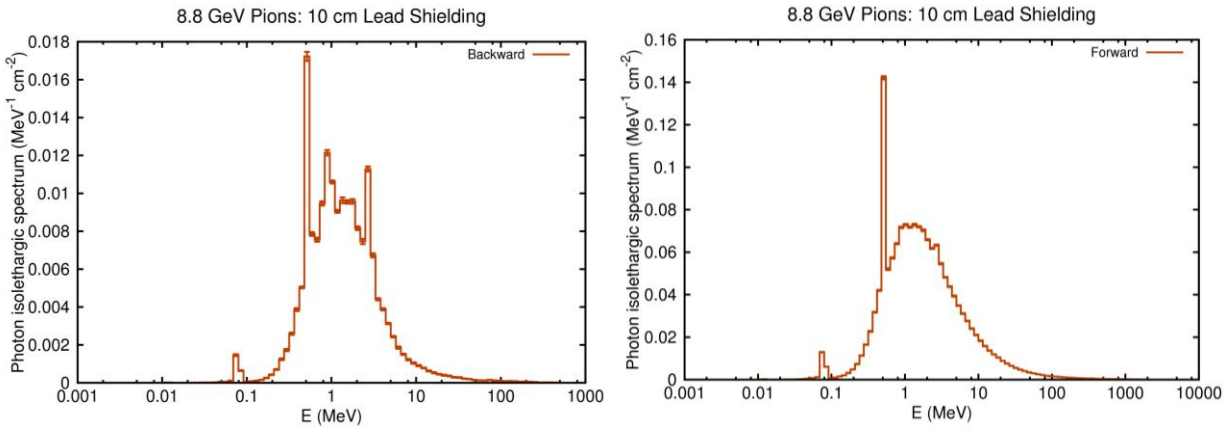

Figure 67. Photon isolethargic spectrum for backward and forward produced photons in a 10 cm thick lead shielding.

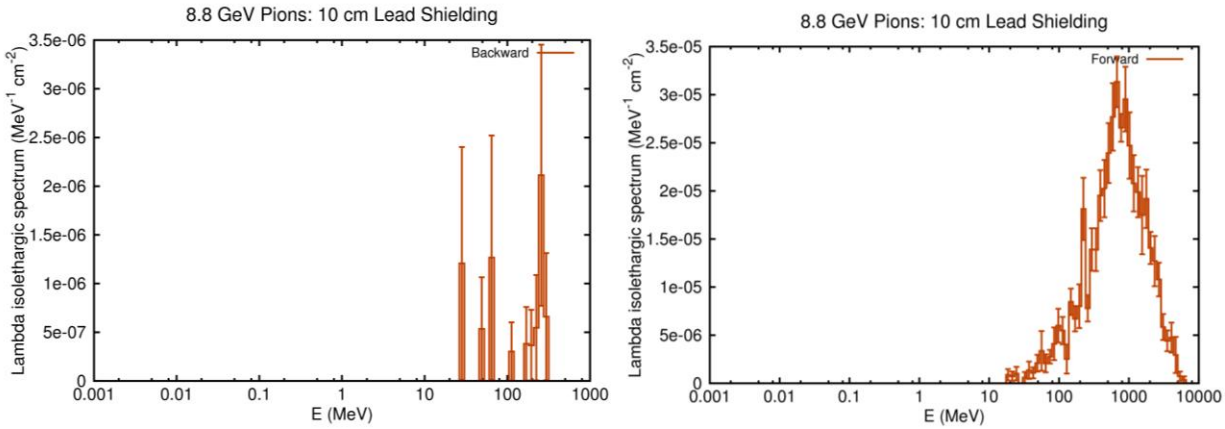

Figure 68. Lambda isolethargic spectrum for backward and forward produced lambdas in a 10 cm thick lead shielding.

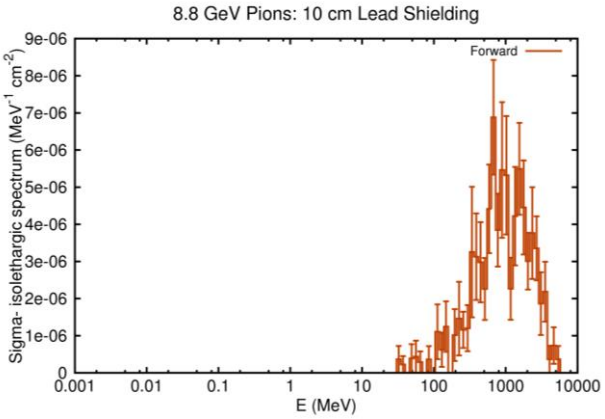

Figure 69. Sigma- isolethargic spectrum forward produced sigma- in a 10 cm thick lead shielding.

In the case of the electrons, the total deposited energy is shown in Figure 70 in units of MeV/cm^3. The average deposited energy in the entire lead block was 8400 MeV per incoming electron. The fluences integrated over all the secondary particles energies are shown in Figures 71-75 and Figures 76-81.

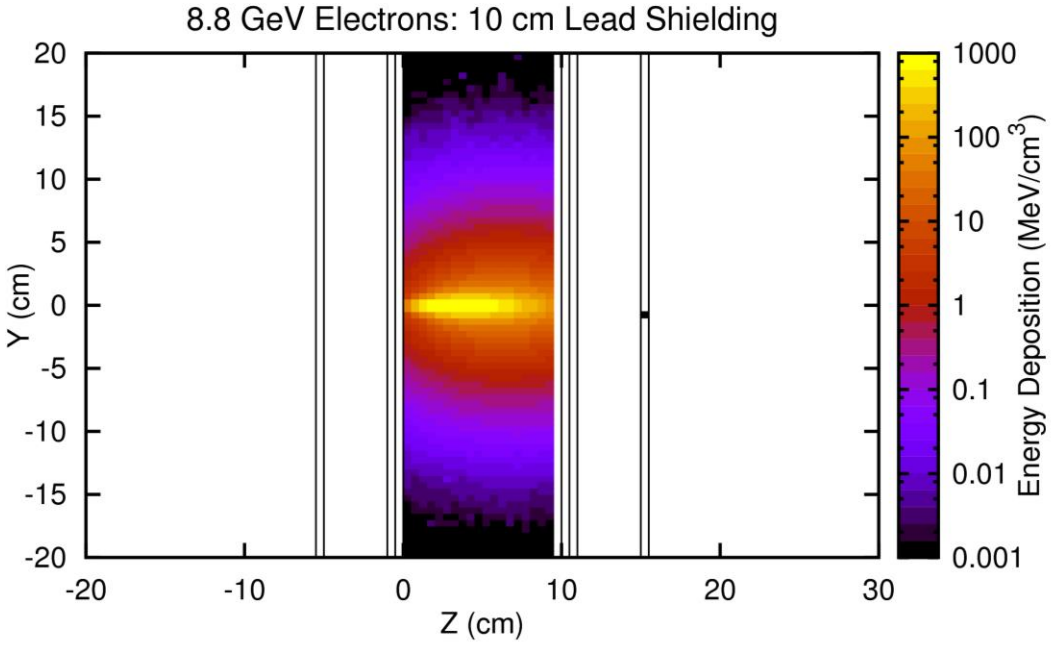

Figure 70. Total deposited energy in the 10 cm thick lead block per incoming 8.8 GeV electron.

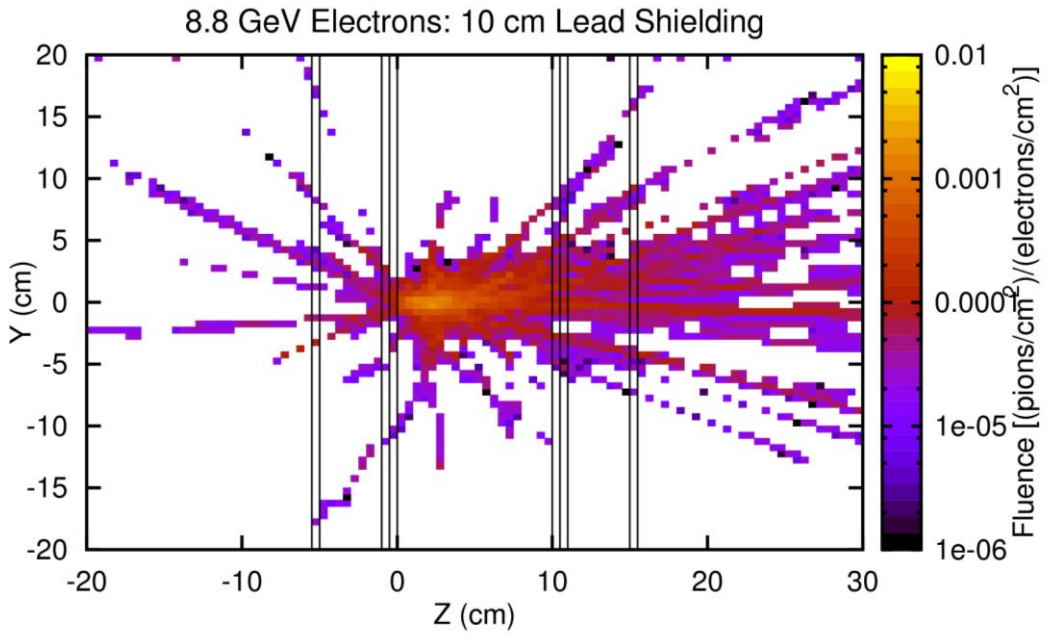

Figure 71. Pion fluence in the case of the 10 cm thick lead block per incoming 8.8 GeV electron.

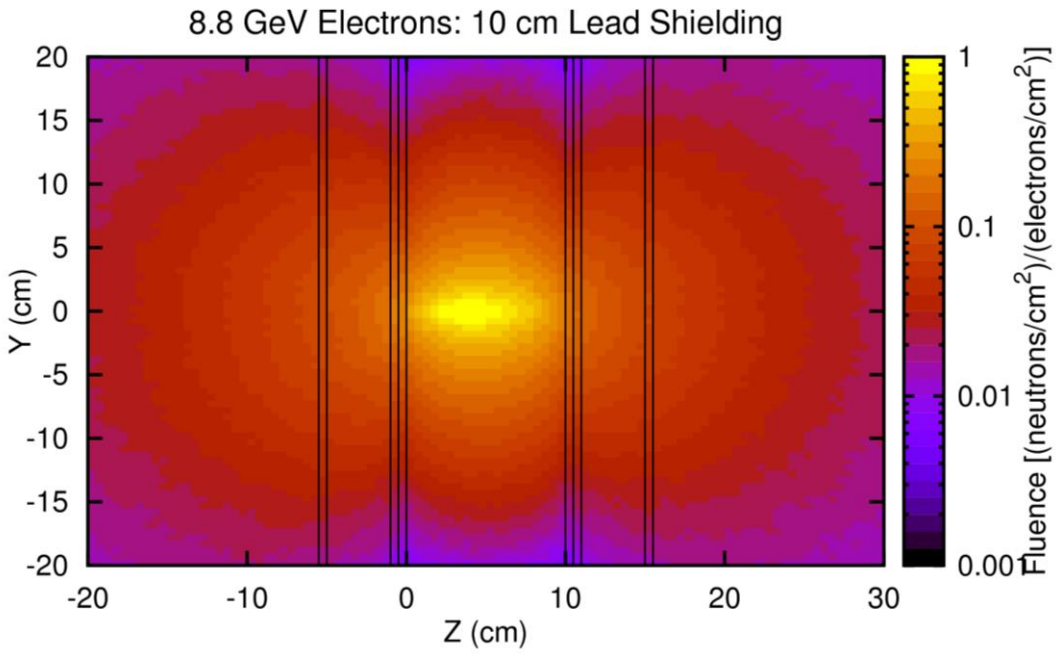

Figure 72. Neutron fluence in the case of the 10 cm thick lead block per incoming 8.8 GeV electron.

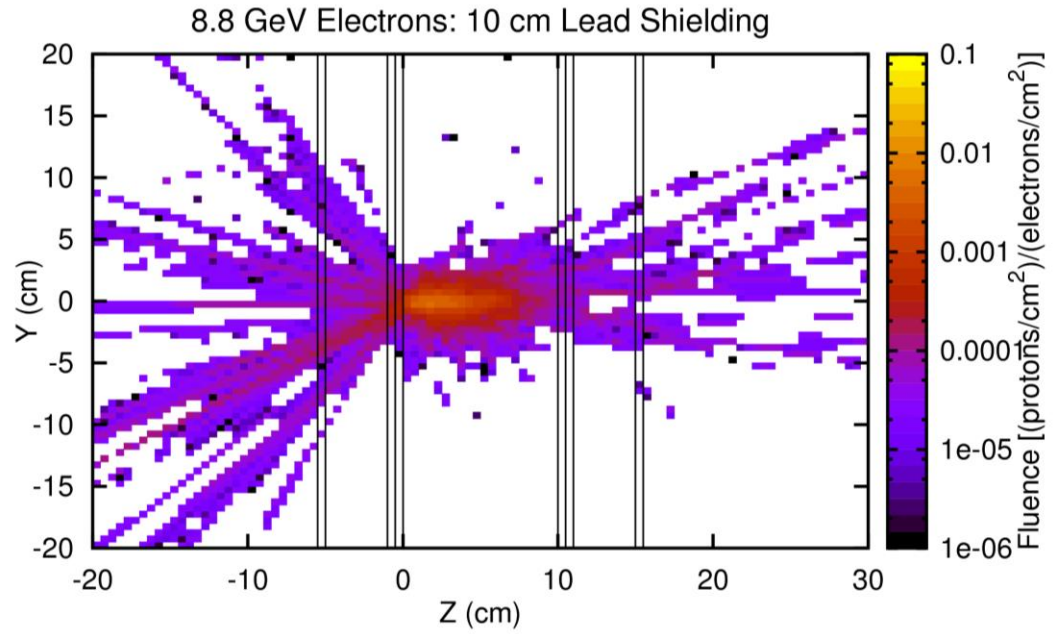

Figure 73. Proton fluence in the case of the 10 cm thick lead block per incoming 8.8 GeV electron.

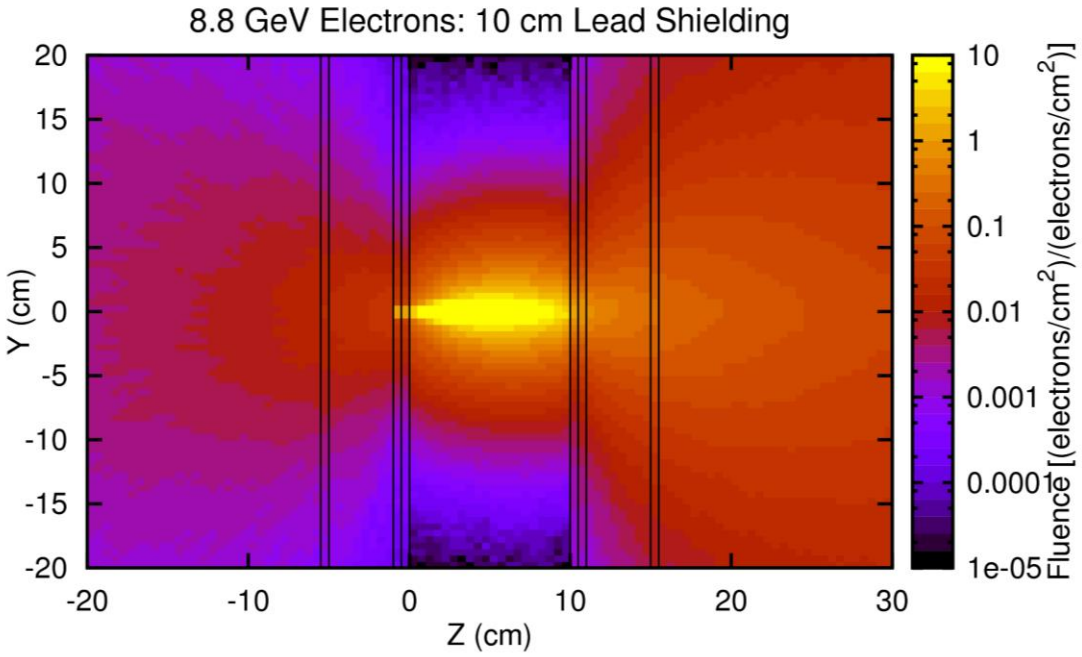

Figure 74. Electron fluence in the case of the 10 cm thick lead block per incoming 8.8 GeV electron.

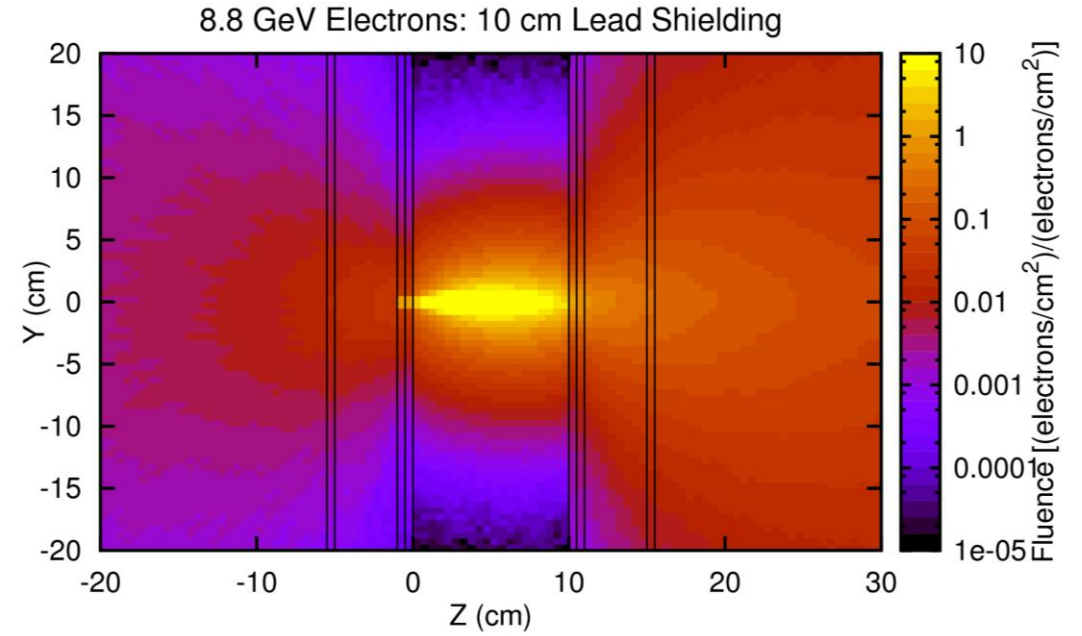

Figure 75. Photon fluence in the case of the 10 cm thick lead block per incoming 8.8 GeV electron.

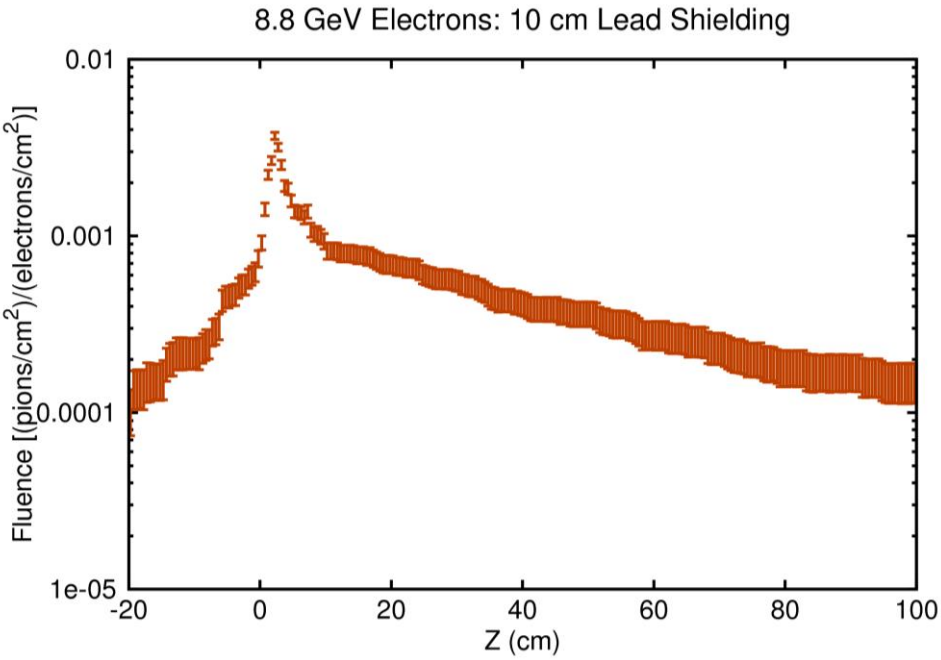

Figure 76. Energy integrated pion fluence as a function of position.

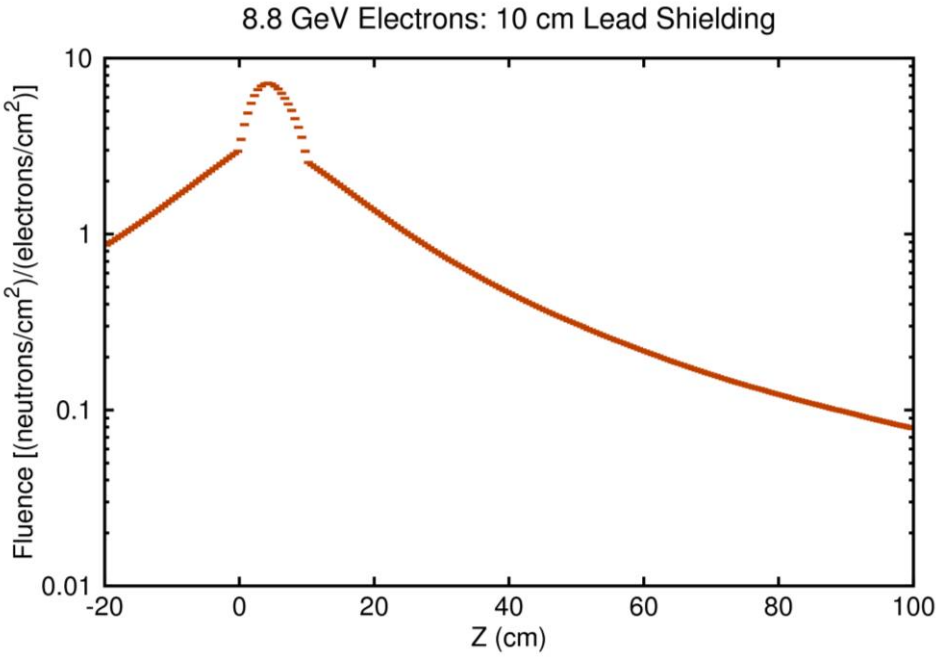

Figure 77. Energy integrated neutron fluence as a function of position.

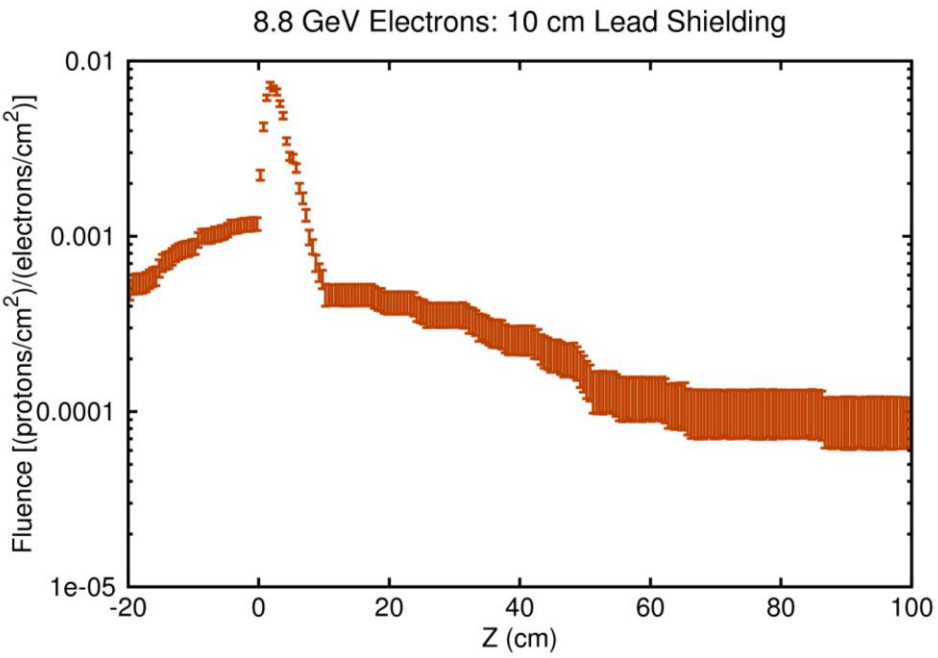

Figure 78. Energy integrated proton fluence as a function of position.

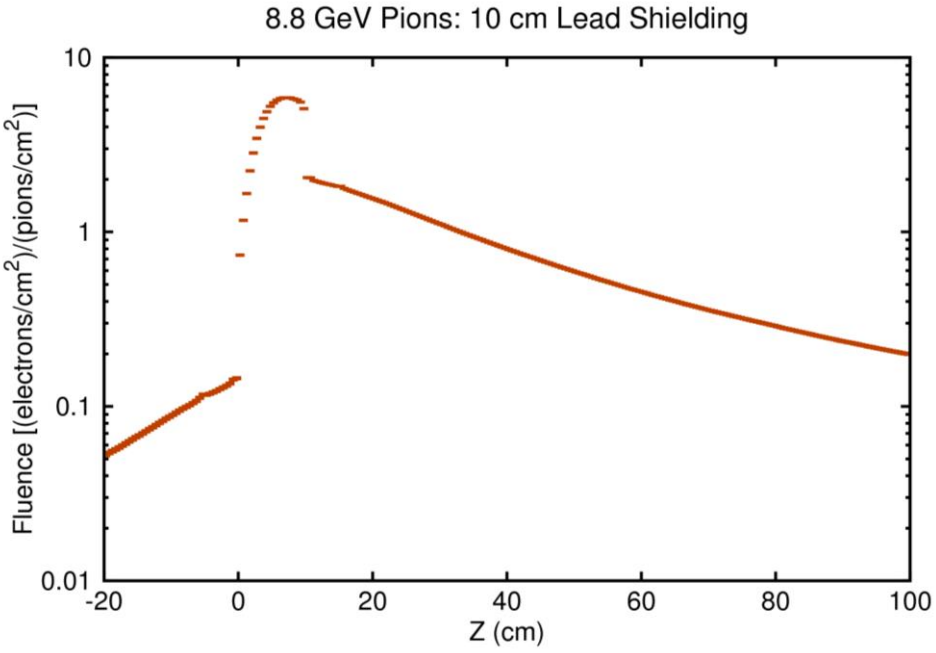

Figure 79. Energy integrated electron fluence as a function of position.

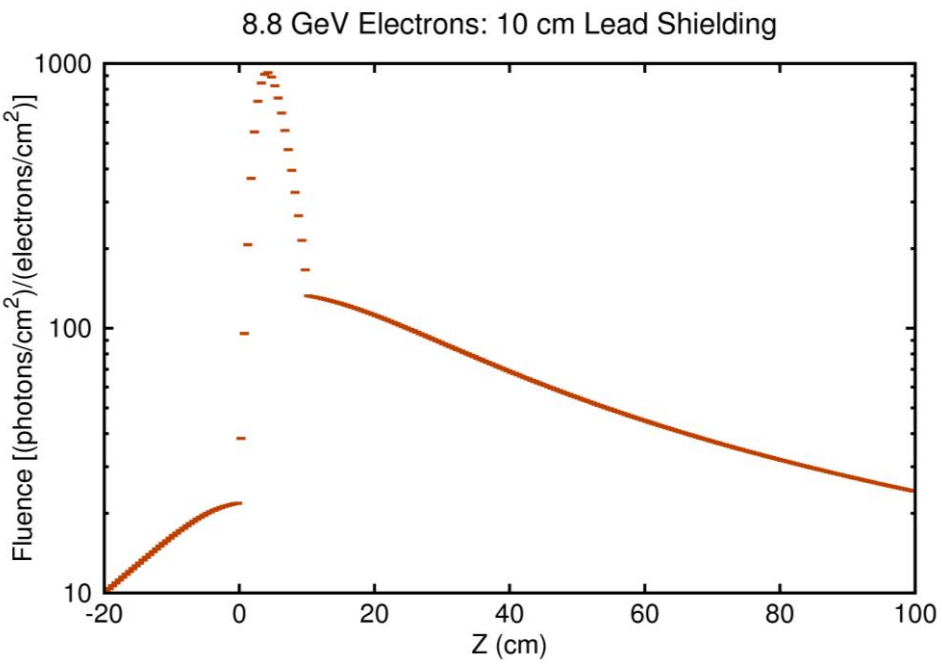

Figure 80. Energy integrated photon fluence as a function of position.

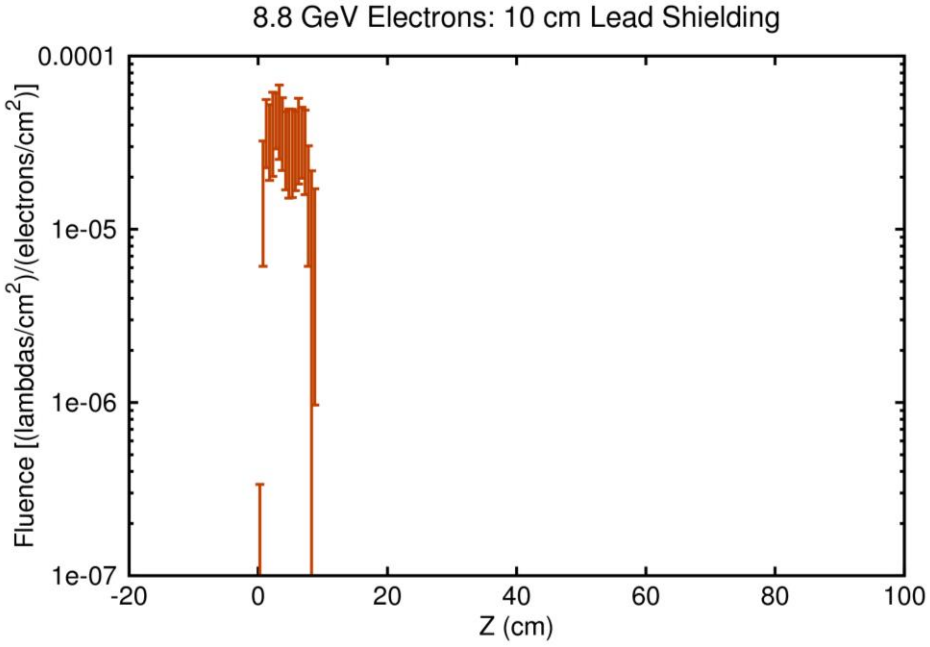

Figure 81. Energy integrated lambda fluence as a function of position.

The fluences shown in Figures 76-81 are integrated over all the secondary particles energies and can be used to calculate the background rates, but, to fully understand the background, it is also important to know the secondary particles energy spectra. In Figures 82-86 the isolethargic spectra are shown for the secondary particles produced by the shielding in forward and backward directions. The reason for using isolethatrgic spectra is that the dynamic range of the energies of the secondary particles requires a logarithmic energy scale. For such a scale the area under the isolethargic spectrum curve is proportional to number of particles in a particular energy interval.

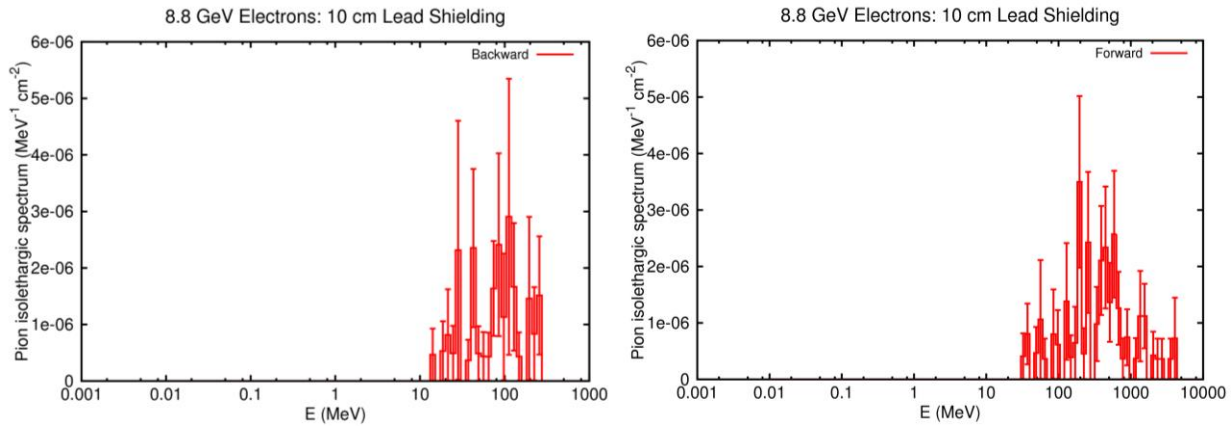

Figure 82. Pion isolethargic spectrum for backward and forward produced pions in a 10 cm thick lead shielding.

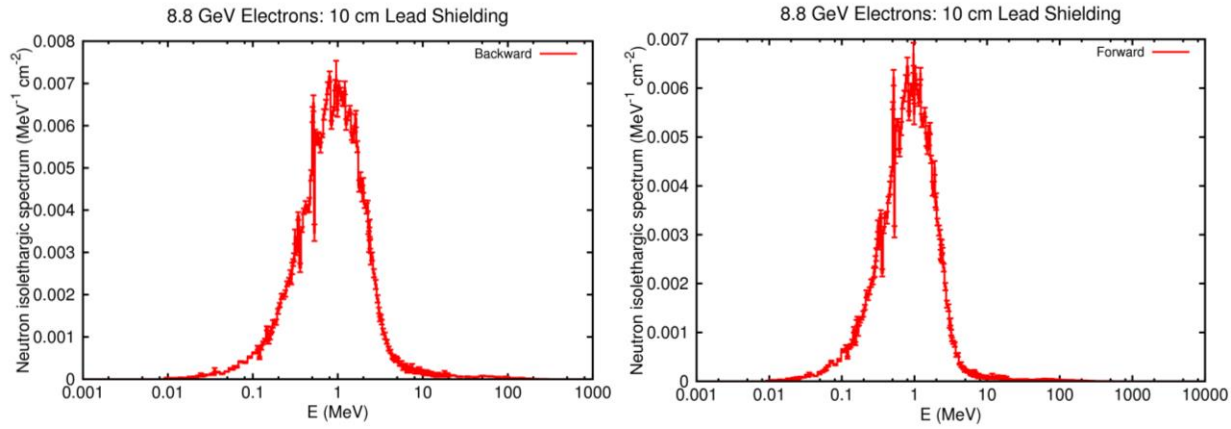

Figure 83. Neutron isolethargic spectrum for backward and forward produced neutrons in a 10 cm thick lead shielding.

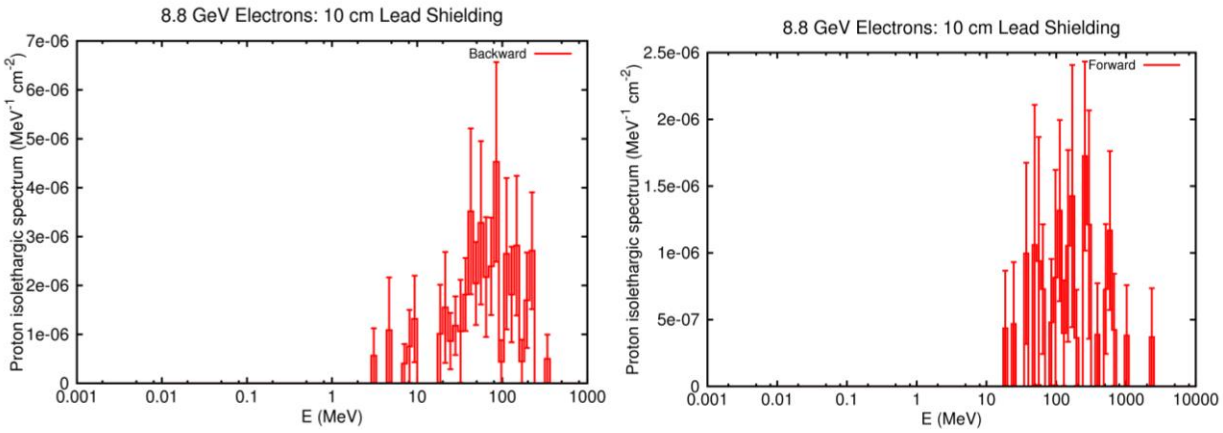

Figure 84. Proton isolethargic spectrum for backward and forward produced protons in a 10 cm thick lead shielding.

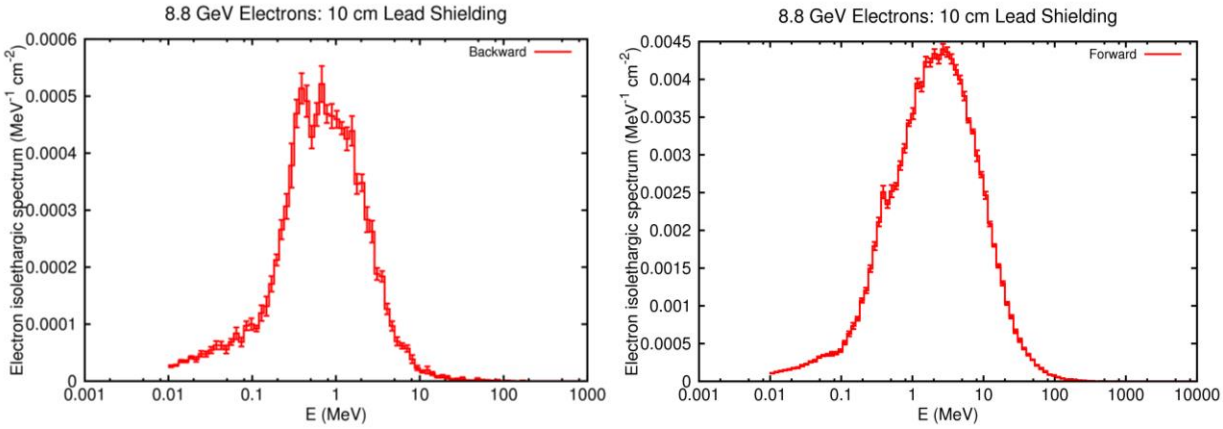

Figure 85. Electron isolethargic spectrum for backward and forward produced electrons in a 10 cm thick lead shielding.

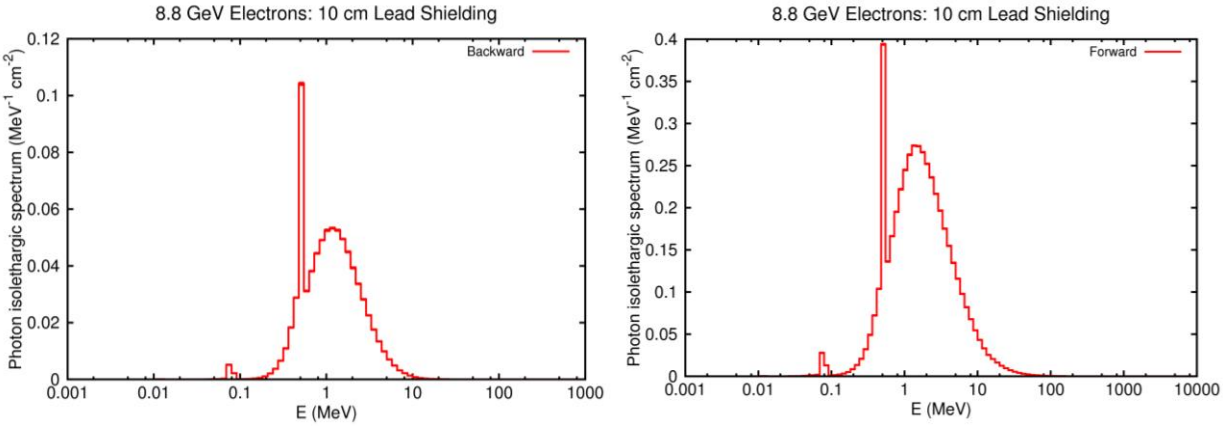

Figure 86. Photon isolethargic spectrum for backward and forward produced photons in a 10 cm thick lead shielding.

IV. Results for 20 cm thick lead shielding

In this section we study the effects of pions and electrons impinging on a 20 cm x 20 cm x 20 cm lead block. In addition to the total deposited energy in the block, the fluences of pions, muons, neutrons, protons, electrons, photons, lambdas and sigma- are also calculated in units of number of particles per cm^2 normalized to number of incoming particles per cm^2. With such a choice of units one only needs to multiply shown fluences with primary particles rates (which can be calculated separately) to get the fluences expected in the Moller experiment. In the simulation the cutoff energy threshold for all the particles was 10^{-5} GeV, except for the neutrons where the cutoff threshold was 10^{-8} GeV.

In the case of the pions, the total deposited energy is shown in Figure 87 in units of MeV/cm^3. The average deposited energy in the entire lead block was 2750 MeV per incoming pion. The fluences integrated over all the secondary particles energies are shown in Figures 88-95 and Figures 96-103.

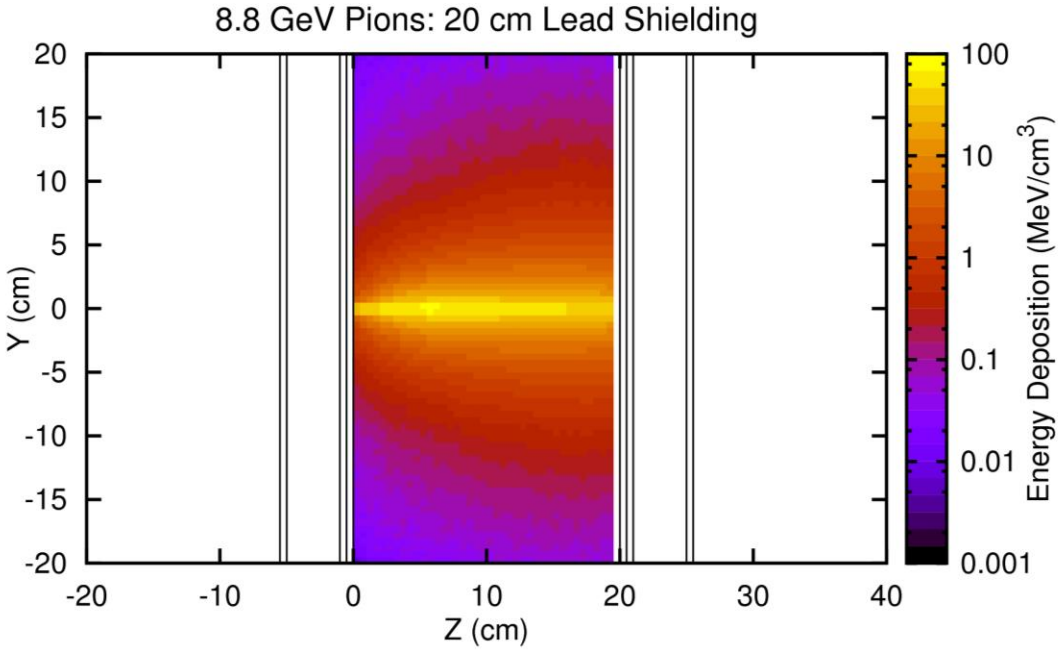

Figure 87. Total deposited energy in the 20 cm thick lead block per incoming 8.8 GeV pion.

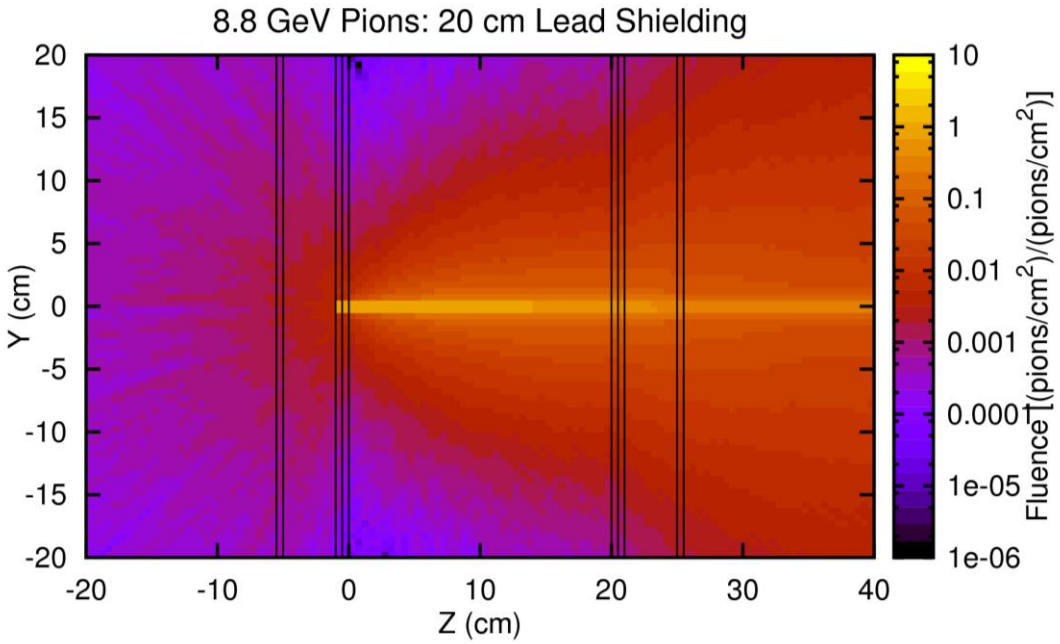

Figure 88. Pion fluence in the case of the 20 cm thick lead block per incoming 8.8 GeV pion.

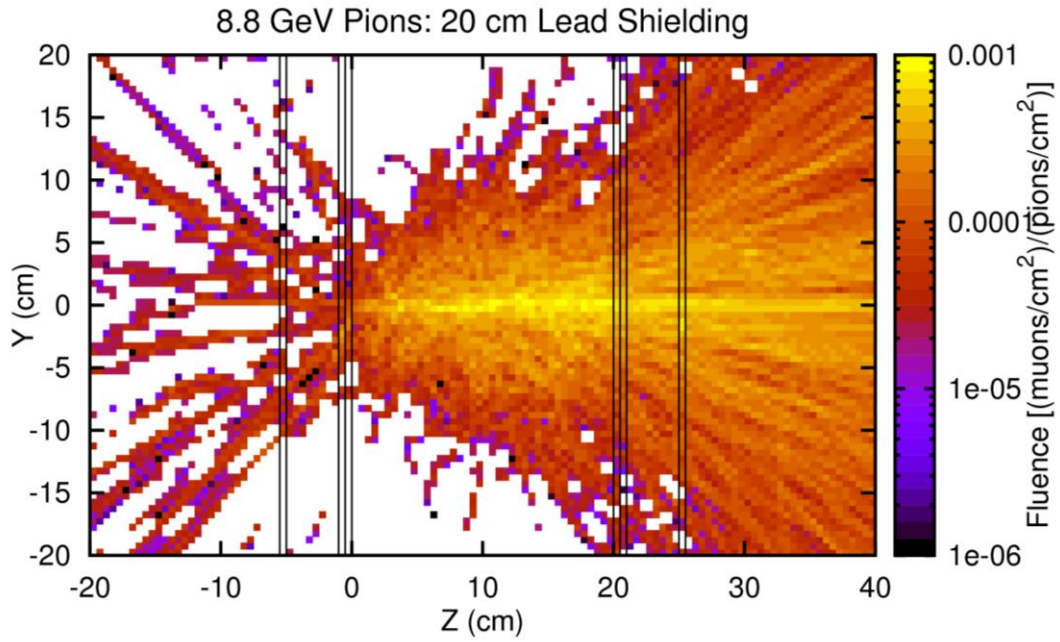

Figure 89. Muon fluence in the case of the 20 cm thick lead block per incoming 8.8 GeV pion.

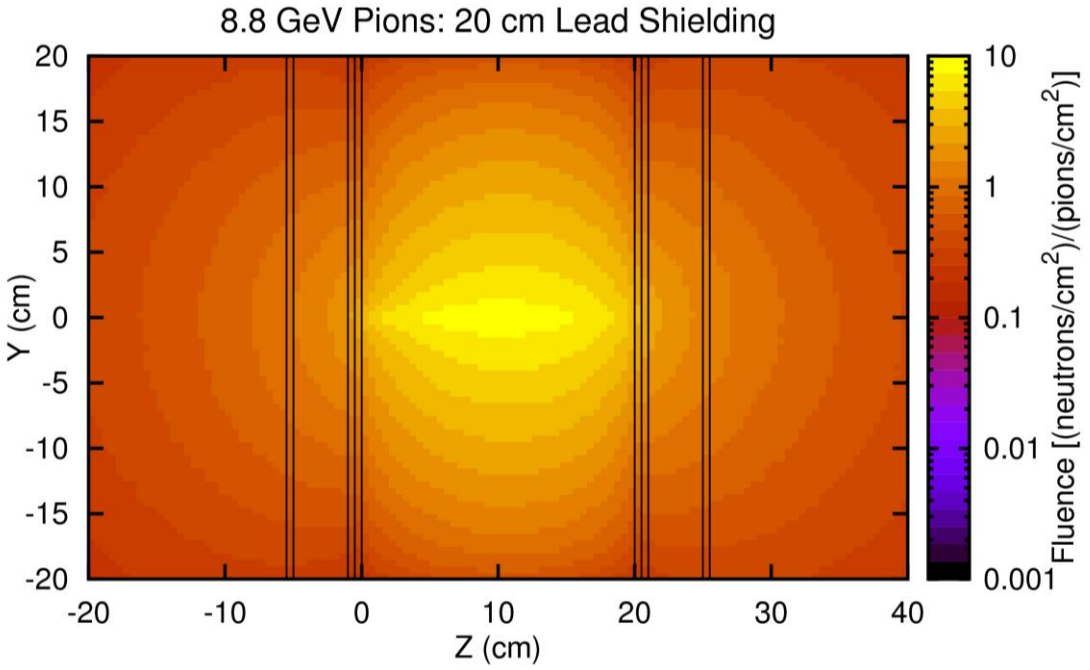

Figure 90. Neutron fluence in the case of the 20 cm thick lead block per incoming 8.8 GeV pion.

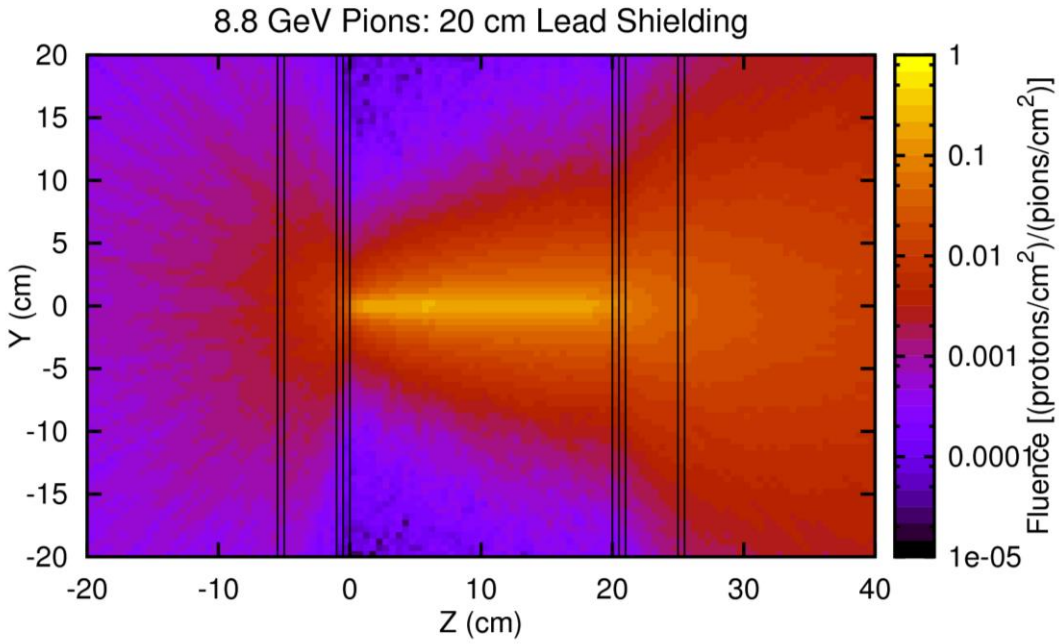

Figure 91. Proton fluence in the case of the 20 cm thick lead block per incoming 8.8 GeV pion.

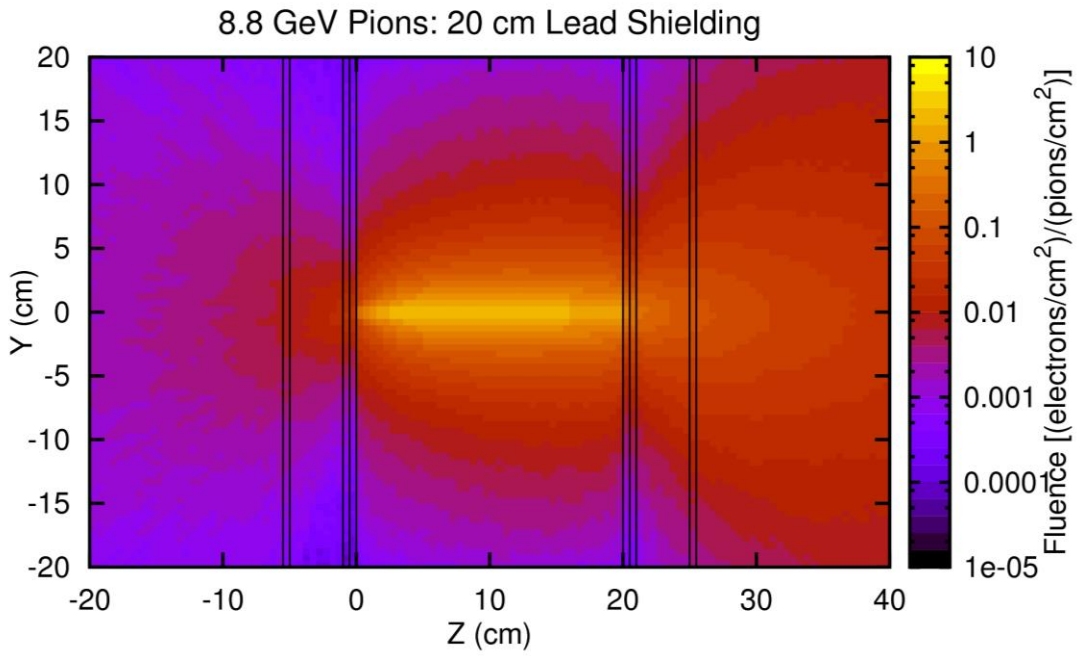

Figure 92. Electron fluence in the case of the 20 cm thick lead block per incoming 8.8 GeV pion.

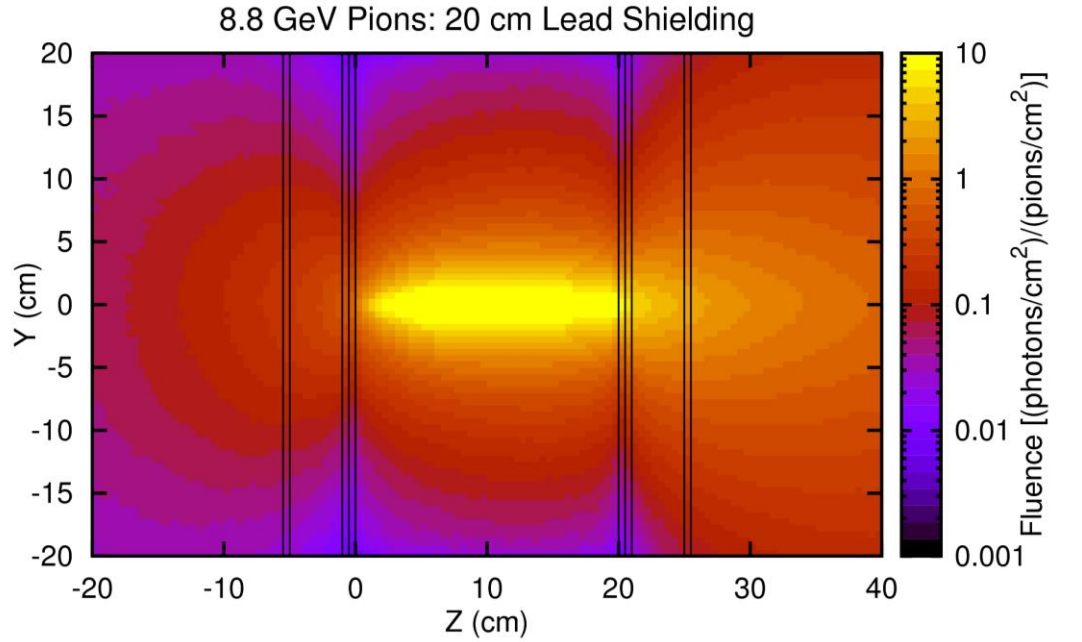

Figure 93. Photon fluence in the case of the 20 cm thick lead block per incoming 8.8 GeV pion.

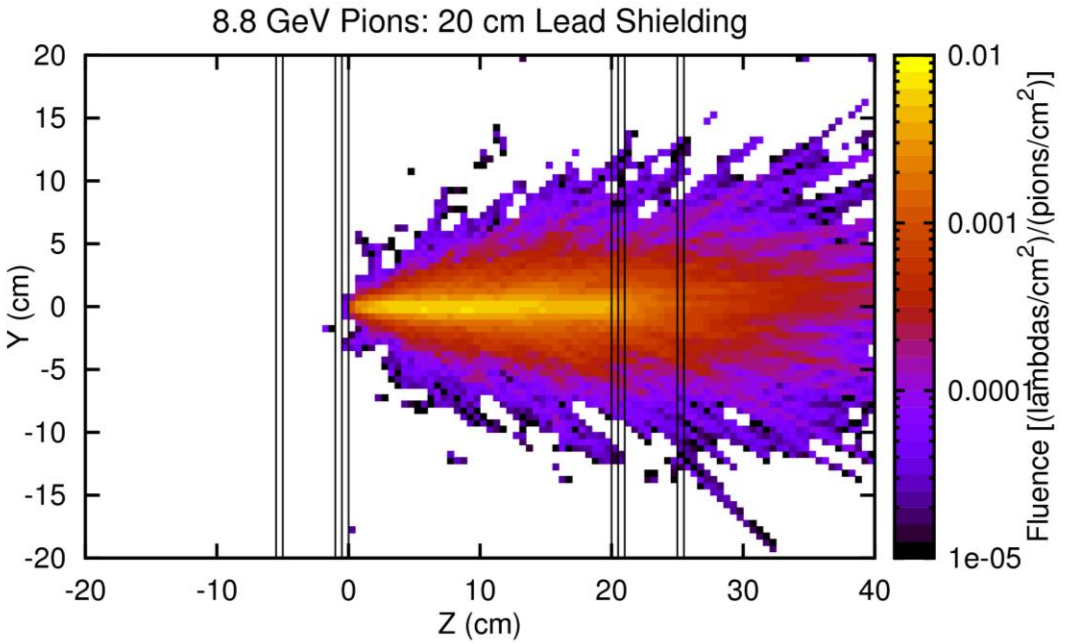

Figure 94. Lambda fluence in the case of the 20 cm thick lead block per incoming 8.8 GeV pion.

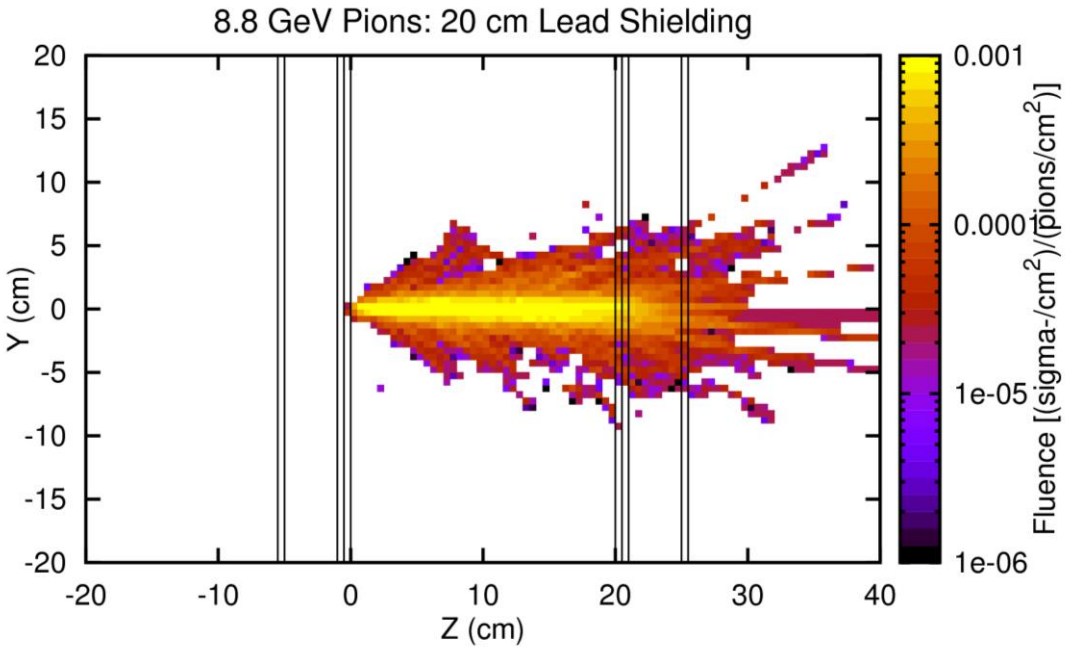

Figure 95. Sigma- fluence in the case of the 20 cm thick lead block per incoming 8.8 GeV pion.

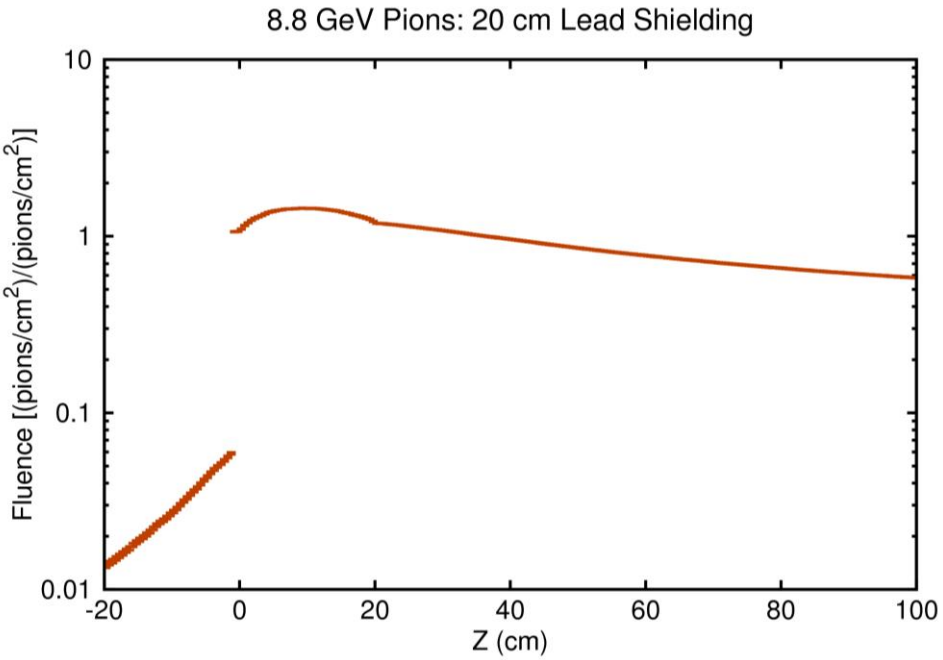

Figure 96. Energy integrated pion fluence as a function of position.

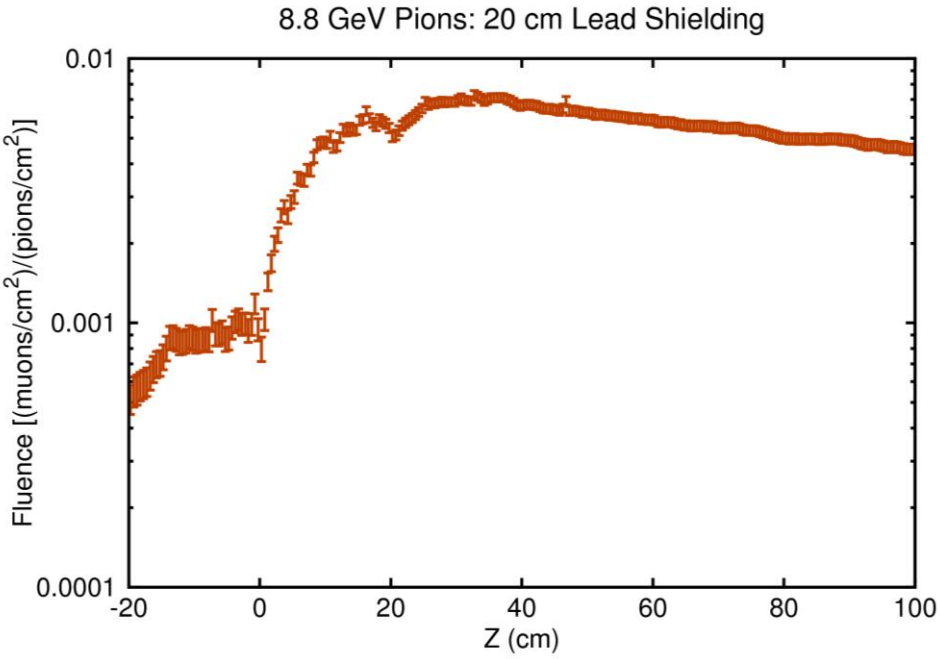

Figure 97. Energy integrated muon fluence as a function of position.

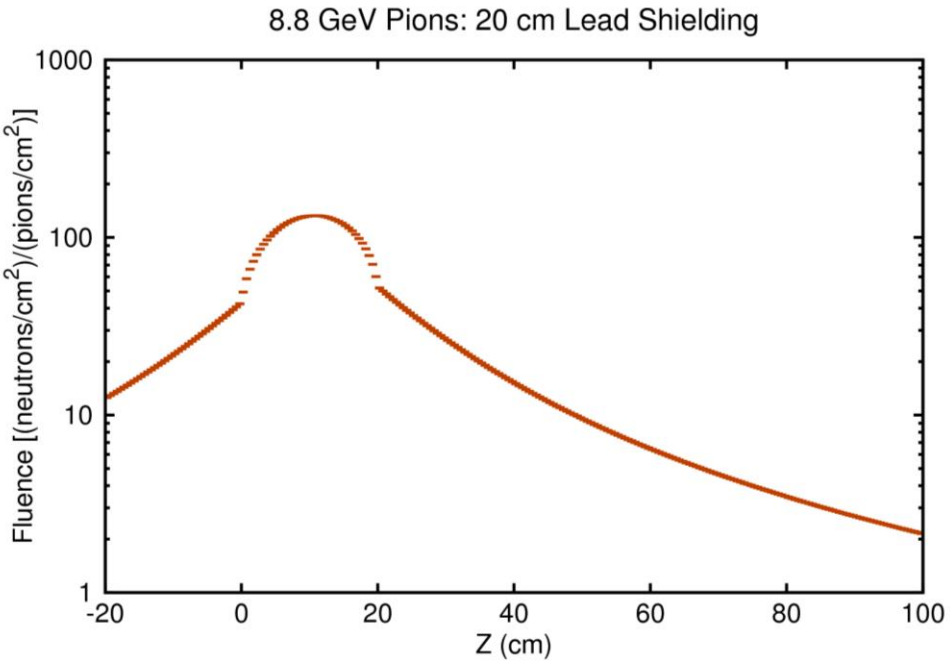

Figure 98. Energy integrated neutron fluence as a function of position.

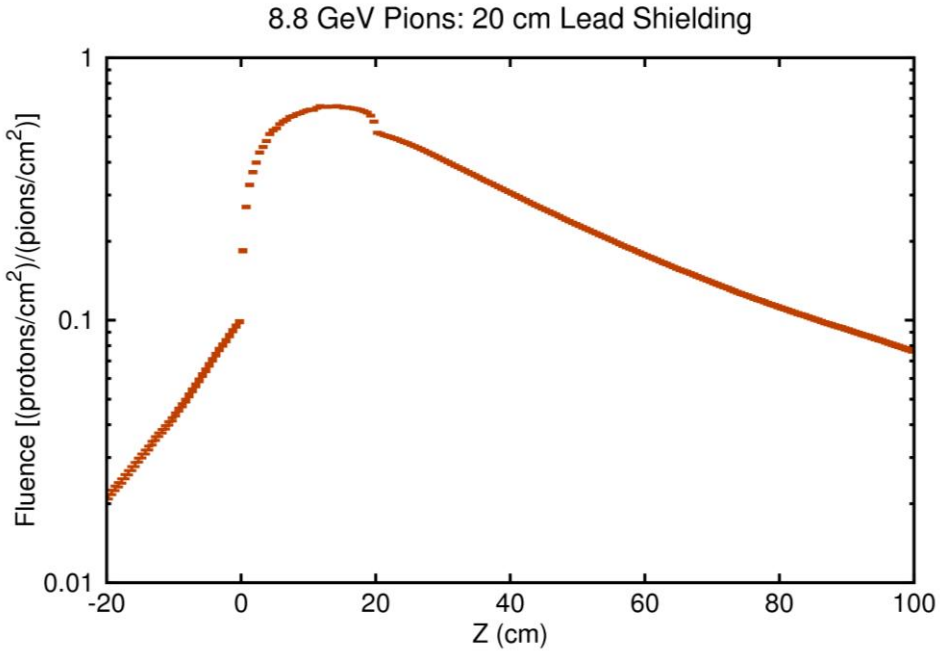

Figure 99. Energy integrated proton fluence as a function of position.

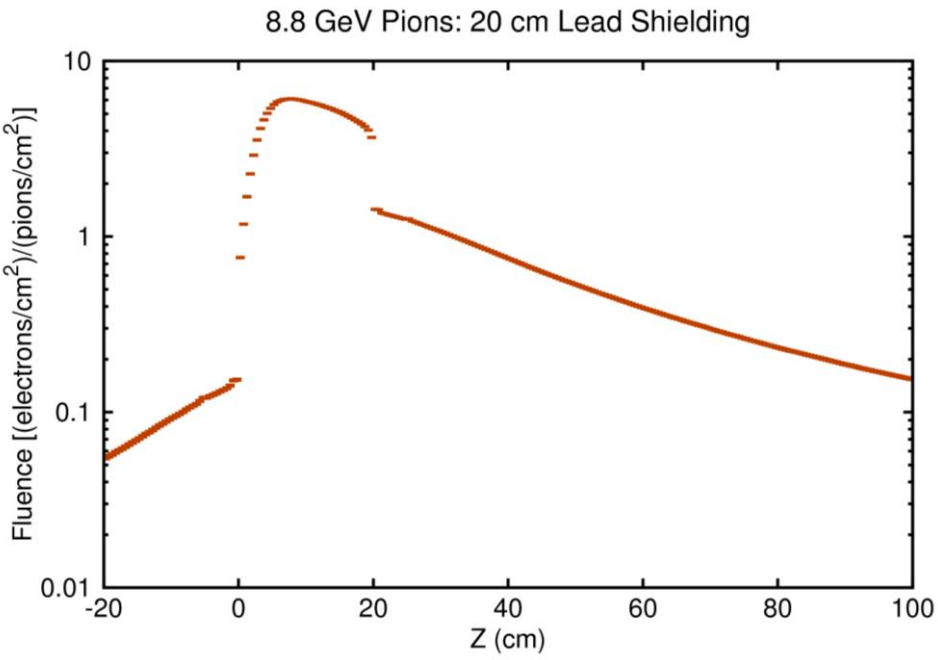

Figure 100. Energy integrated electron fluence as a function of position.

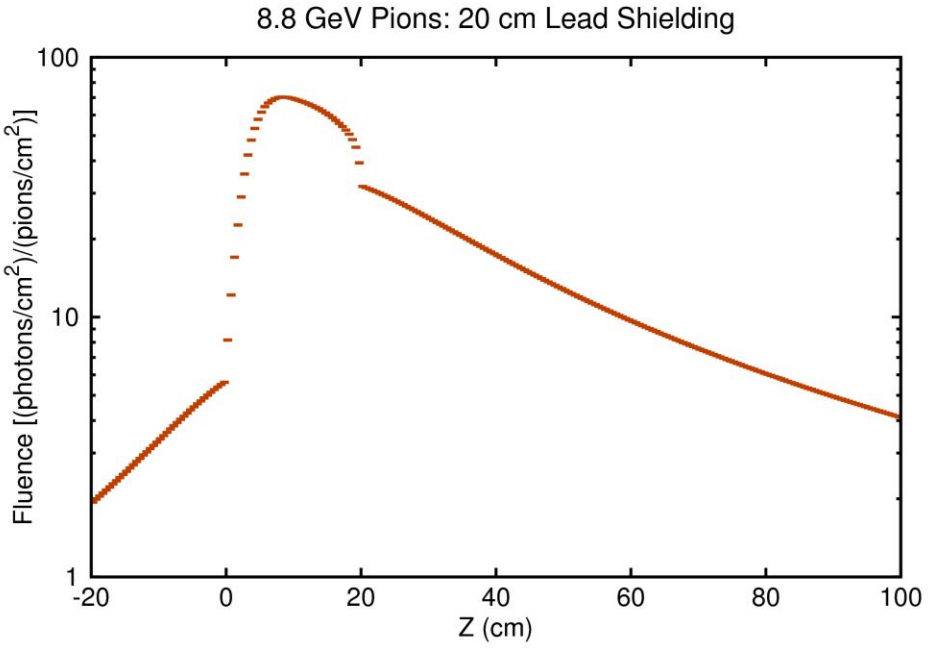

Figure 101. Energy integrated photon fluence as a function of position.

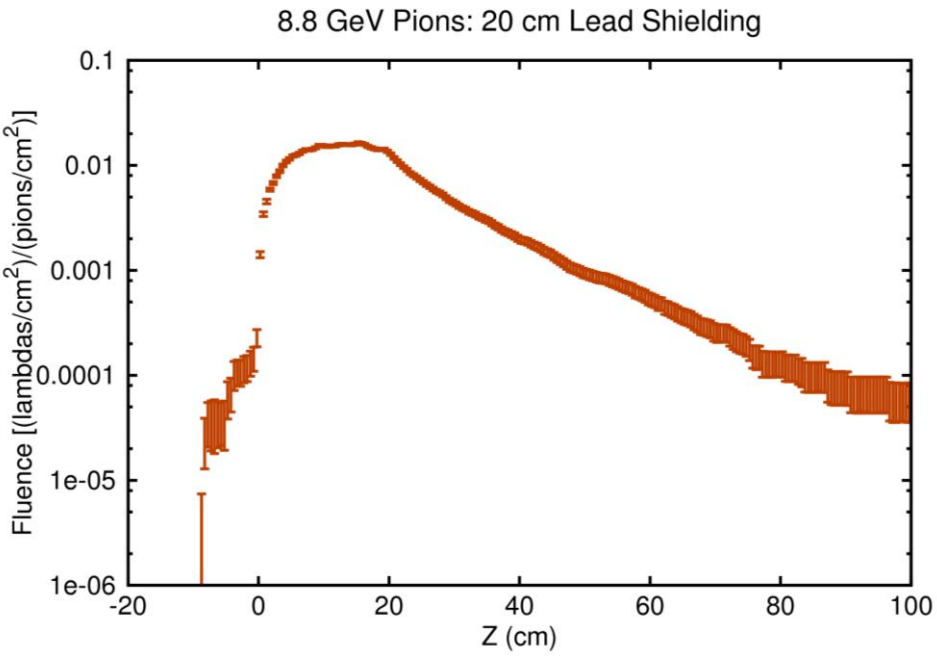

Figure 102. Energy integrated lambda fluence as a function of position.

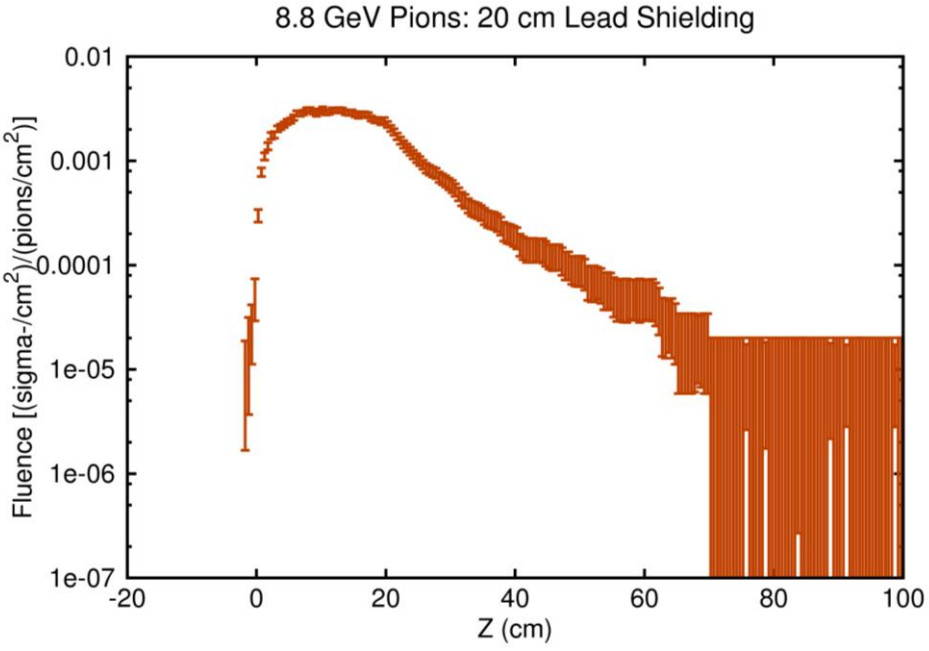

Figure 103. Energy integrated sigma- fluence as a function of position.

The fluences shown in Figures 96-103 are integrated over all the secondary particles energies and can be used to calculate the background rates, but, to fully understand the background, it is also important to know the secondary particles energy spectra. In Figures 104-111 the isolethargic spectra are shown for the secondary particles produced by the shielding in forward and backward directions. The reason for using isolethatrgic spectra is that the dynamic range of the energies of the secondary particles requires a logarithmic energy scale. For such a scale the area under the isolethargic spectrum curve is proportional to the number of particles in a particular energy interval.

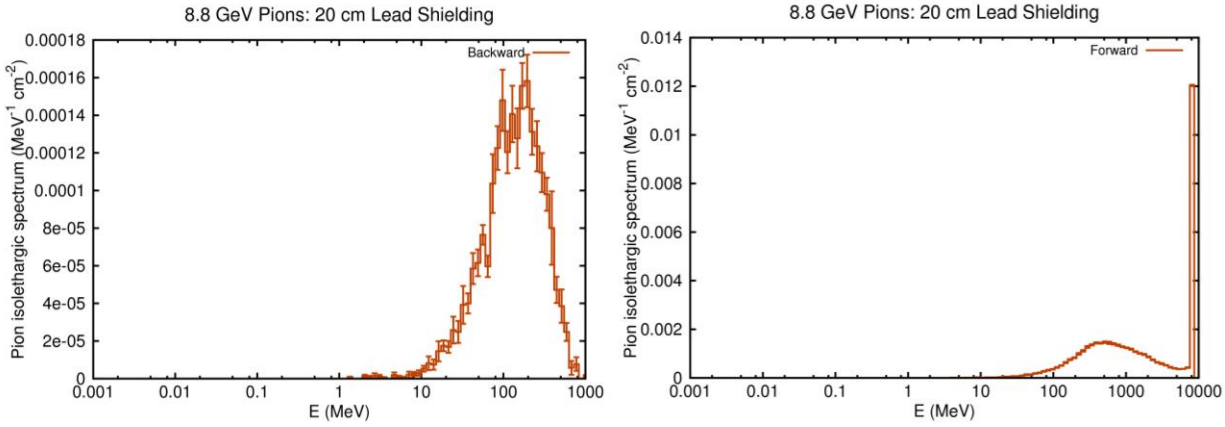

Figure 104. Pion isolethargic spectrum for backward and forward produced pions in a 20 cm thick lead shielding.

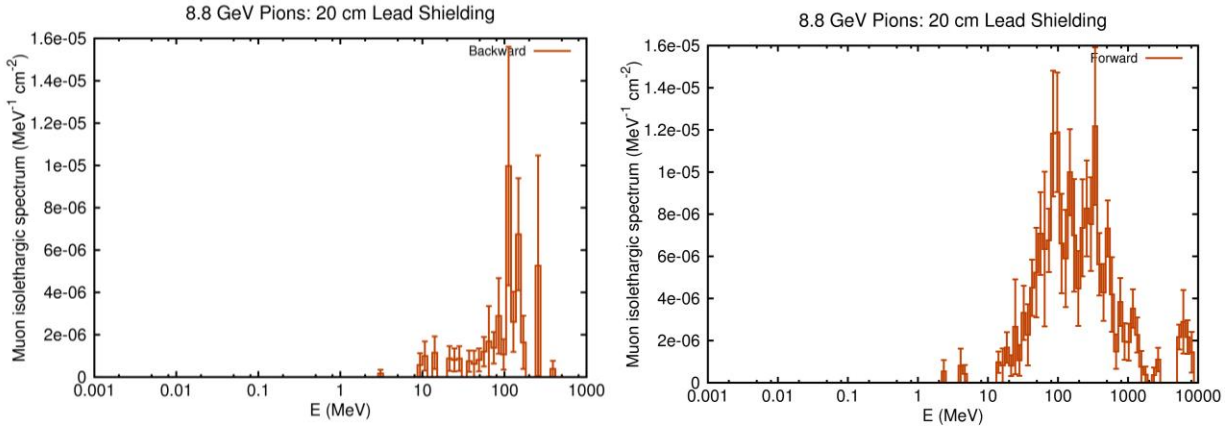

Figure 105. Muon isolethargic spectrum for backward and forward produced muons in a 20 cm thick lead shielding.

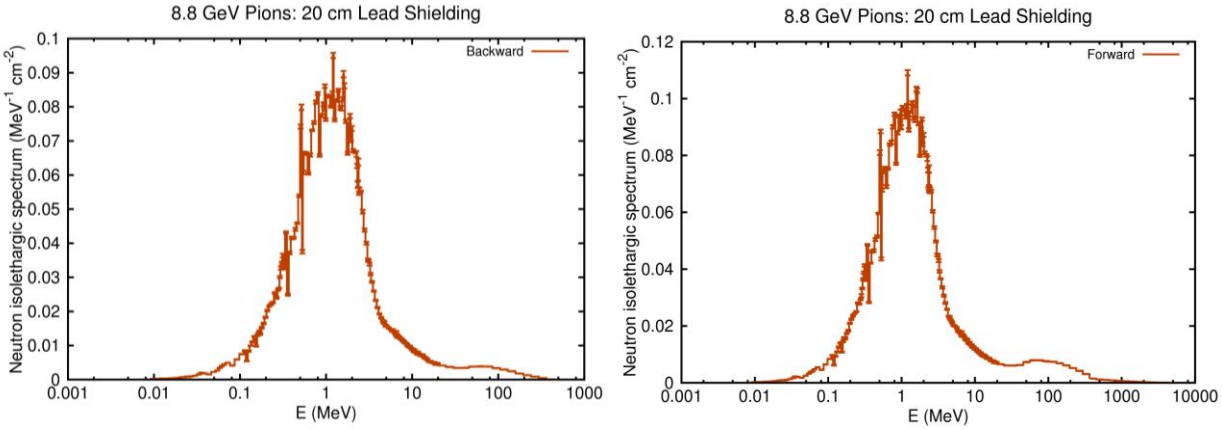

Figure 106. Neutron isolethargic spectrum for backward and forward produced neutrons in a 20 cm thick lead shielding.

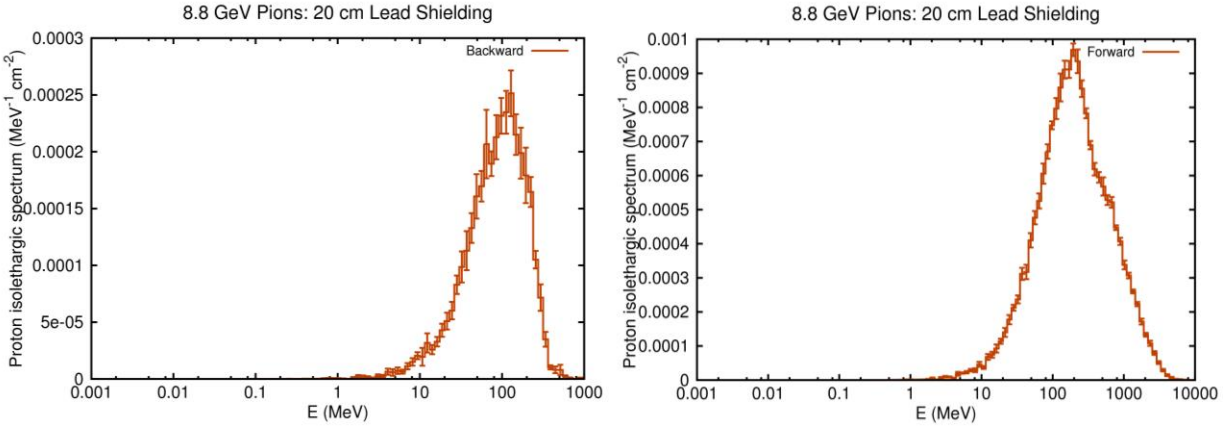

Figure 107. Proton isolethargic spectrum for backward and forward produced protons in a 20 cm thick lead shielding.

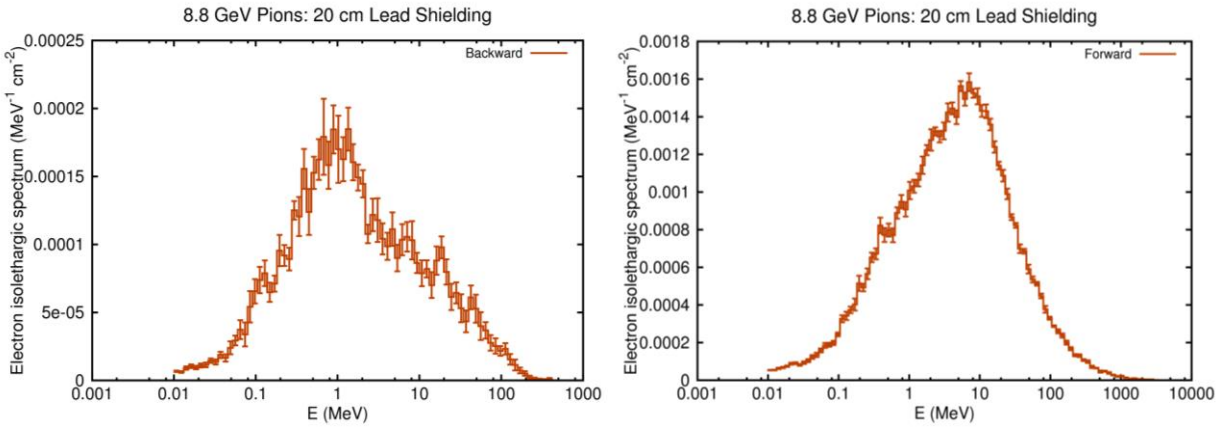

Figure 108. Electron isolethargic spectrum for backward and forward produced electrons in a 20 cm thick lead shielding.

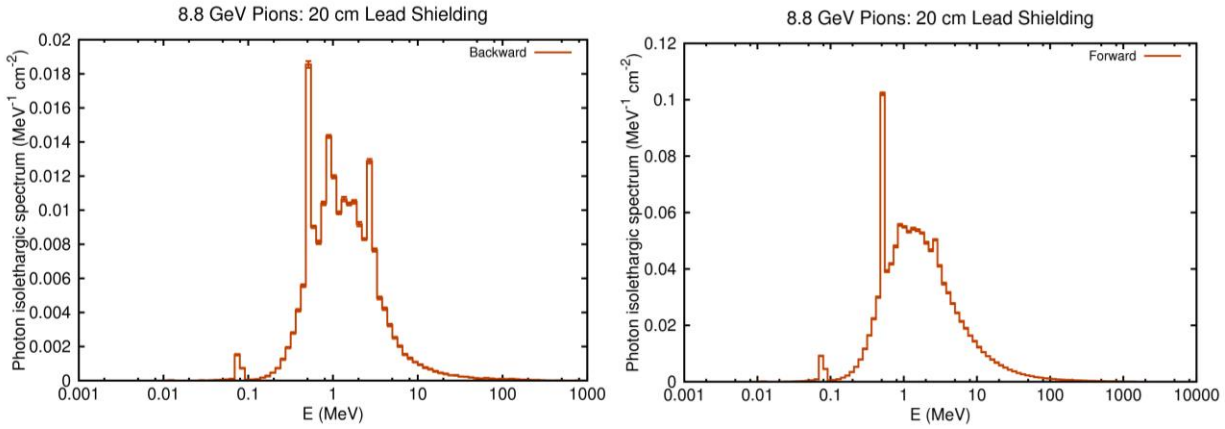

Figure 109. Photon isolethargic spectrum for backward and forward produced photons in a 20 cm thick lead shielding.

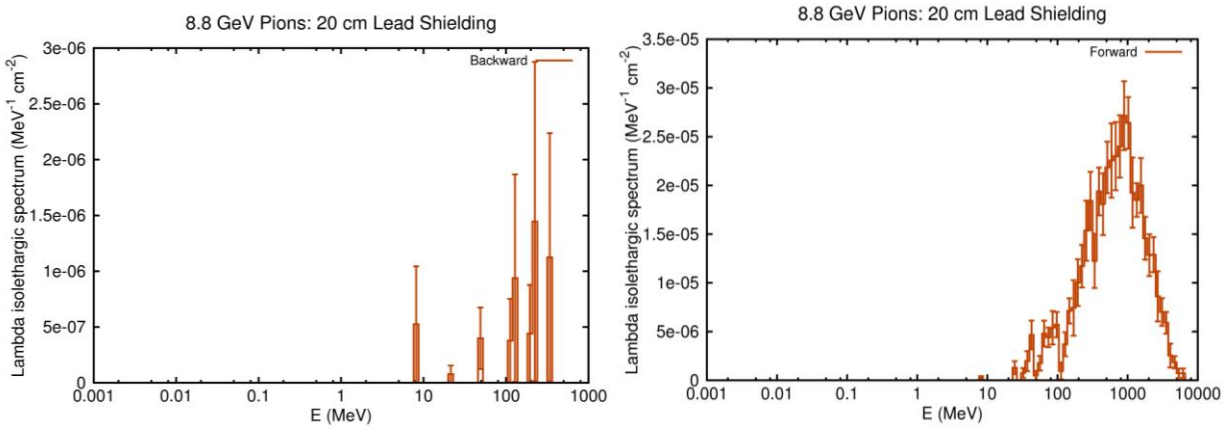

Figure 110. Lambda isolethargic spectrum for backward and forward produced lambdas in a 20 cm thick lead shielding.

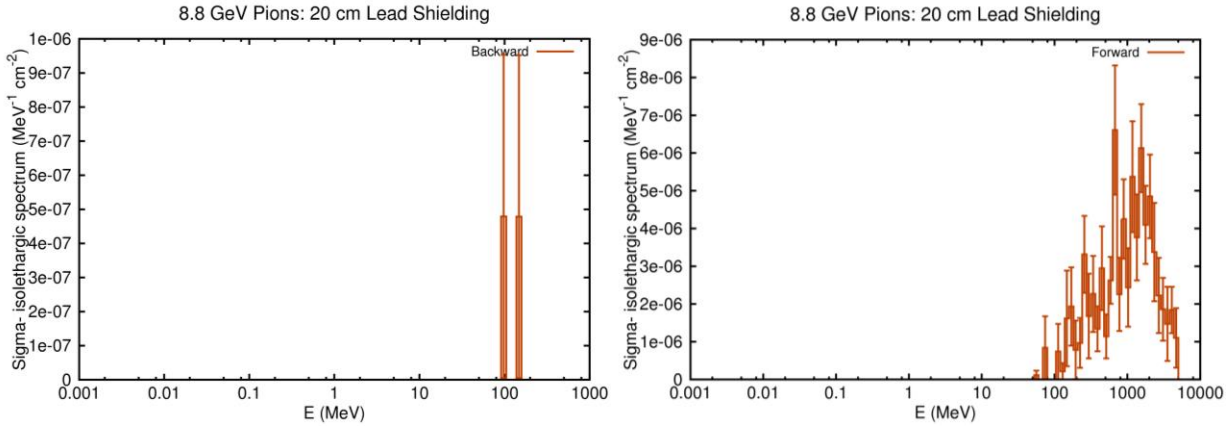

Figure 111. Sigma- isolethargic spectrum for backward and forward produced sigma- in a 20 cm thick lead shielding.

In the case of the electrons, the total deposited energy is shown in Figure 112 in units of MeV/cm^3. The average deposited energy in the entire lead block was 8750 MeV per incoming electron. The fluences integrated over all secondary particles energies are shown in Figures 113-117 and Figures 118-123.

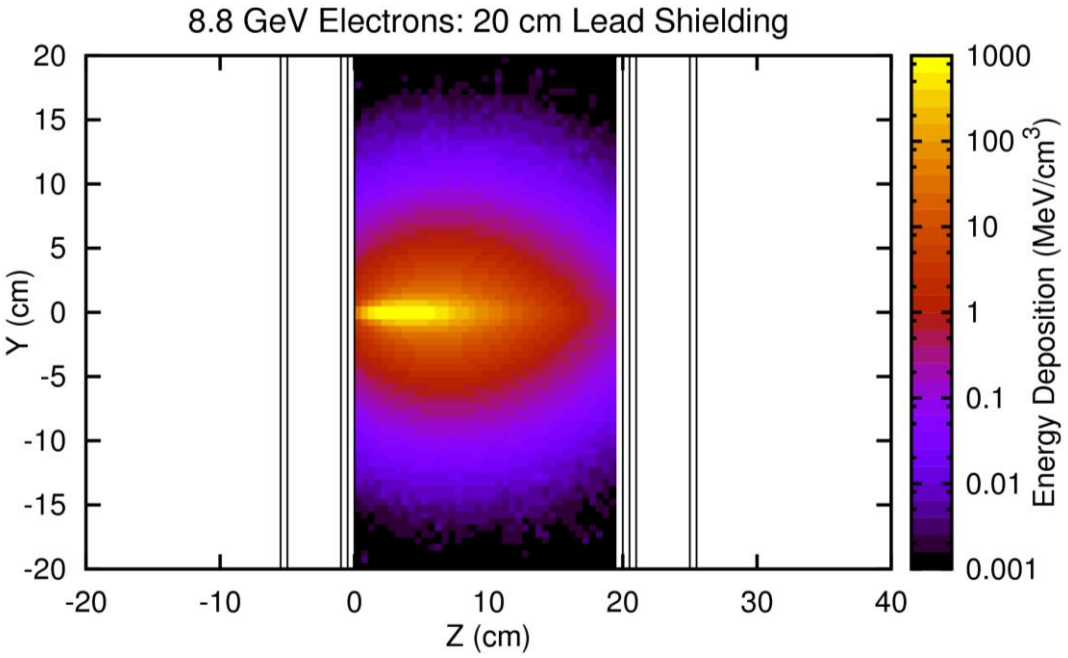

Figure 112. Total deposited energy in the 20 cm thick lead block per incoming 8.8 GeV electron.

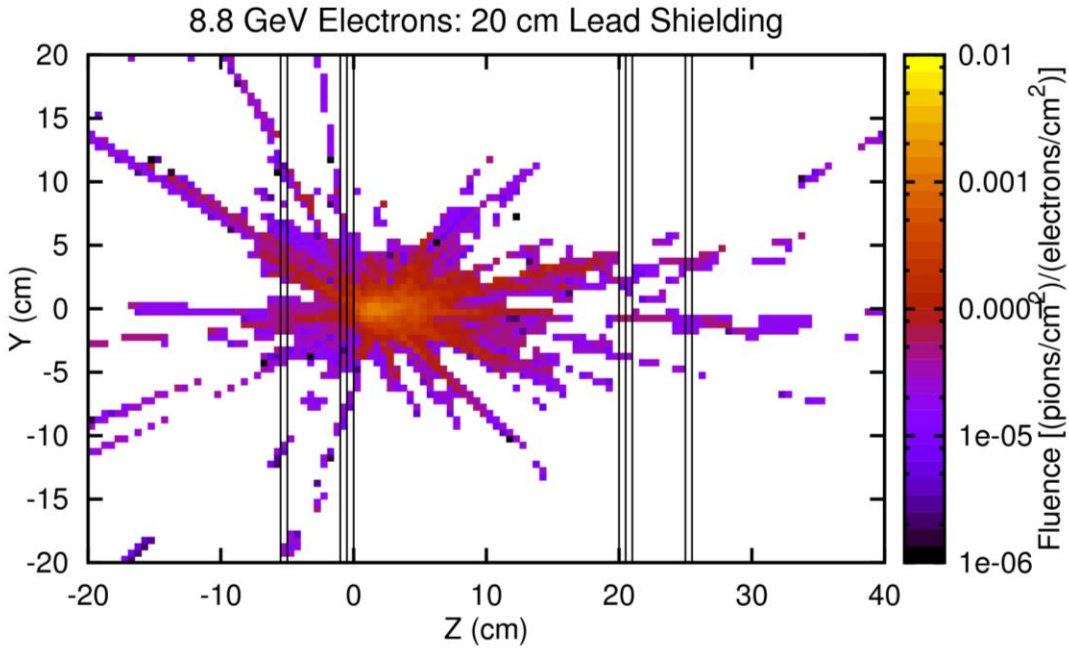

Figure 113. Pion fluence in the case of the 20 cm thick lead block per incoming 8.8 GeV electron.

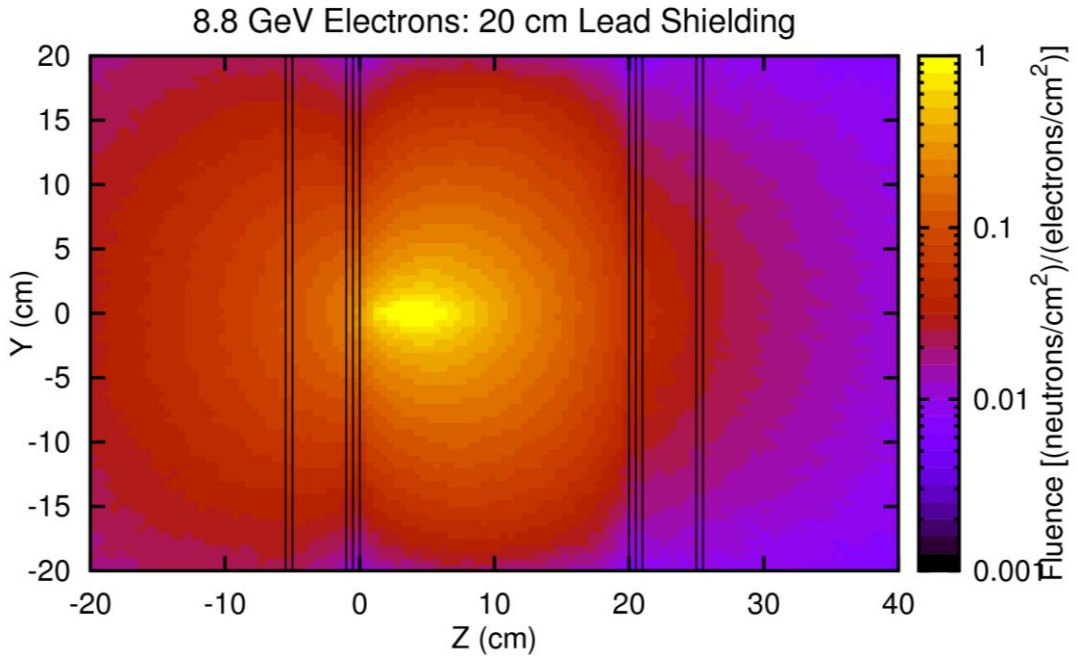

Figure 114. Neutron fluence in the case of the 20 cm thick lead block per incoming 8.8 GeV electron.

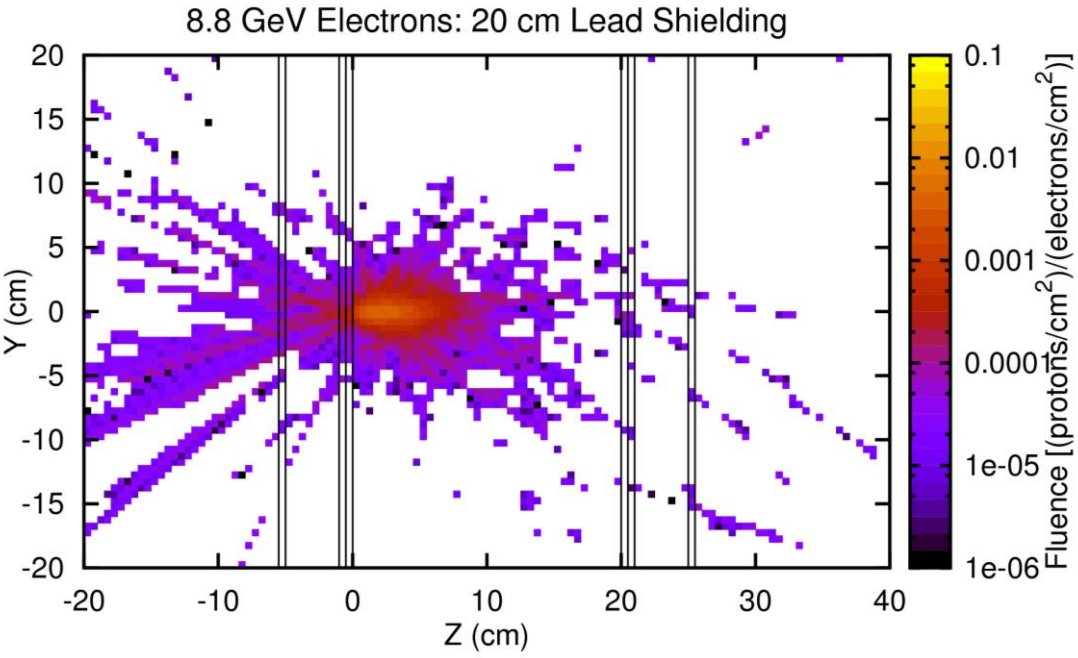

Figure 115. Proton fluence in the case of the 20 cm thick lead block per incoming 8.8 GeV electron.

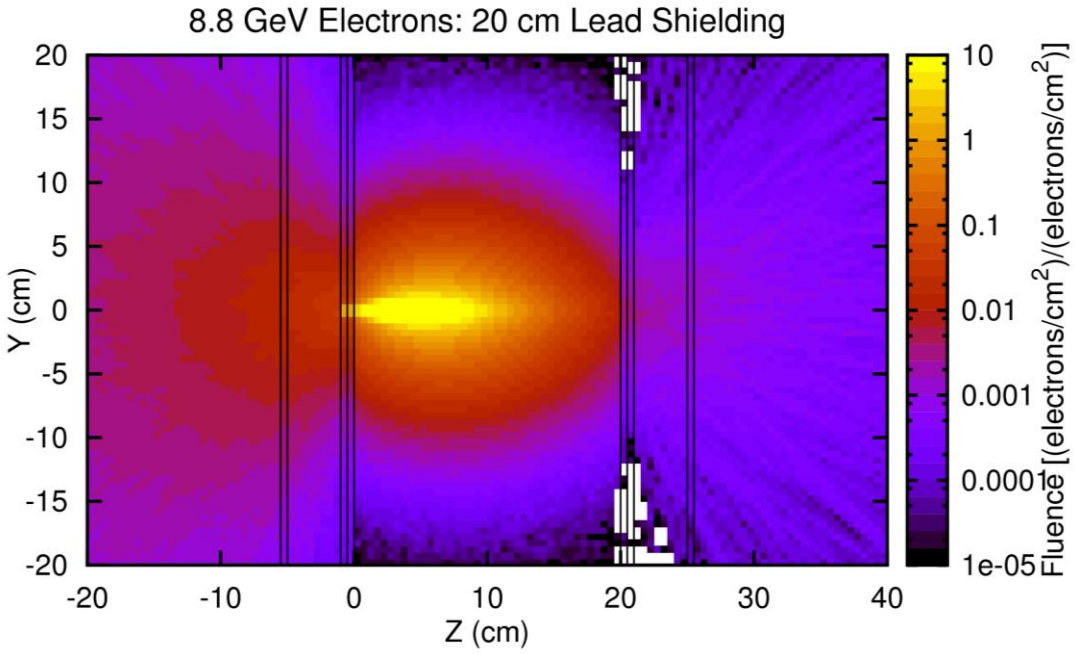

Figure 116. Electron fluence in the case of the 20 cm thick lead block per incoming 8.8 GeV electron.

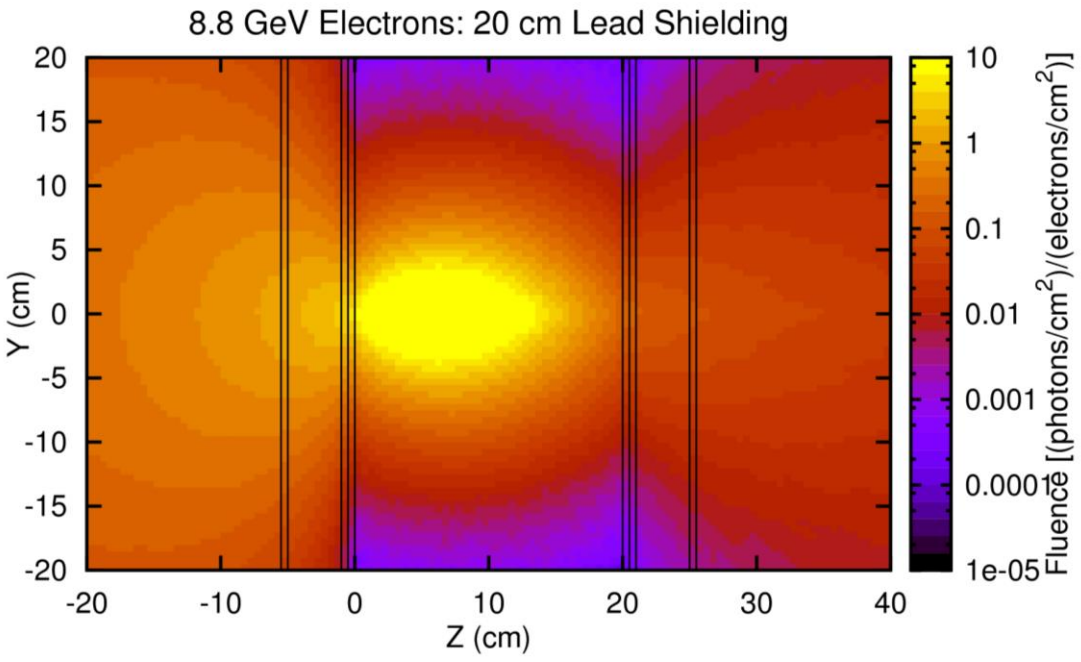

Figure 117. Photon fluence in the case of the 20 cm thick lead block per incoming 8.8 GeV electron.

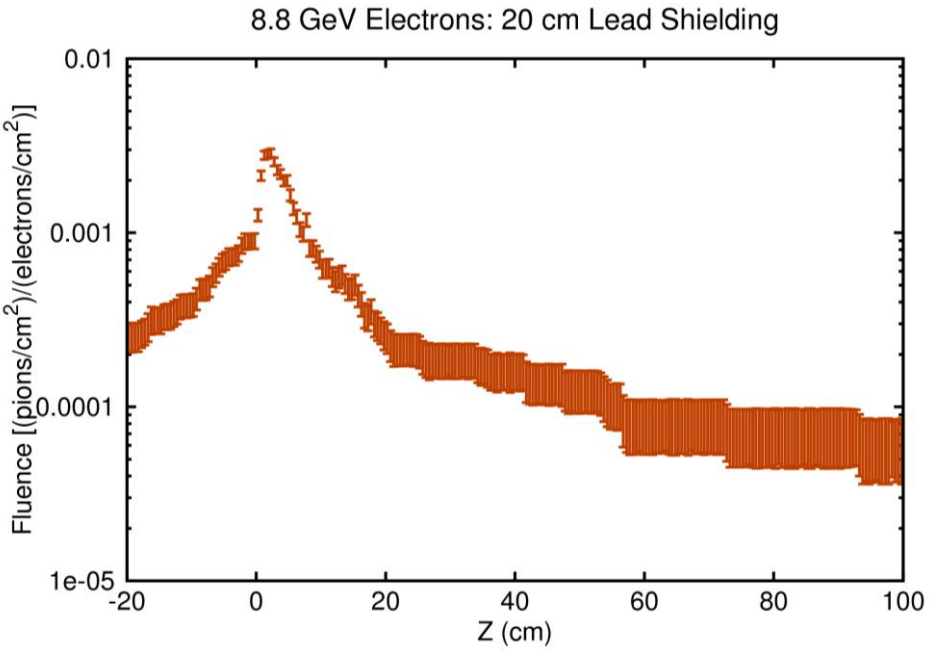

Figure 118. Energy integrated pion fluence as a function of position.

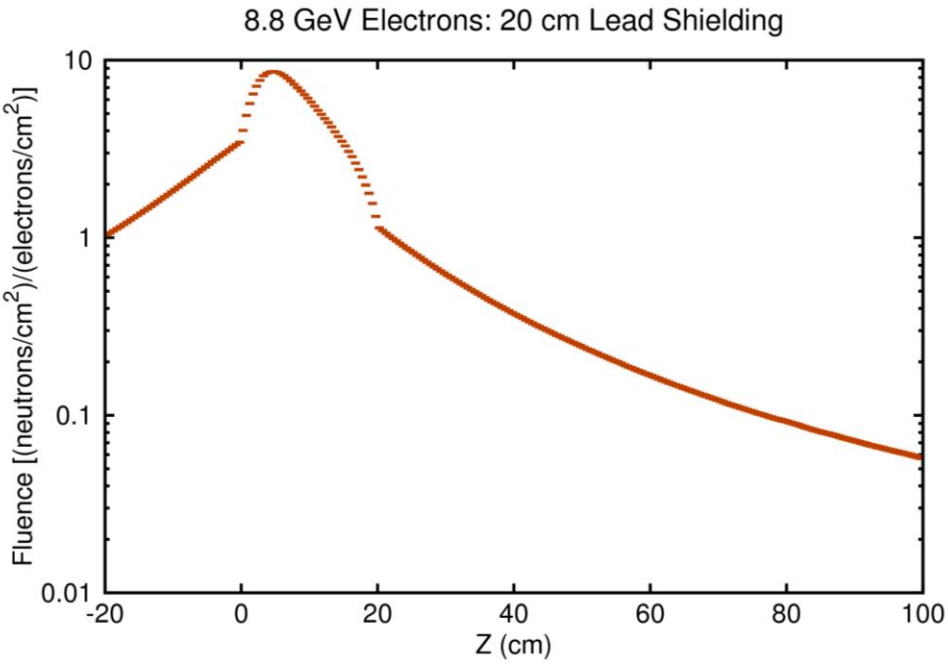

Figure 119. Energy integrated neutron fluence as a function of position.

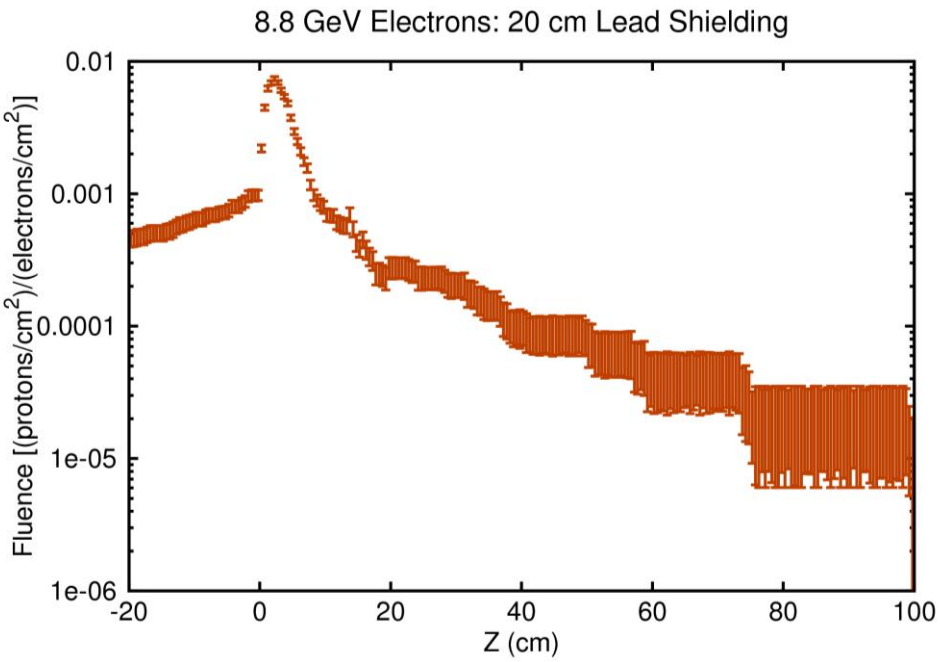

Figure 120. Energy integrated proton fluence as a function of position.

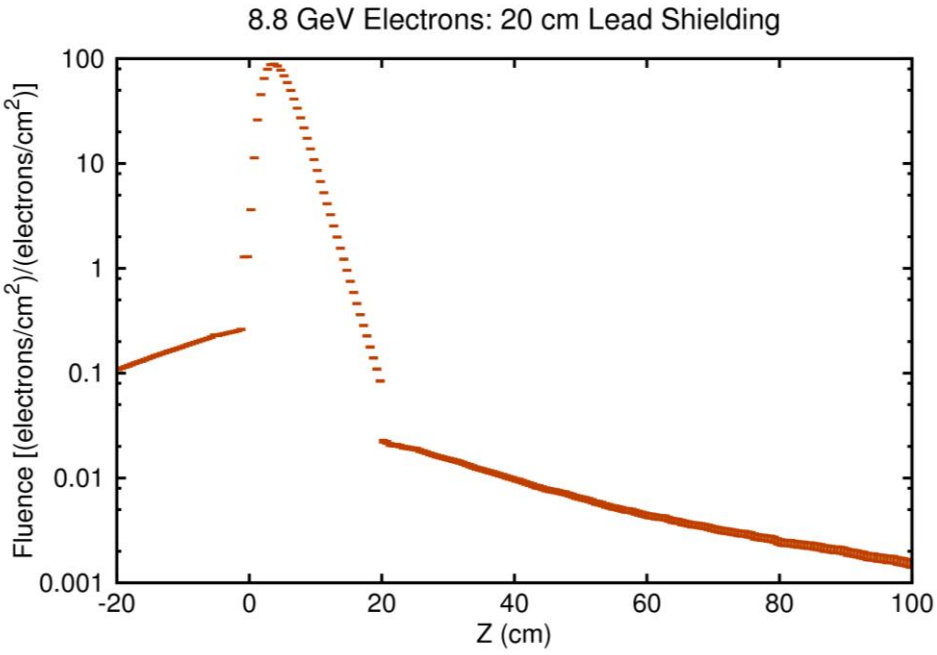

Figure 121. Energy integrated electron fluence as a function of position.

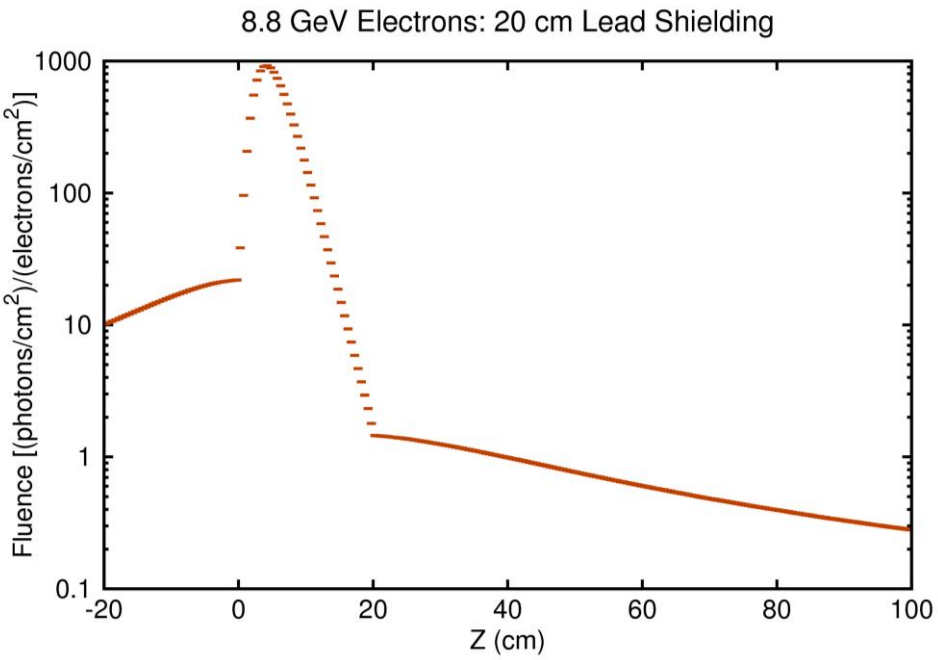

Figure 122. Energy integrated photon fluence as a function of position.

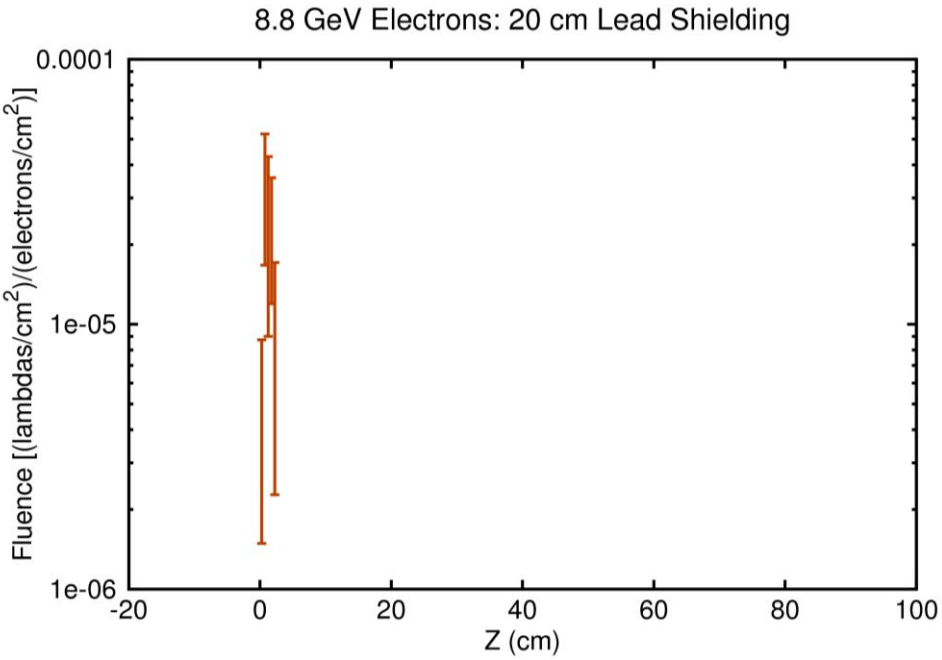

Figure 123. Energy integrated lambda fluence as a function of position.

The fluences shown in Figures 118-123 are integrated over all the secondary particles energies and can be used to calculate the background rates, but, to fully understand the background, it is also important to know the secondary particles energy spectra. In Figures 124-128 the isolethargic spectra are shown for the secondary particles produced by the shielding in forward and backward directions. The reason for using isolethatrgic spectra is that the dynamic range of the energies of the secondary particles requires a logarithmic energy scale. For such a scale the area under the isolethargic spectrum curve is proportional to number of particles in a particular energy interval.

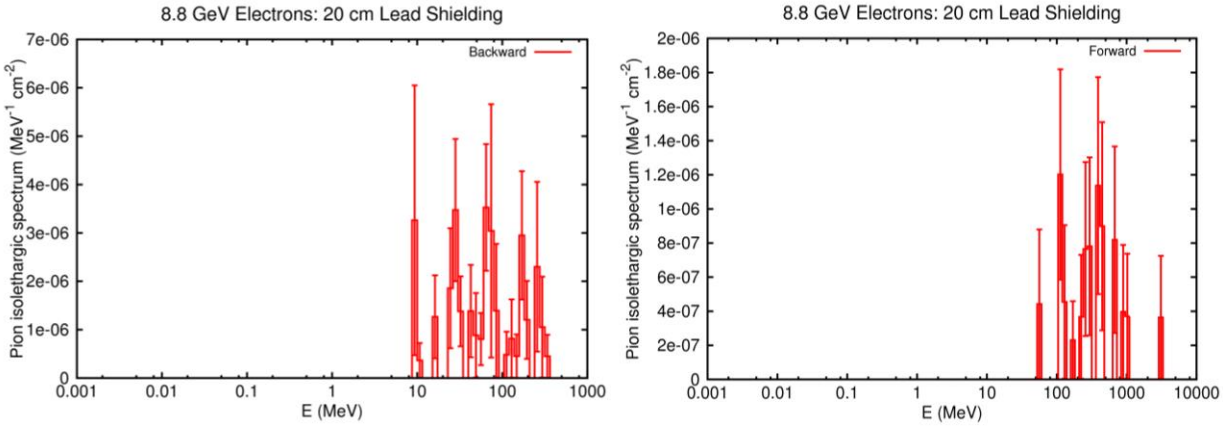

Figure 124. Pion isolethargic spectrum for backward and forward produced pions in a 20 cm thick lead shielding.

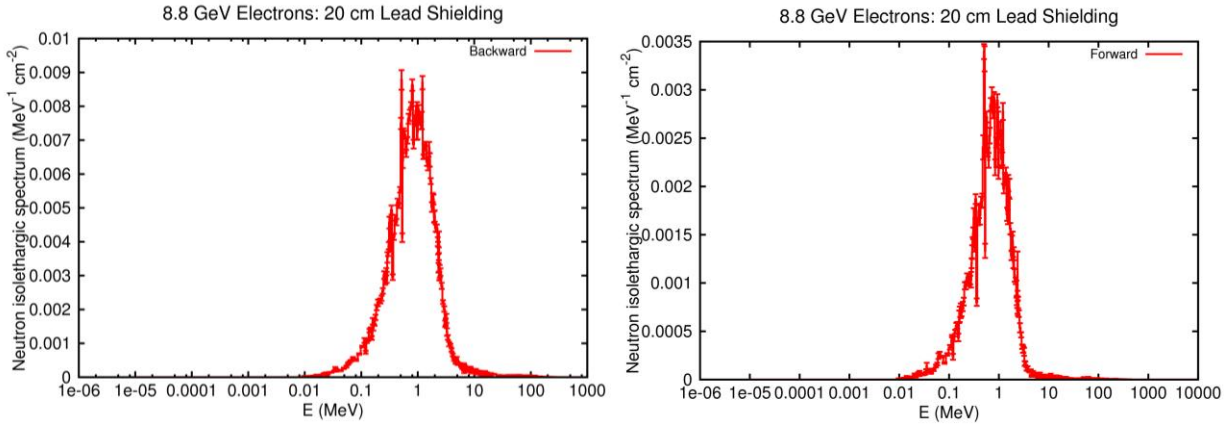

Figure 125. Neutron isolethargic spectrum for backward and forward produced neutrons in a 20 cm thick lead shielding.

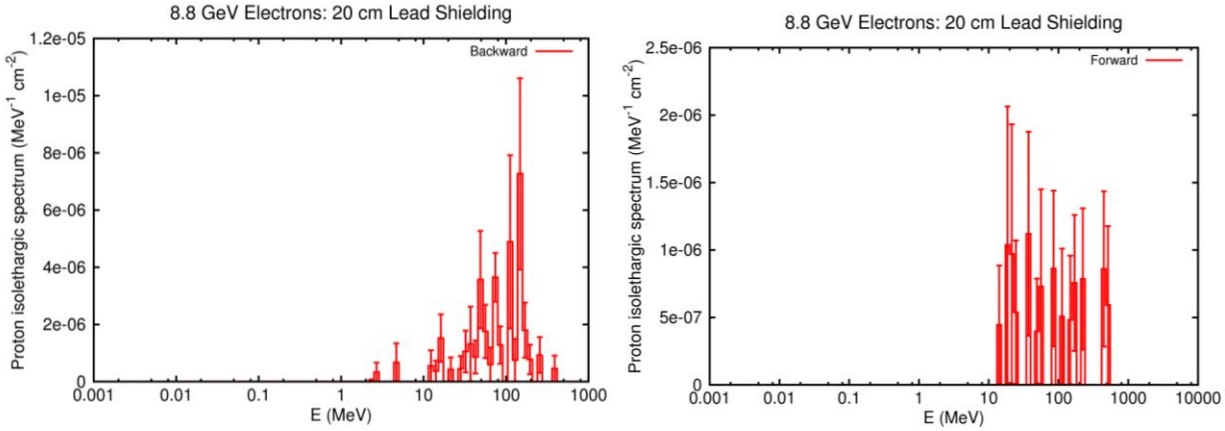

Figure 126. Proton isolethargic spectrum for backward and forward produced protons in a 20 cm thick lead shielding.

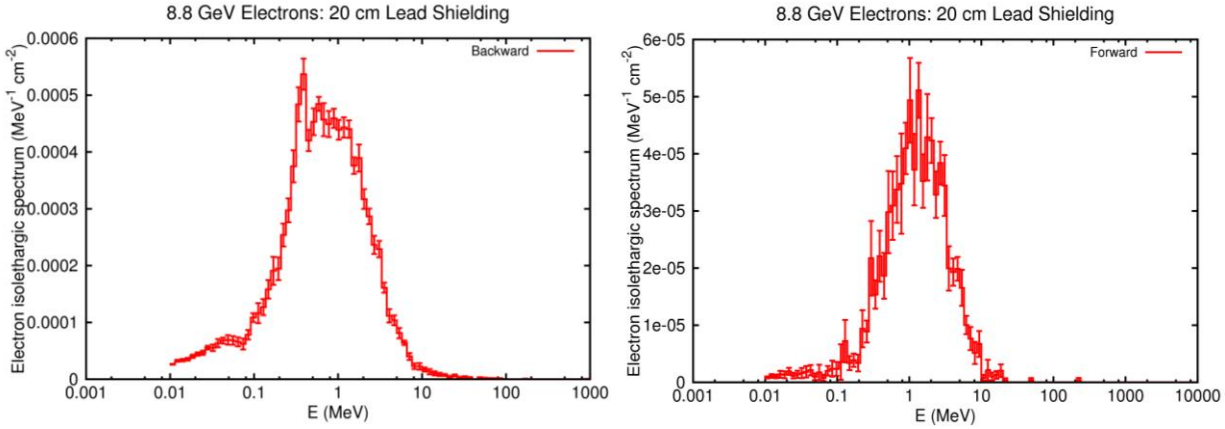

Figure 127. Electron isolethargic spectrum for backward and forward produced electrons in a 20 cm thick lead shielding.

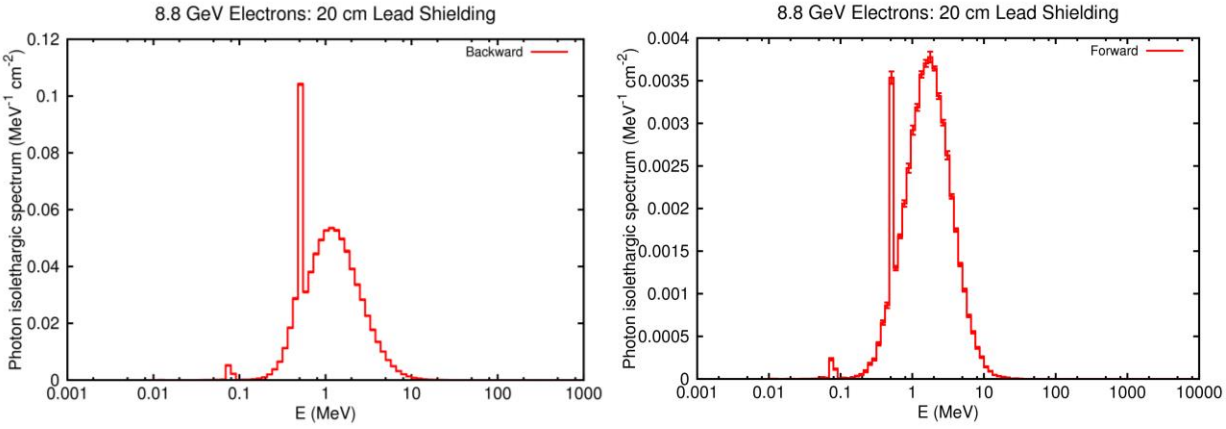

Figure 128. Photon isolethargic spectrum for backward and forward produced photons in a 20 cm thick lead shielding.

V Results for 50 cm thick lead shielding

In this section we study the effects of pions and electrons impinging on a 20 cm x 20 cm x 50 cm lead block. In addition to the total deposited energy in the block, the fluences of pions, muons, neutrons, protons, electrons, photons, lambdas and sigma- are also calculated in units of number of particles per cm^2 normalized to number of incoming particles per cm^2. With such a choice of units one only needs to multiply shown fluences with primary particles rates (which can be calculated separately) to get the fluences expected in the Moller experiment. In the simulation the cutoff energy threshold for all the particles was 10^{-5} GeV, except for the neutrons where the cutoff threshold was 10^{-8} GeV.

In the case of the pions, the total deposited energy is shown in Figure 129 in units of MeV/cm^3. The average deposited energy in the entire lead block was 5220 MeV per incoming pion. The fluences integrated over all secondary particles energies are shown in Figures 130-137 and Figures 138-145.

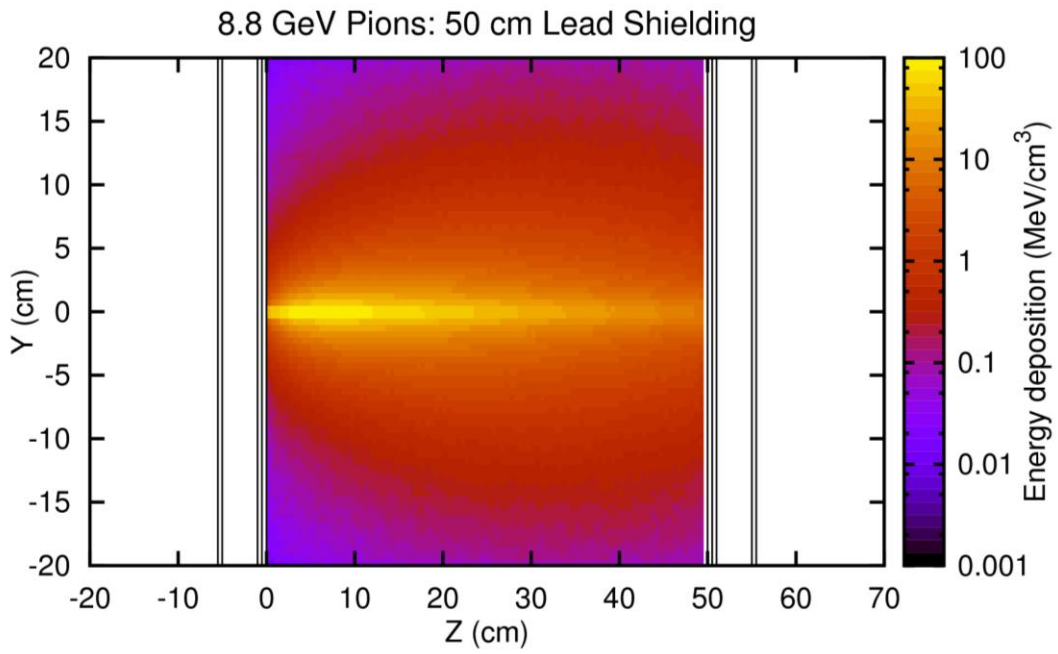

Figure 129. Total deposited energy in the 50 cm thick lead block per incoming 8.8 GeV pion.

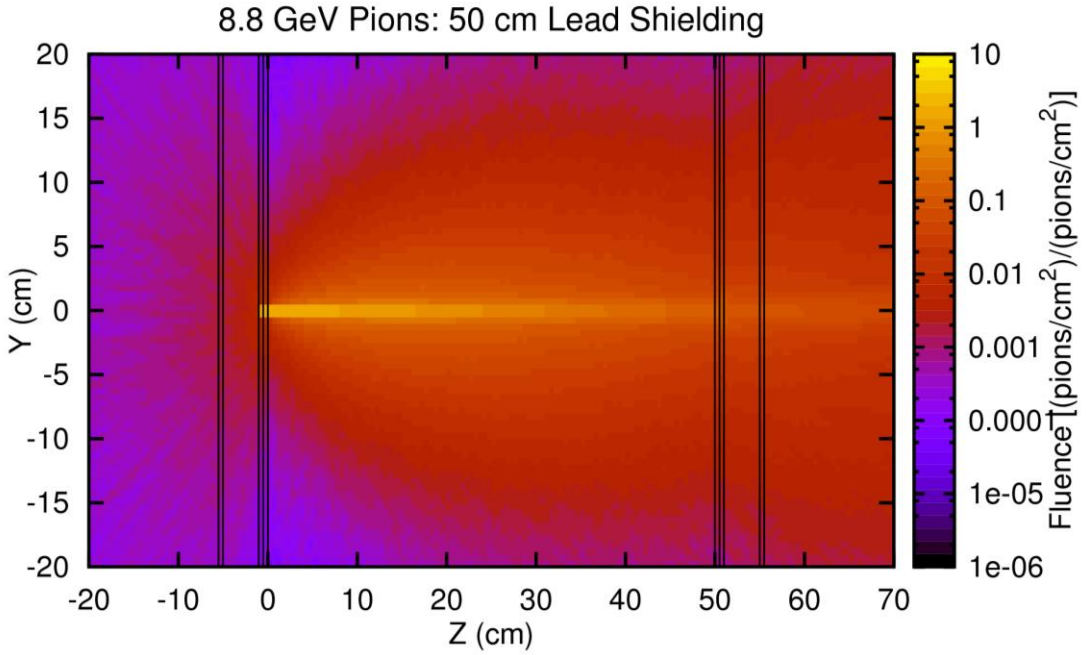

Figure 130. Pion fluence in the case of the 50 cm thick lead block per incoming 8.8 GeV pion.

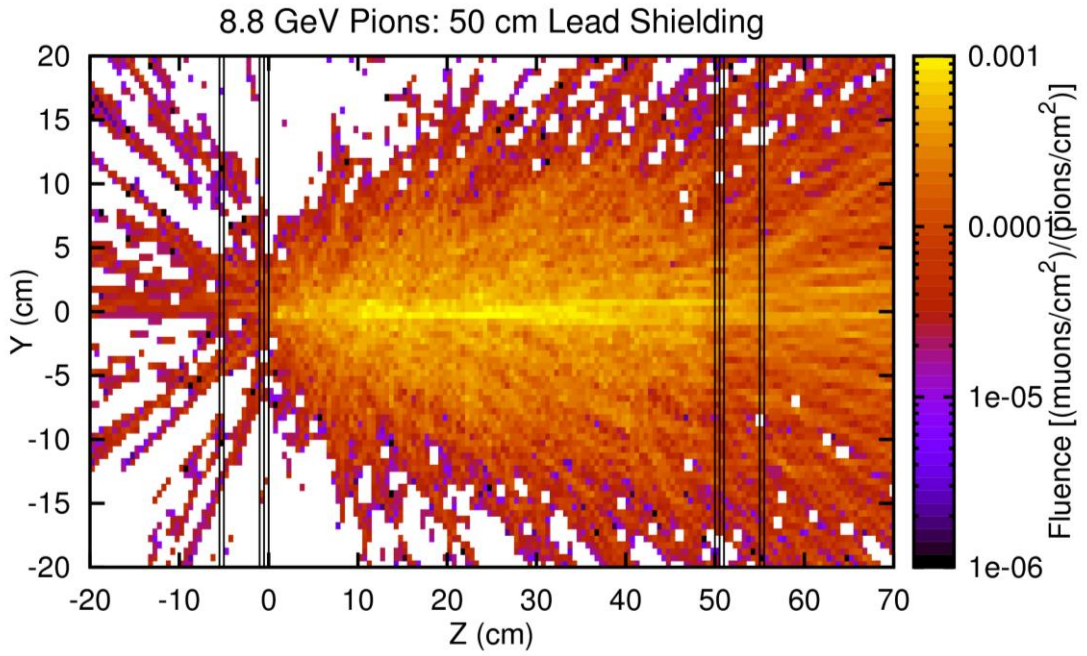

Figure 131. Muon fluence in the case of the 50 cm thick lead block per incoming 8.8 GeV pion.

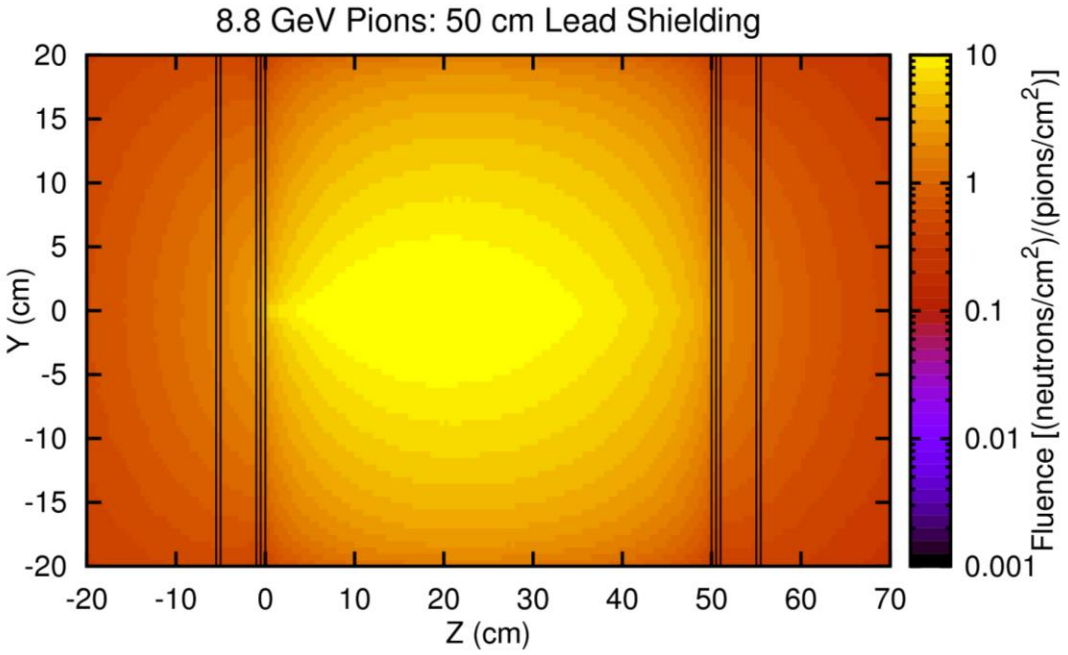

Figure 132. Neutron fluence in the case of the 50 cm thick lead block per incoming 8.8 GeV pion.

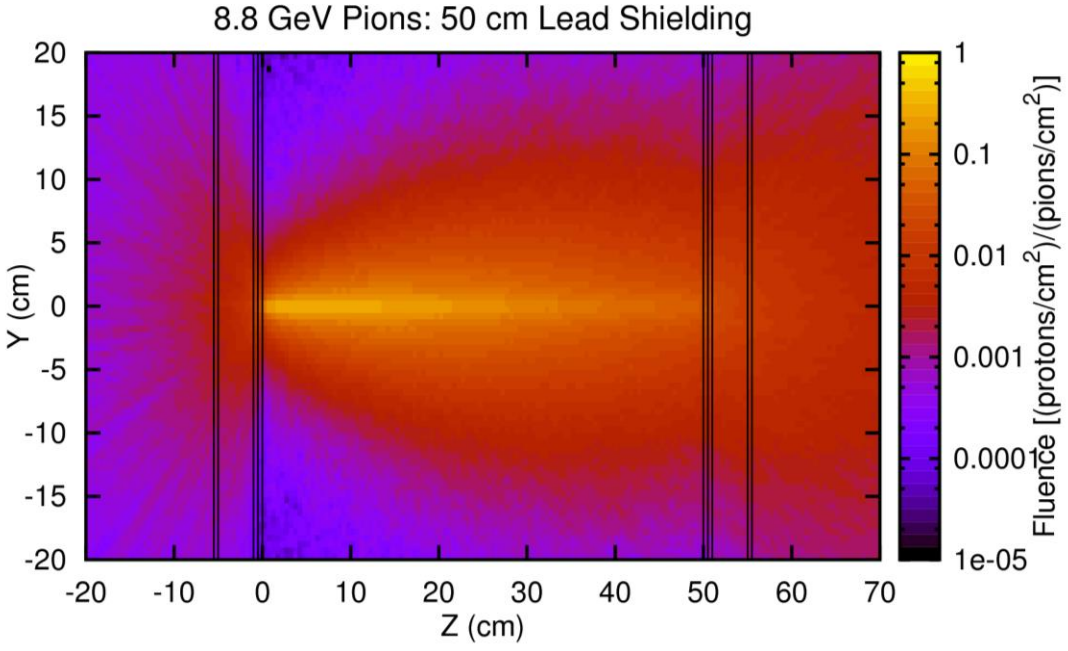

Figure 133. Proton fluence in the case of the 50 cm thick lead block per incoming 8.8 GeV pion.

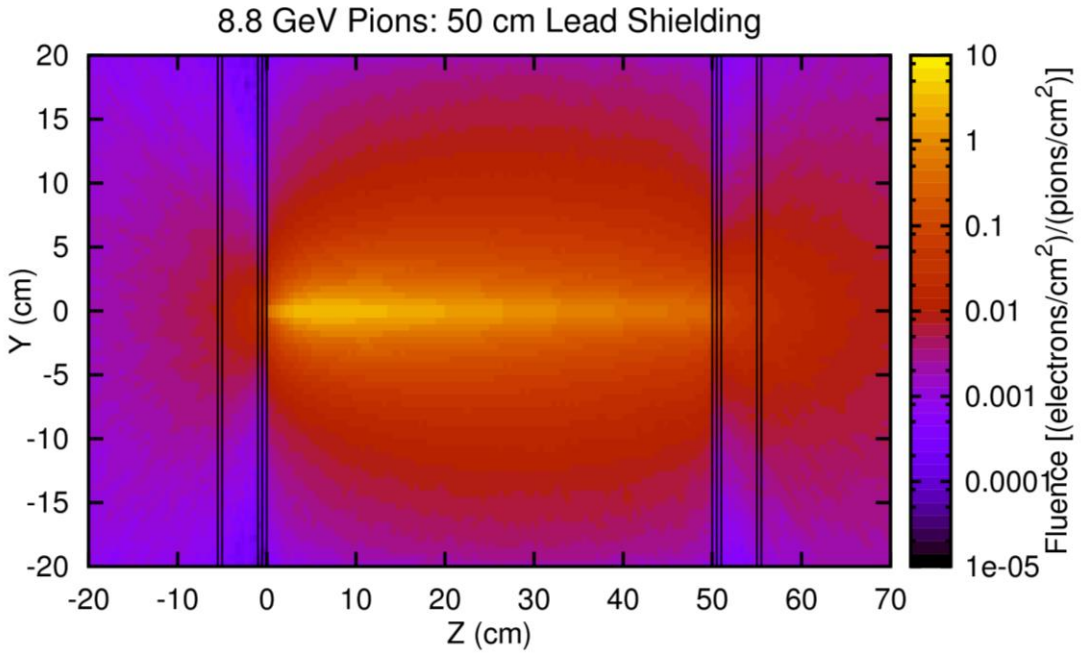

Figure 134. Electron fluence in the case of the 50 cm thick lead block per incoming 8.8 GeV pion.

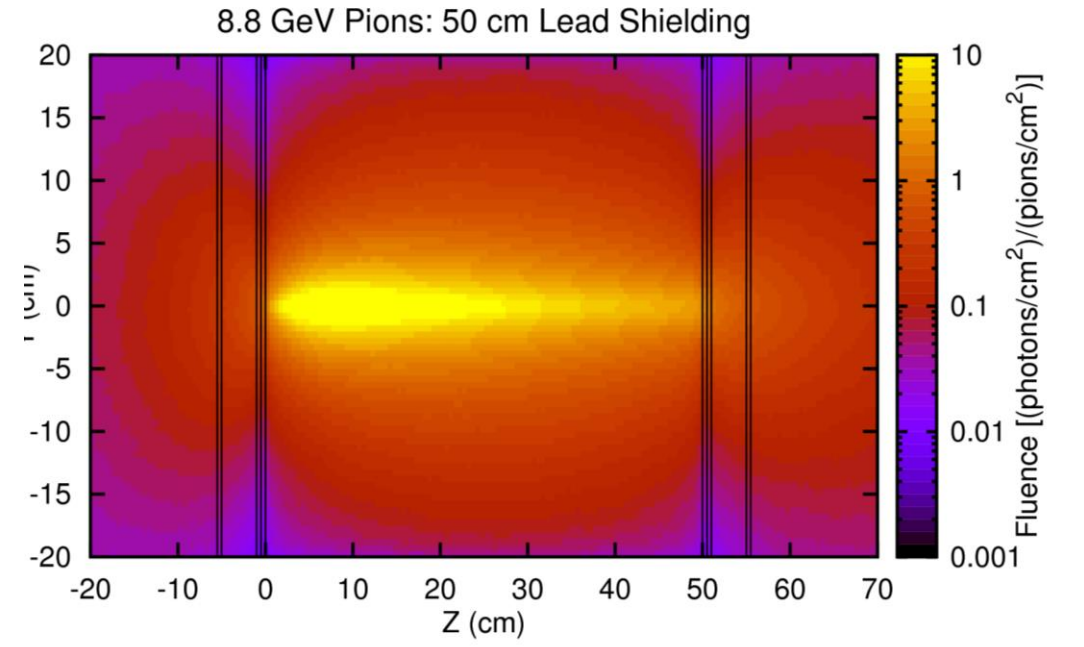

Figure 135. Photon fluence in the case of the 50 cm thick lead block per incoming 8.8 GeV pion.

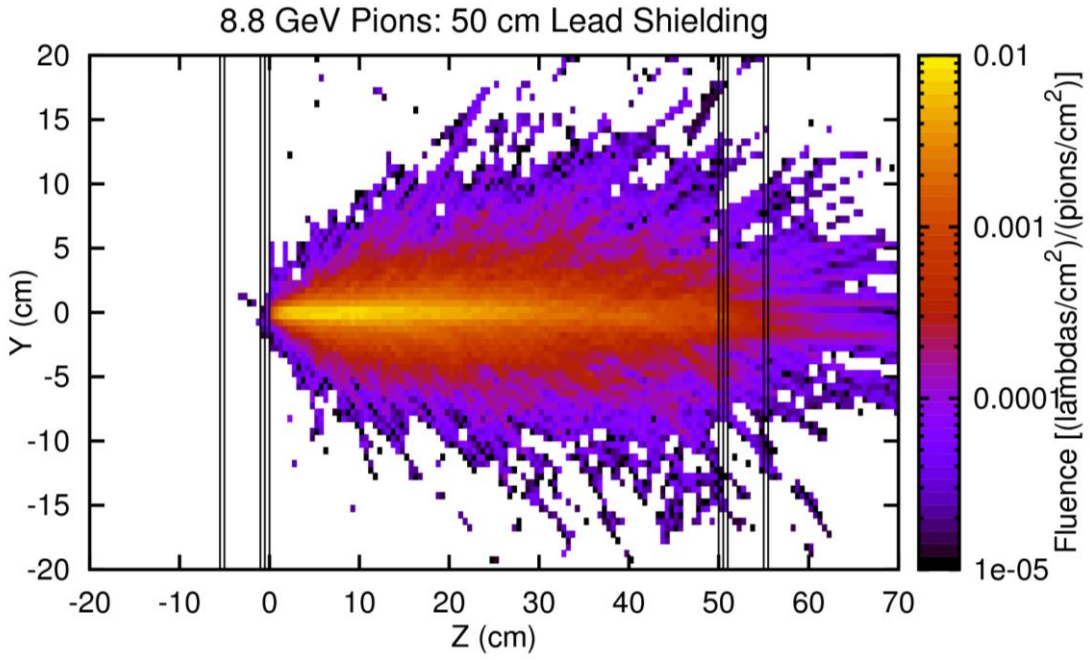

Figure 136. Lambda fluence in the case of the 50 cm thick lead block per incoming 8.8 GeV pion.

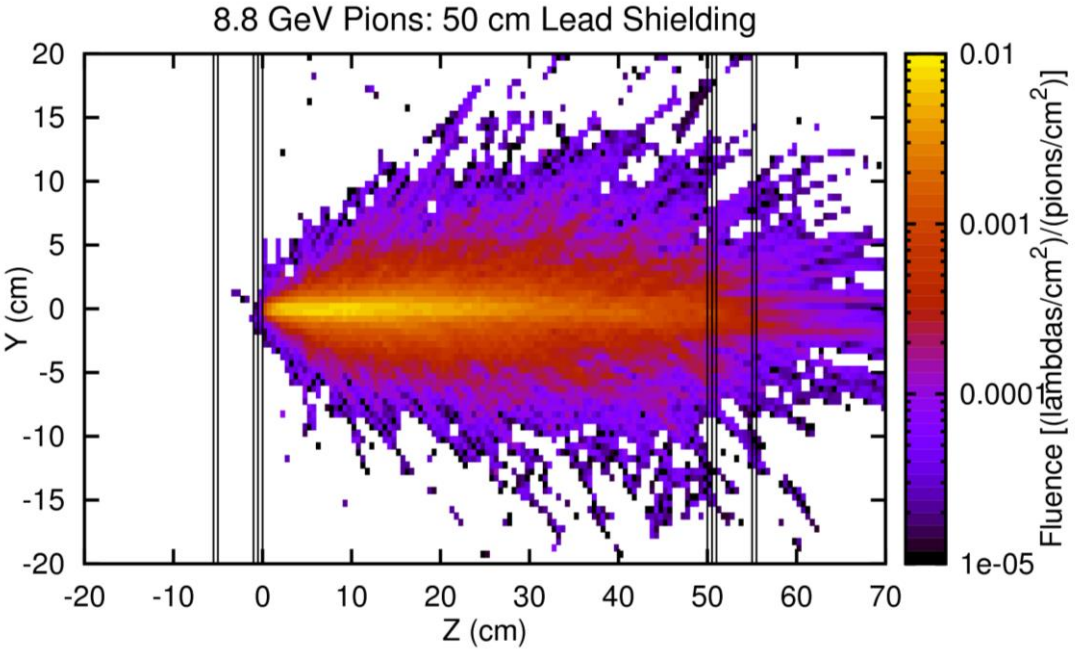

Figure 137. Sigma- fluence in the case of the 50 cm thick lead block per incoming 8.8 GeV pion.

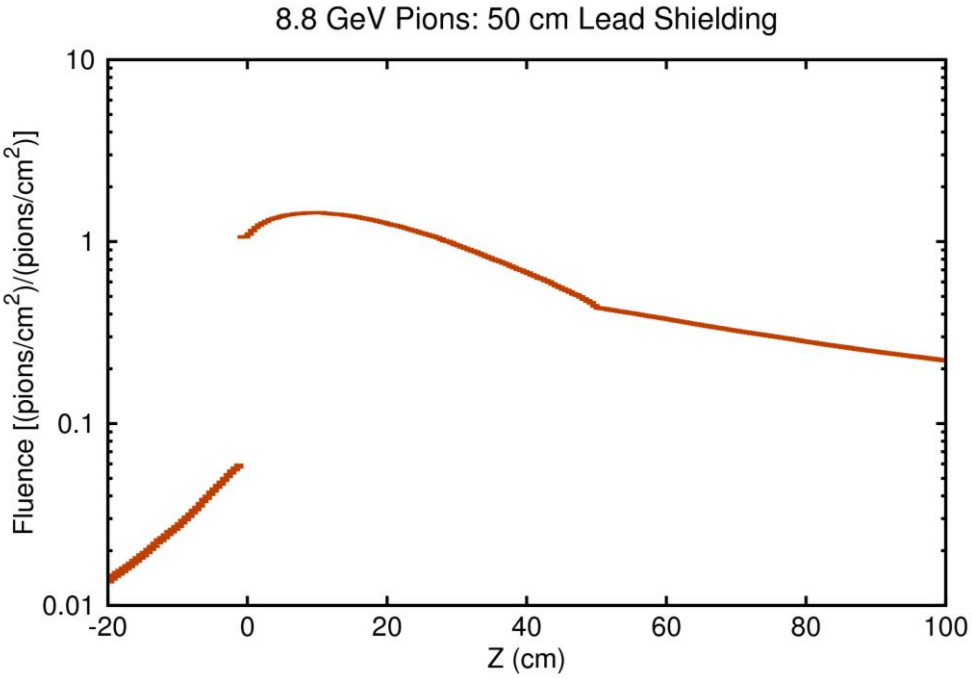

Figure 138. Energy integrated pion fluence as a function of position.

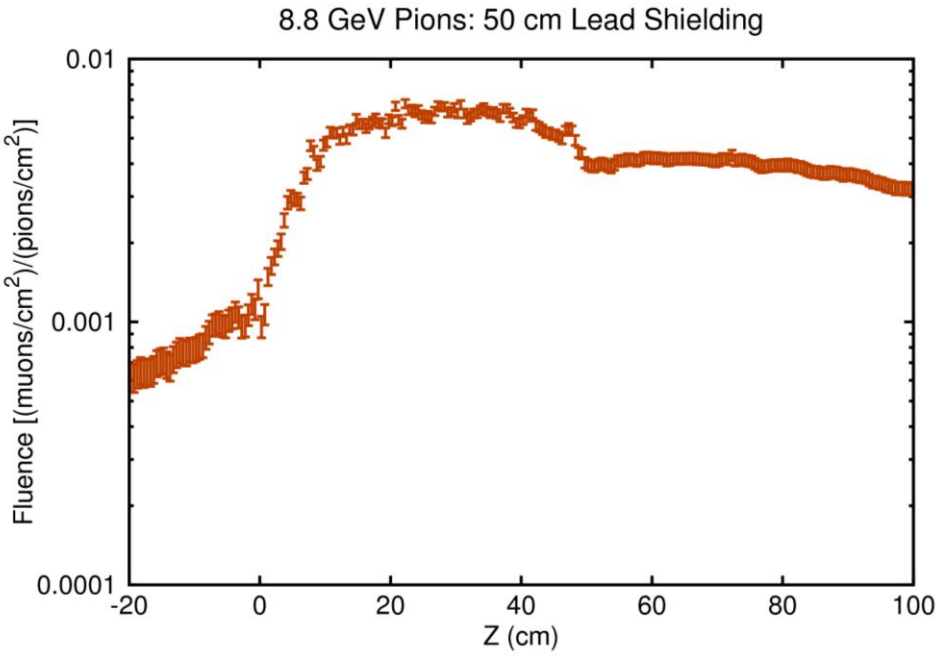

Figure 139. Energy integrated muon fluence as a function of position.

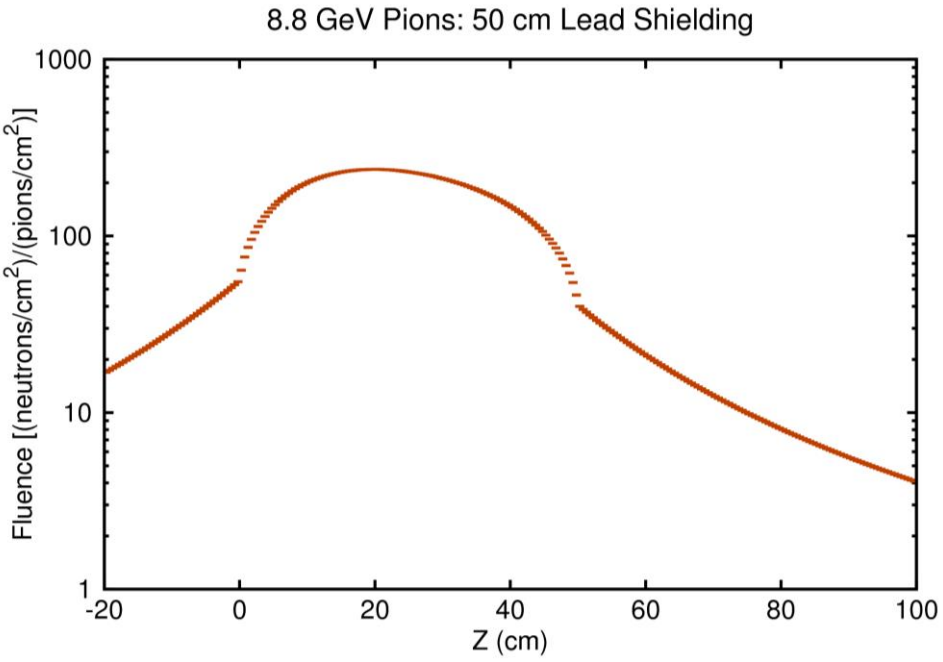

Figure 140. Energy integrated neutron fluence as a function of position.

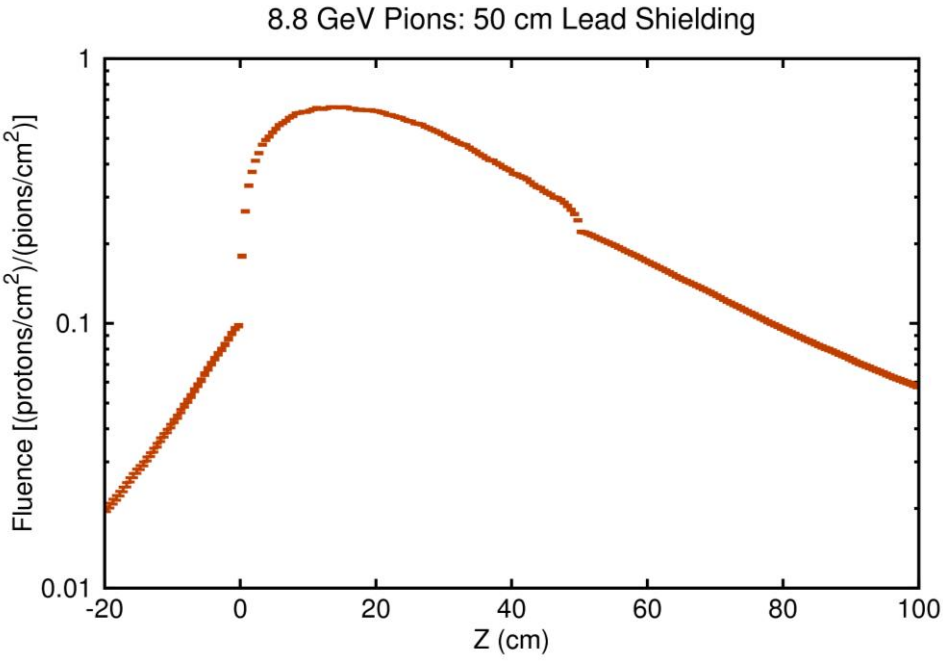

Figure 141. Energy integrated proton fluence as a function of position.

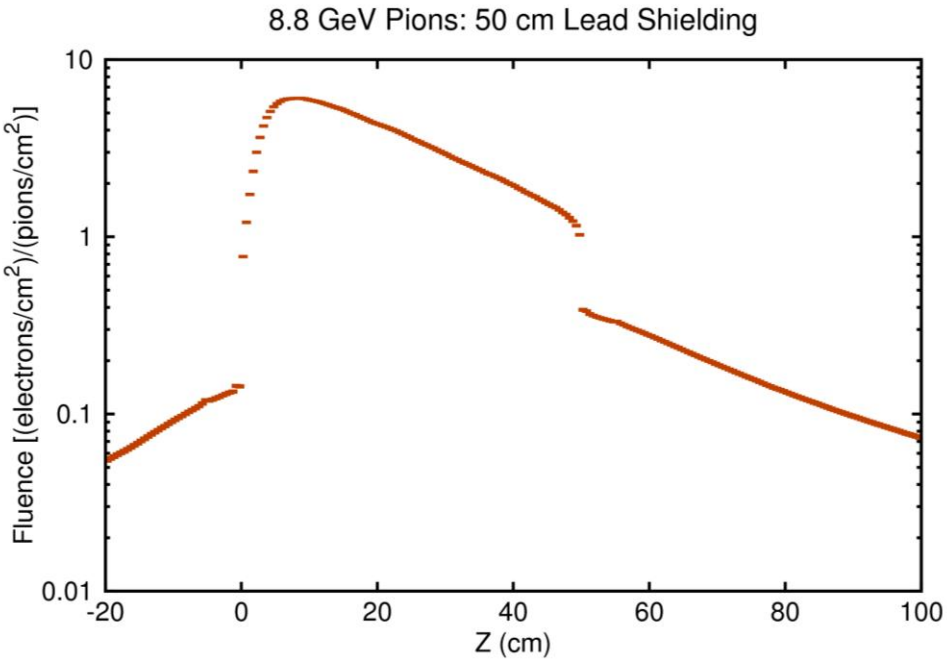

Figure 142. Energy integrated electron fluence as a function of position.

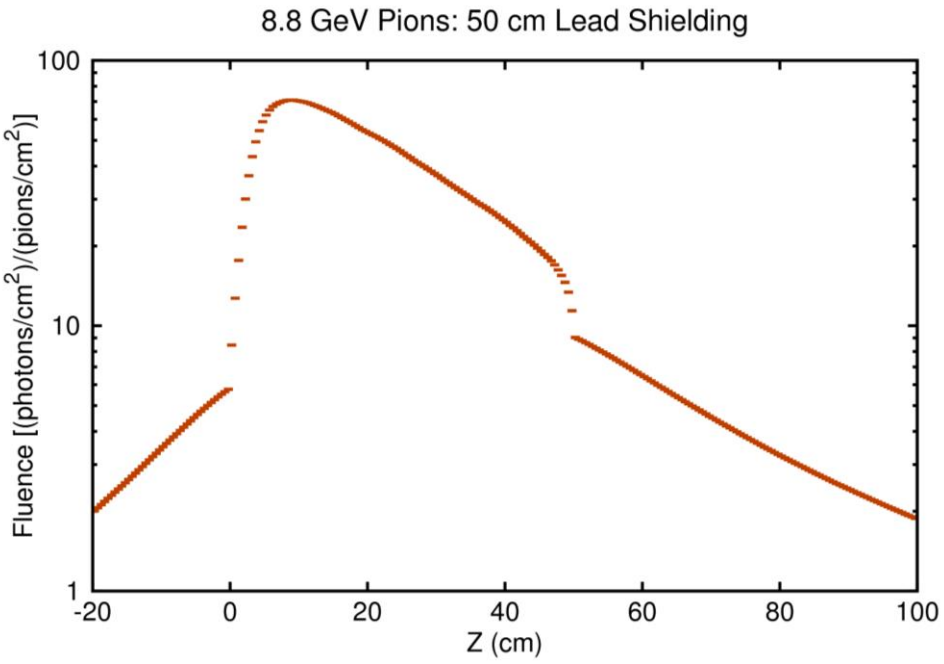

Figure 143. Energy integrated photon fluence as a function of position.

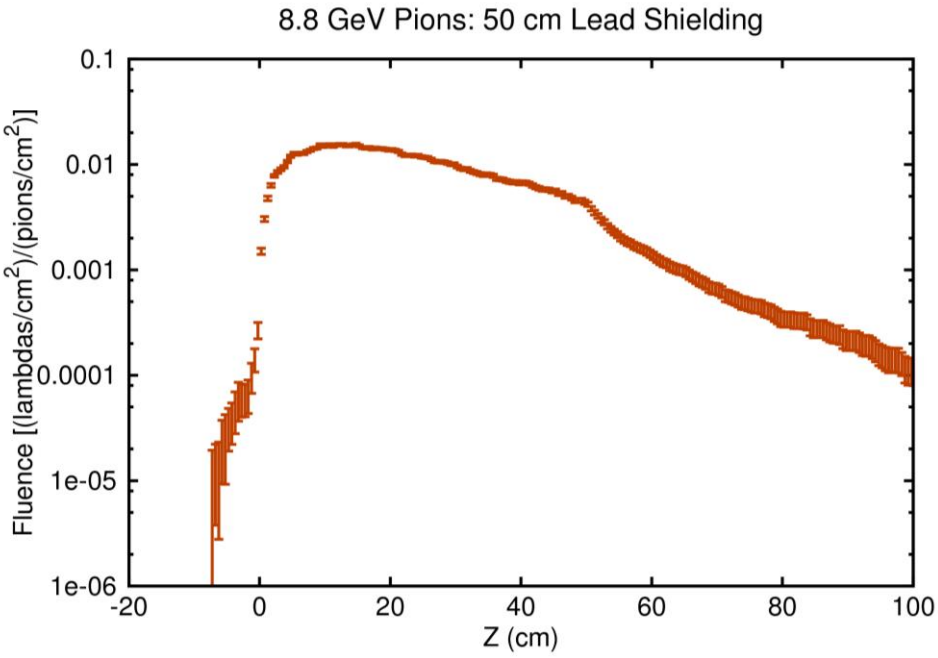

Figure 144. Energy integrated lambda fluence as a function of position.

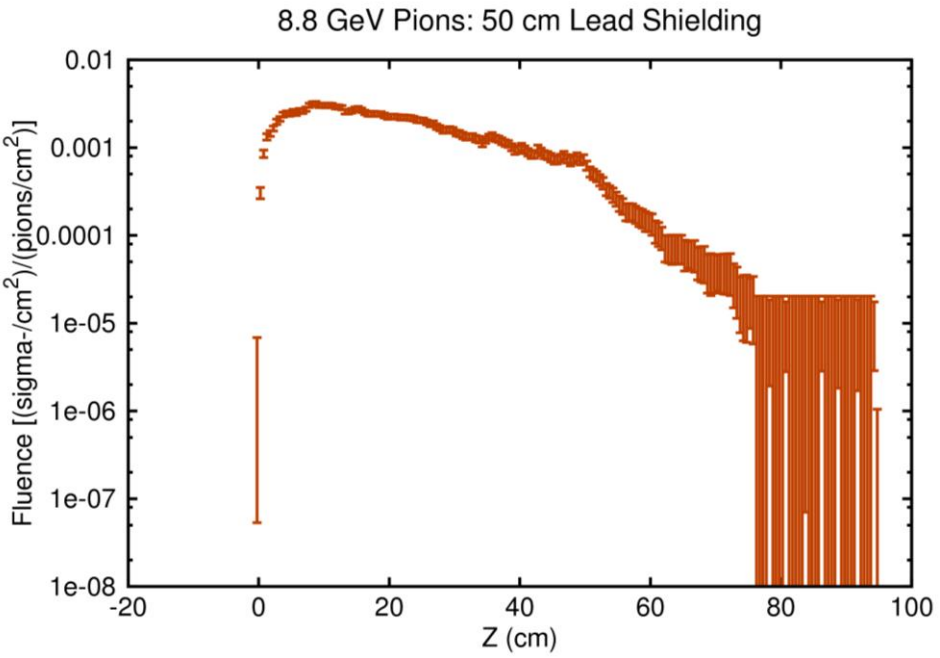

Figure 145. Energy integrated sigma- fluence as a function of position.

The fluences shown in Figures 138-145 are integrated over all secondary particles energies and can be used to calculate the background rates, but, to fully understand the background, it is also important to know the secondary particles energy spectra. In Figures 146-153 the isolethargic spectra are shown for the secondary particles produced by the shielding in forward and backward directions. The reason for using isolethatrgic spectra is that the dynamic range of the energies of the secondary particles requires a logarithmic energy scale. For such a scale the area under the isolethargic spectrum curve is proportional to number of particles in a particular energy interval.

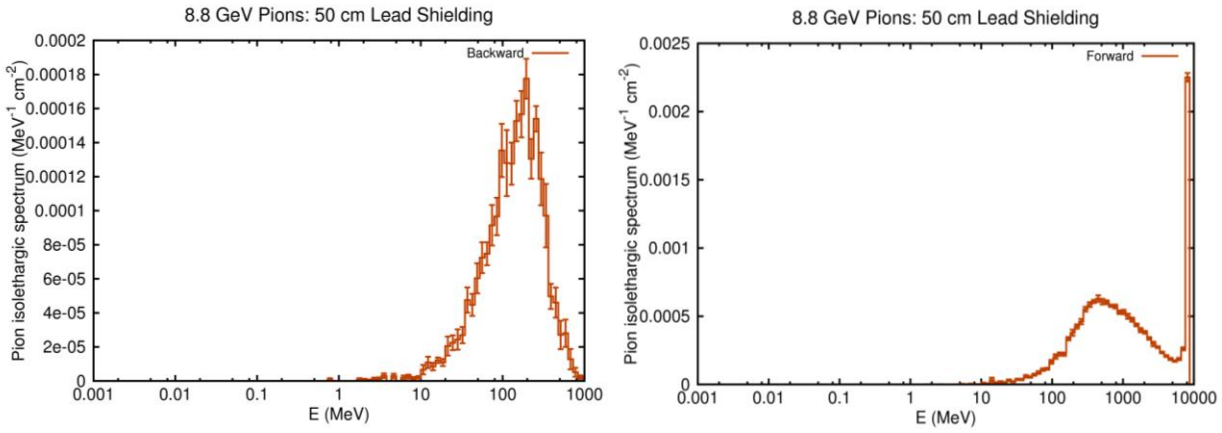

Figure 146. Pion isolethargic spectrum for backward and forward produced pions in a 50 cm thick lead shielding.

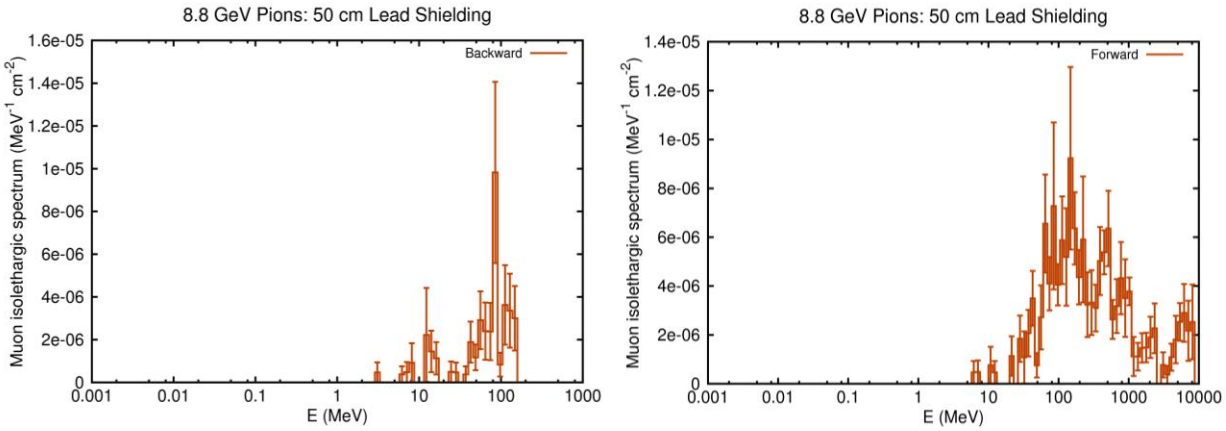

Figure 147. Muon isolethargic spectrum for backward and forward produced muons in a 50 cm thick lead shielding.

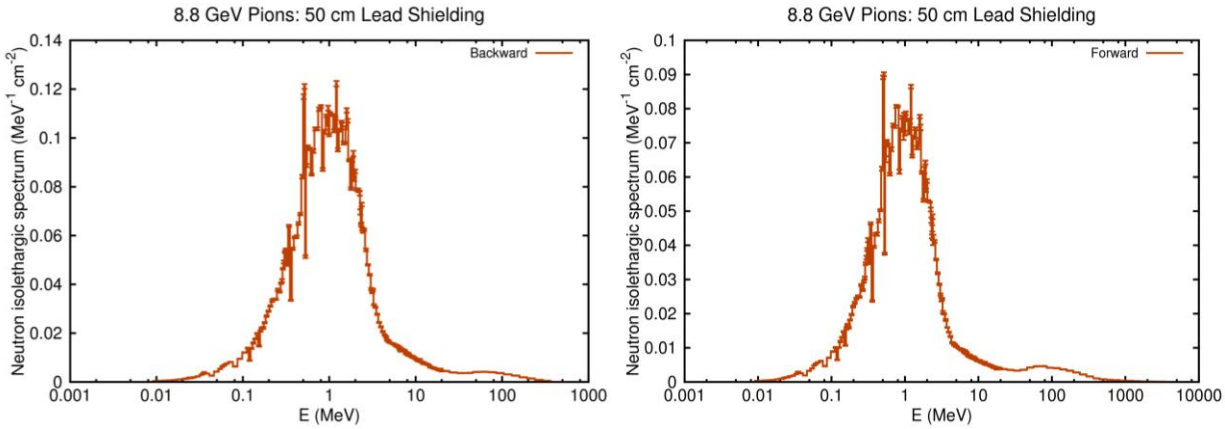

Figure 148. Neutron isolethargic spectrum for backward and forward produced neutrons in a 50 cm thick lead shielding.

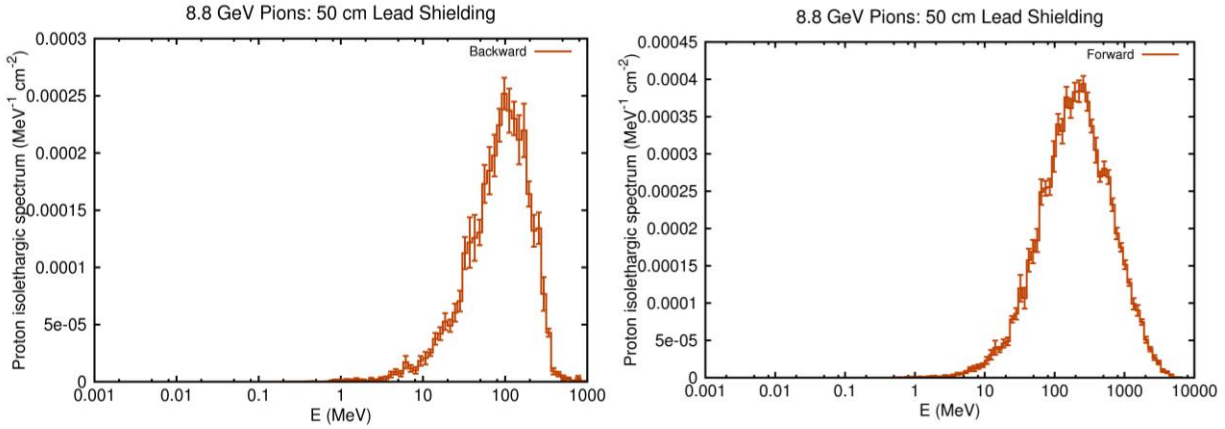

Figure 149. Proton isolethargic spectrum for backward and forward produced protons in a 50 cm thick lead shielding.

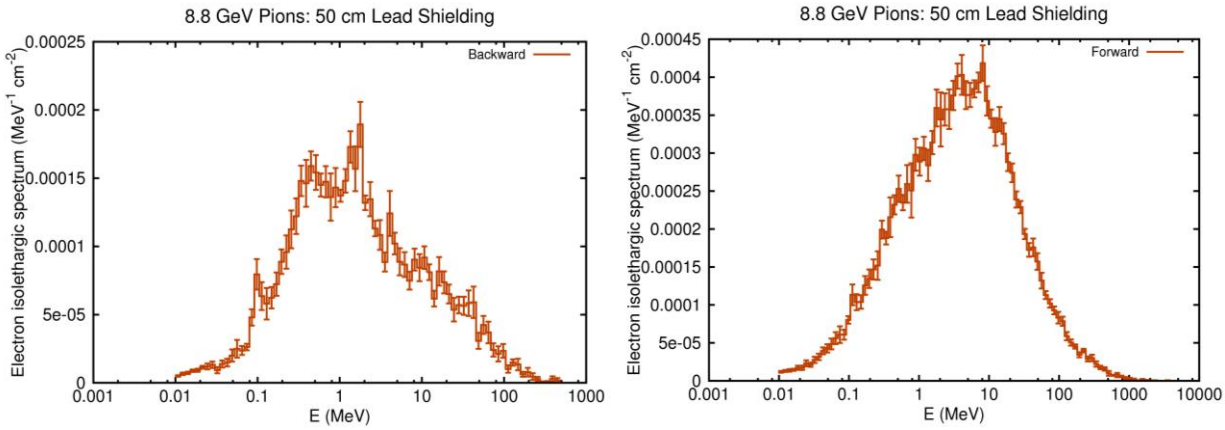

Figure 150. Electron isolethargic spectrum for backward and forward produced electrons in a 50 cm thick lead shielding.

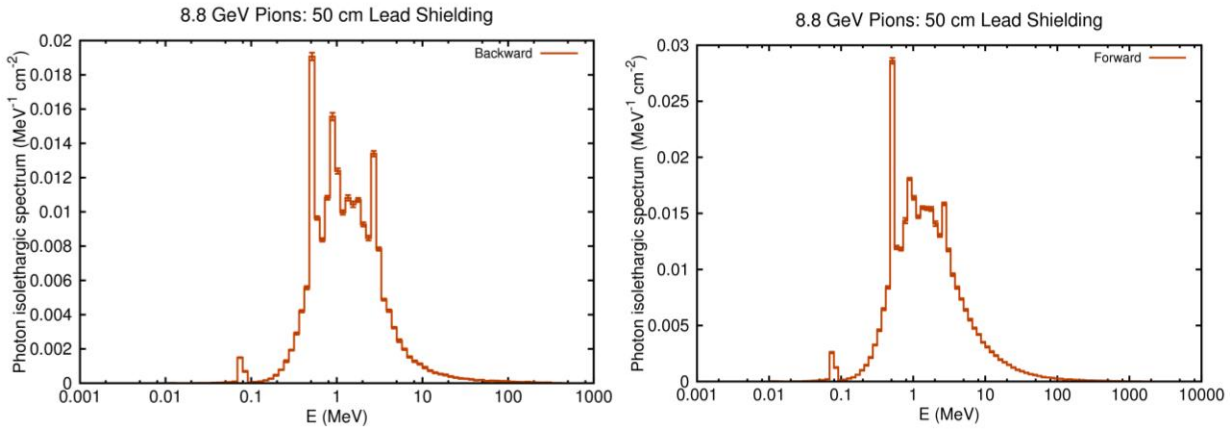

Figure 151. Photon isolethargic spectrum for backward and forward produced photons in a 50 cm thick lead shielding.

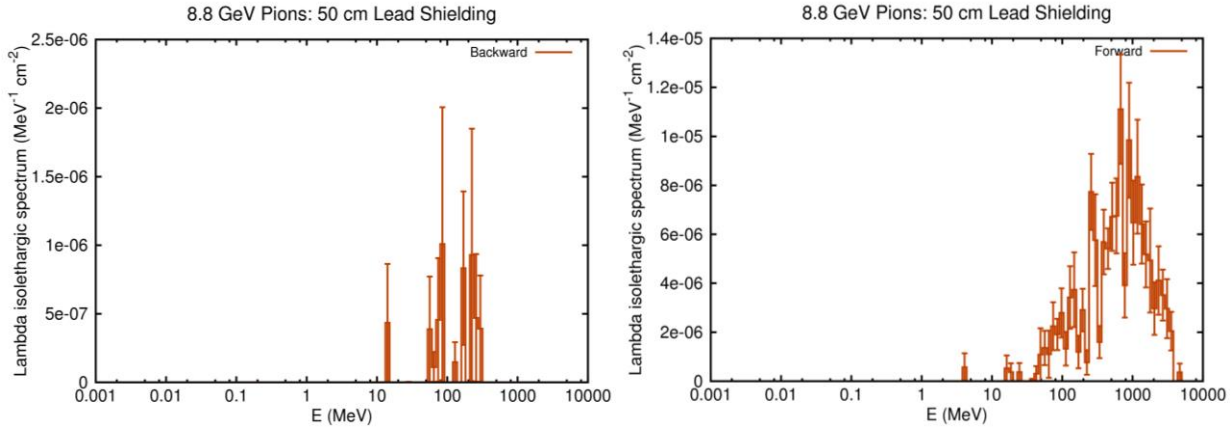

Figure 152. Lambda isolethargic spectrum for backward and forward produced lambdas in a 50 cm thick lead shielding.

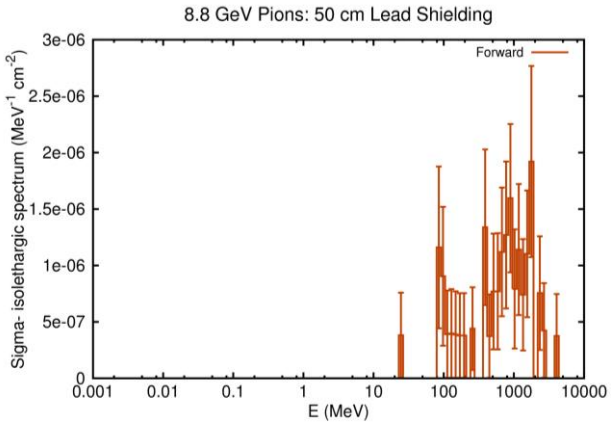

Figure 153. Sigma- isolethargic spectrum for forward produced sigma- in a 50 cm thick lead shielding.

In the case of the electrons, the total deposited energy is shown in Figure 154 in units of MeV/cm^3. The average deposited energy in the entire lead block was 8750 MeV per incoming electron. The fluences integrated over all secondary particles energies are shown in Figures 155-159 and Figures 160-164.

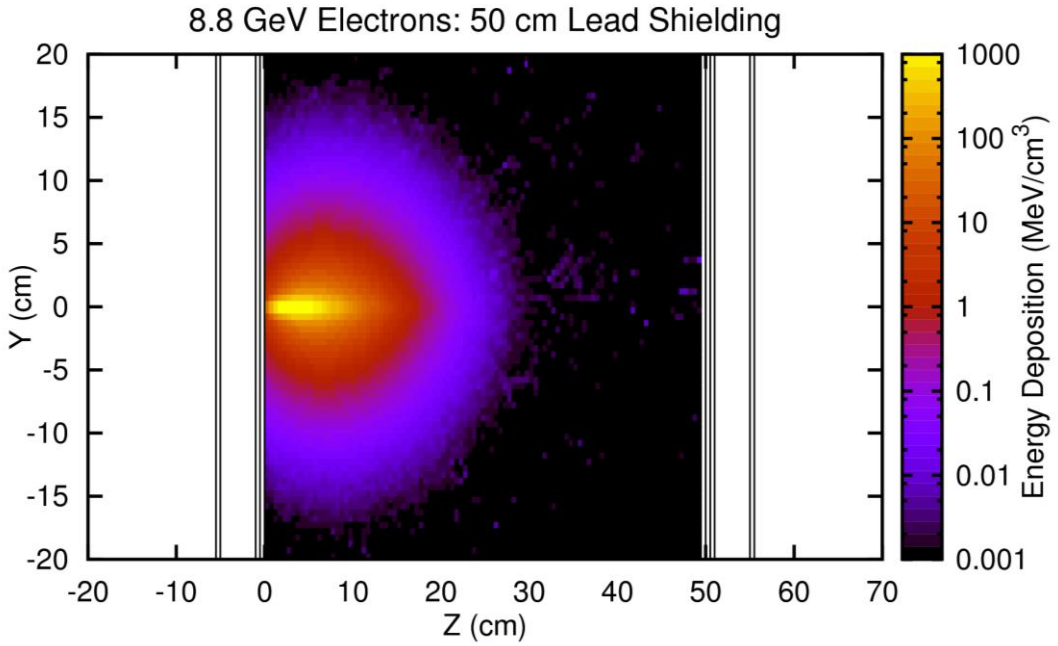

Figure 154. Total deposited energy in the 50 cm thick lead block per incoming 8.8 GeV electron.

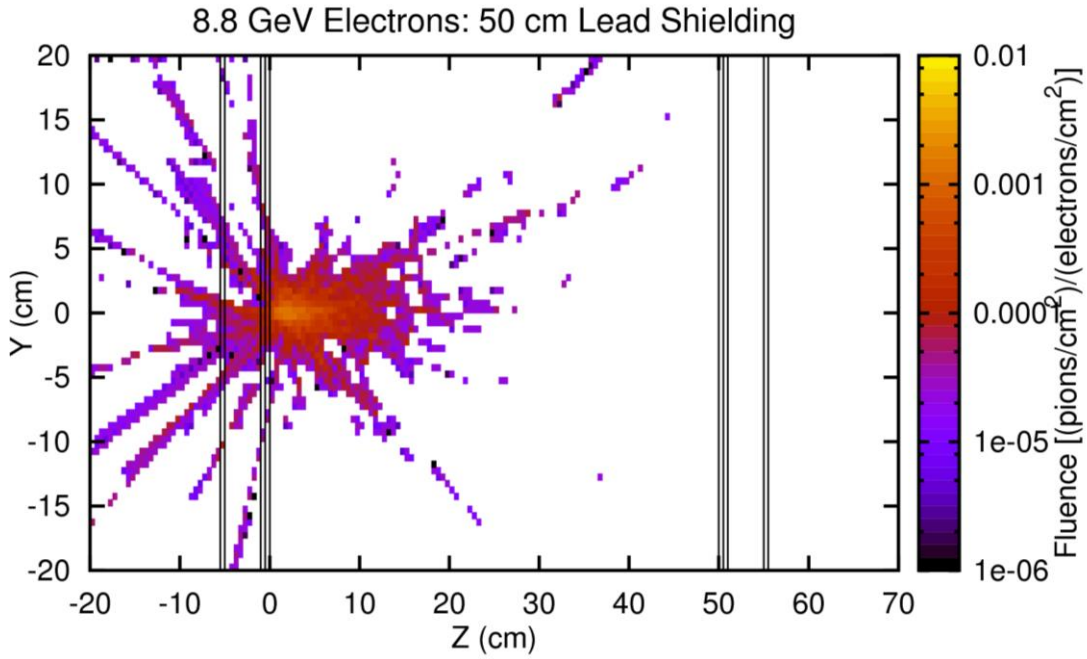

Figure 155. Pion fluence in the case of the 50 cm thick lead block per incoming 8.8 GeV electron.

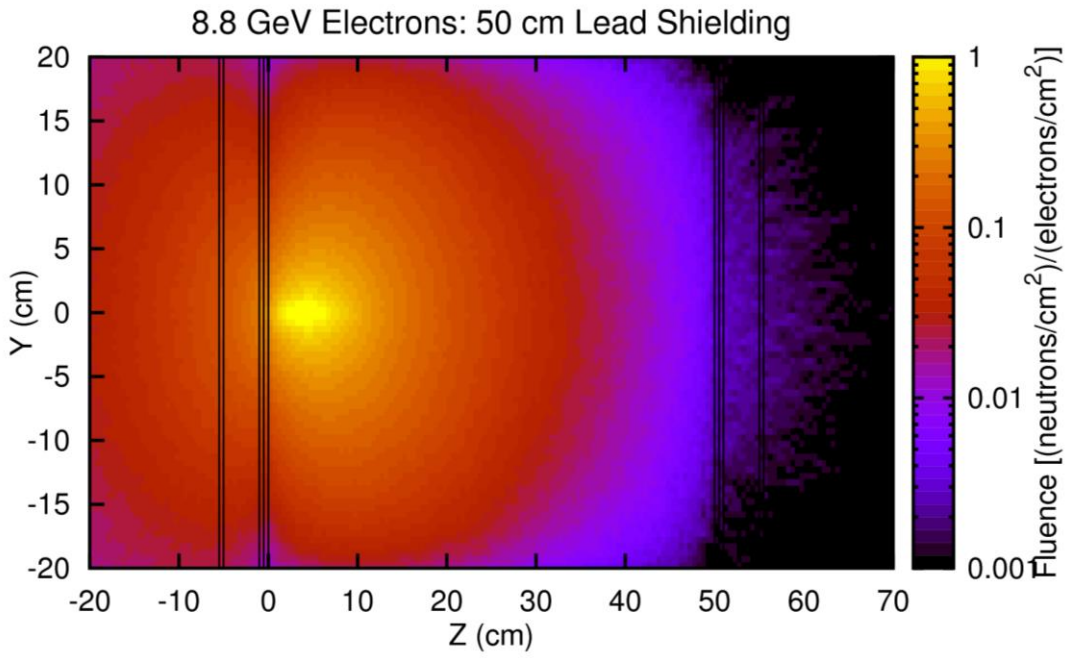

Figure 156. Neutron fluence in the case of the 50 cm thick lead block per incoming 8.8 GeV electron.

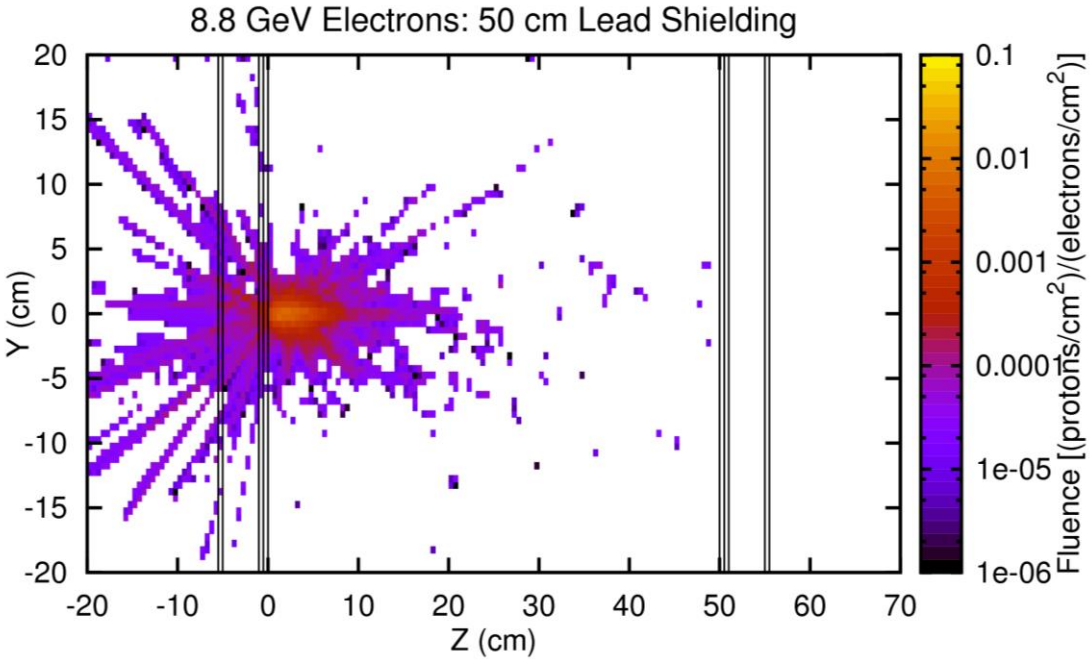

Figure 157. Proton fluence in the case of the 50 cm thick lead block per incoming 8.8 GeV electron.

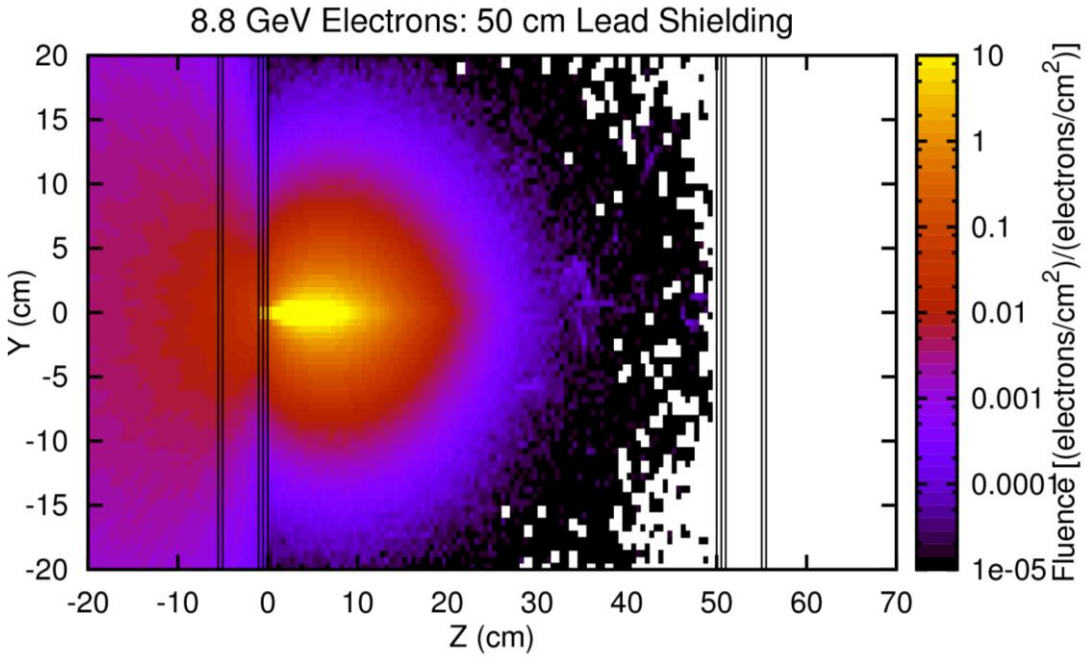

Figure 158. Electron fluence in the case of the 50 cm thick lead block per incoming 8.8 GeV electron.

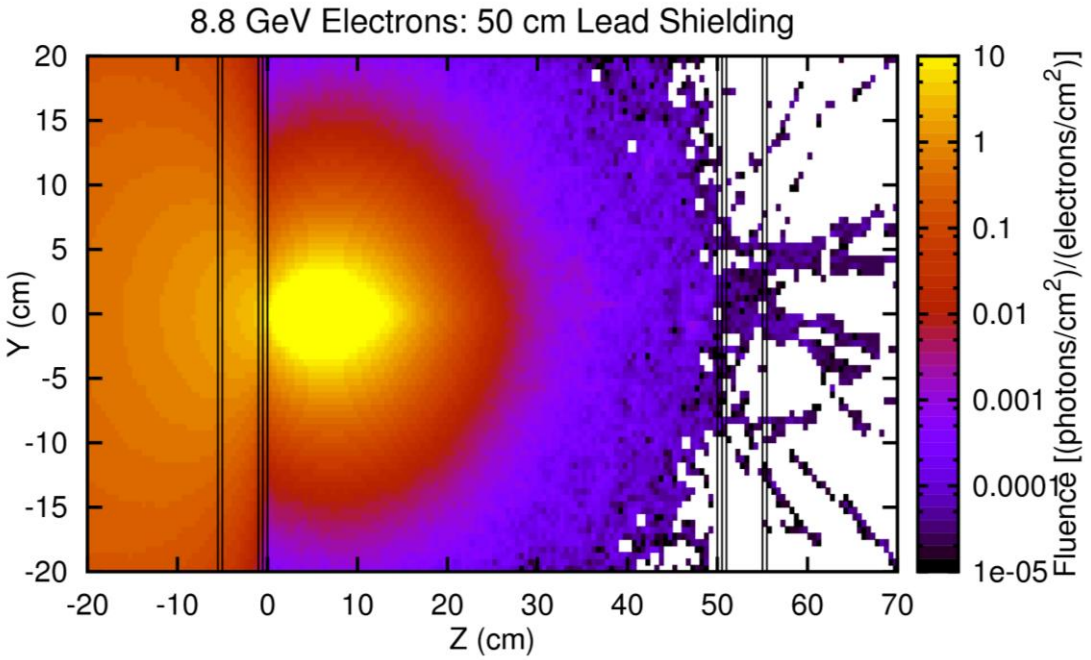

Figure 159. Photon fluence in the case of the 50 cm thick lead block per incoming 8.8 GeV electron.

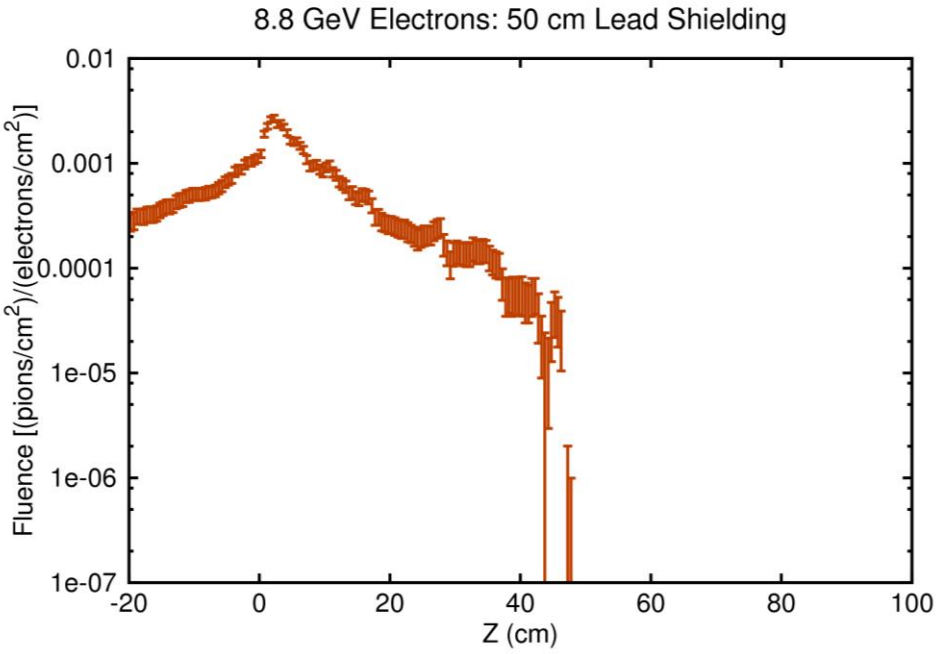

Figure 160. Energy integrated pion fluence as a function of position.

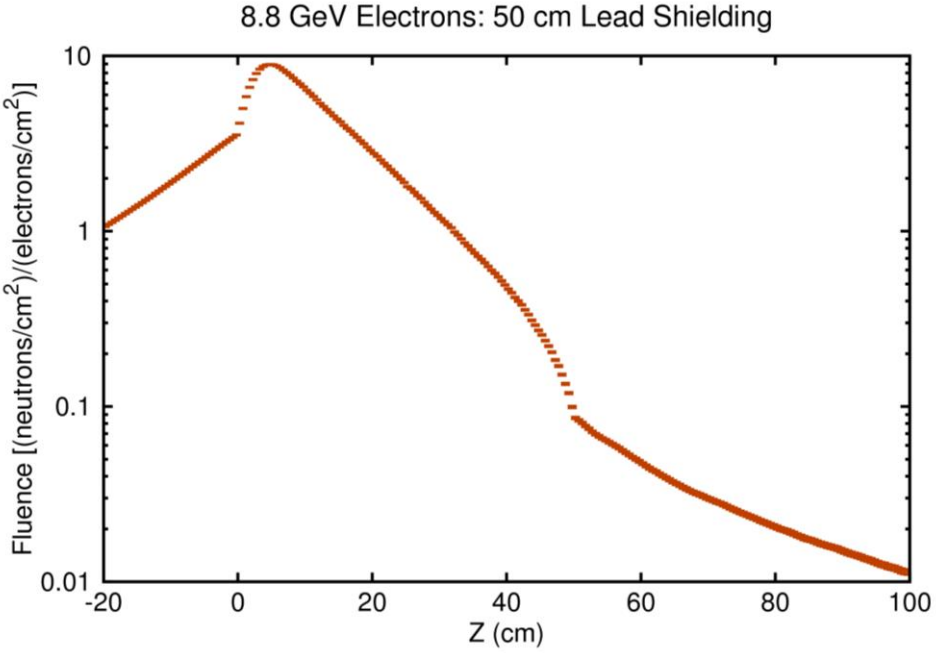

Figure 161. Energy integrated neutron fluence as a function of position.

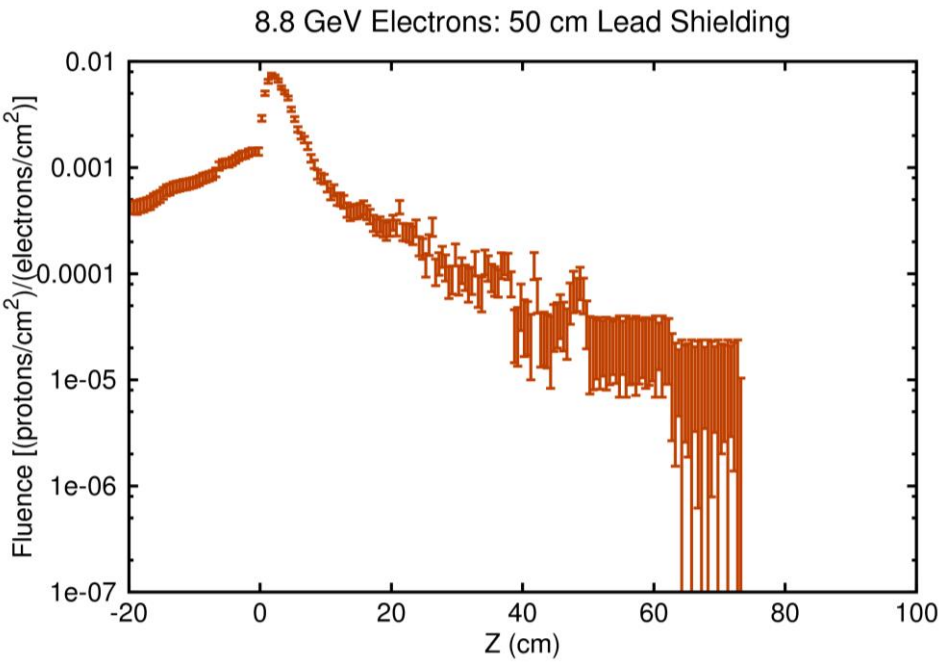

Figure 162. Energy integrated proton fluence as a function of position.

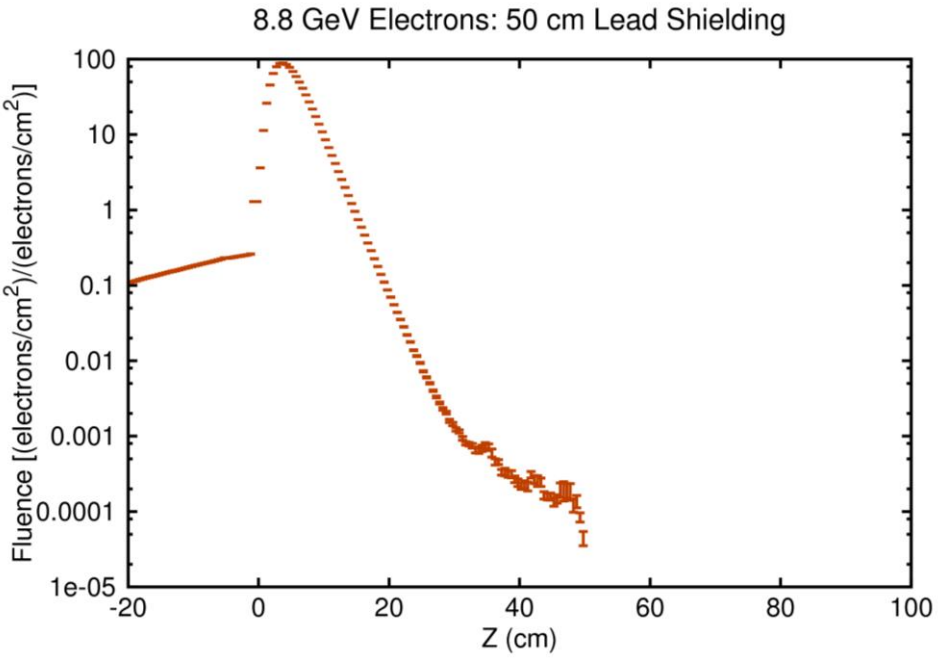

Figure 163. Energy integrated electron fluence as a function of position.

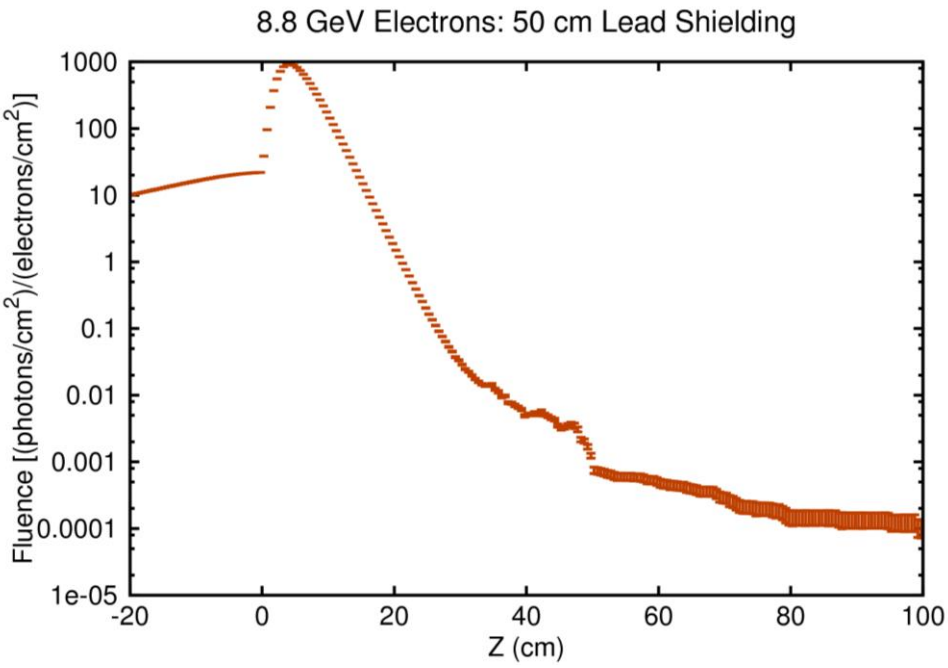

Figure 164. Energy integrated photon fluence as a function of position.

The fluences shown in Figures 160-164 are integrated over all secondary particles energies and can be used to calculate the background rates, but, to fully understand the background, it is also important to know the secondary particles energy spectra. In Figures 165-169 the isolethargic spectra are shown for the secondary particles produced by the shielding in forward and backward directions. The reason for using isolethatrgic spectra is that the dynamic range of the energies of the secondary particles requires a logarithmic energy scale. For such a scale the area under the isolethargic spectrum curve is proportional to number of particles in a particular energy interval.

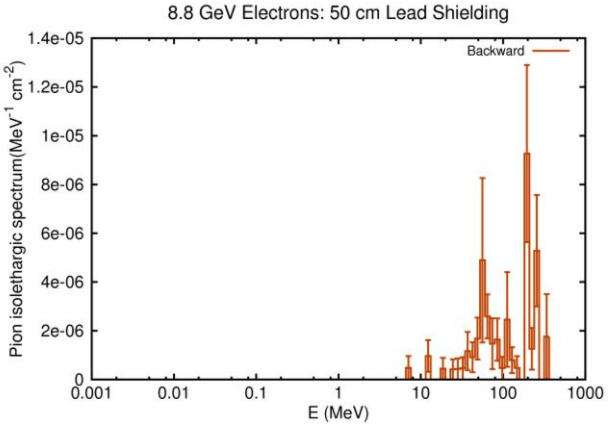

Figure 165. Pion isolethargic spectrum for backward produced pions in a 50 cm thick lead shielding.

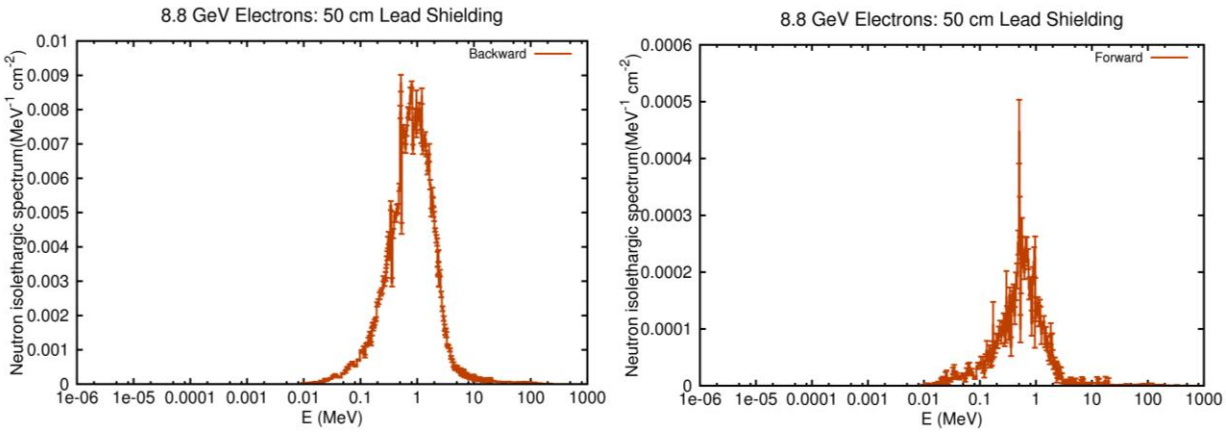

Figure 166. Neutron isolethargic spectrum for backward and forward produced neutrons in a 50 cm thick lead shielding.

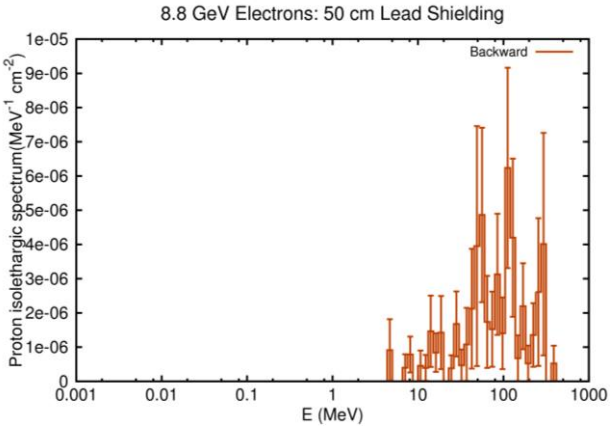

Figure 167. Proton isolethargic spectrum for backward produced protons in a 50 cm thick lead shielding.

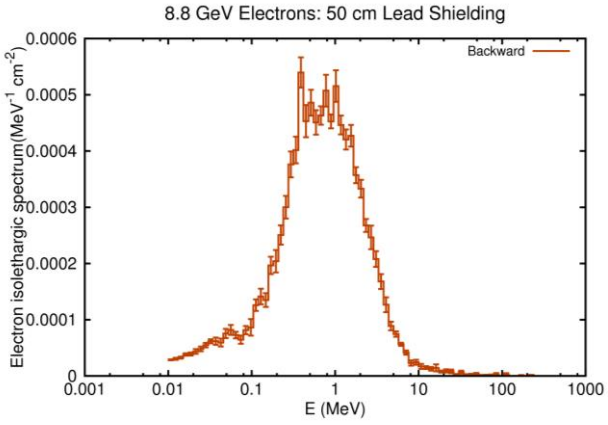

Figure 168. Electron isolethargic spectrum for backward produced electrons in a 50 cm thick lead shielding.

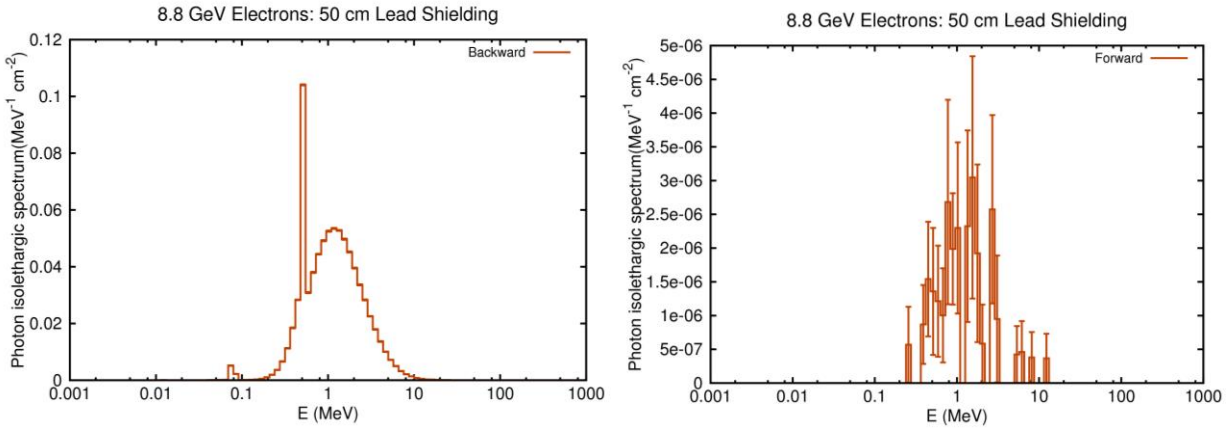

Figure 169. Photon isolethargic spectrum for backward and forward produced photons in a 50 cm thick lead shielding.

VI Summary

The following two tables summarize in more details the results shown in previous figures. Table 2 shows the types, the rates and the energy ranges of the secondary particles produced by the 8.8 GeV electrons in the 5, 10, 20 and 50 cm thick lead shielding in the forward and backward directions. Table 3 shows the types, the rates and the energy ranges of secondary particles produced by the 8.8 GeV pions in the 5, 10, 20 and 50 cm thick lead shielding in the forward and backward directions. The secondary particles rates are obtained assuming the electrons rate of 0.1 GHz/cm^2 and pions rates of 0.1 x 10^{-3} GHz/cm^2 (~0.1 % of the electrons rate) as estimate in the Moller experiment proposal [MOLLER2012]. At this stage of the simulation the obtained secondary particles rates are a rough estimate. This is the result of the assumption that, in the energy range of the Moller experiment, the rates are energy independent and that the cross sections of the secondary particles production are energy independent. Luckily, those two assumptions have opposite trends, allowing for the estimates in the tables. It is obvious that with the forthcoming simulations the rates will be improved.

In both tables the energy ranges are shown for the secondary particles except for the pion produced pions where the percentage of the energy unperturbed pions, pions with the original energy, is shown.

While the results in the two tables will help in understanding the effects of the shielding on the pion detector, positioned behind the shielding, and on the main detector system, positioned in front of the shielding, the result can be also used to estimate the secondary particles effects on the main detector system if one decides to put the shielding in front of main detectors.

		Electrons (0.1 GHz/cm^2)							
		Secondary Particles Backward				Secondary Particles Forward			
Lead Shielding:		5 cm	10 cm	20 cm	50 cm	5 cm	10 cm	20 cm	50 cm
π	Rate (GHz/cm^2)	8.5 10^{-5}				1.3 10^{-4}	8.3 10^{-5}	2 10^{-5}	
	Energy (MeV)	10-400				20-2500	25-5000	50-4000	
μ	Rate (GHz/cm^2)		10^{-6}	10^{-6}				10^{-6}	
	Energy (MeV)								
n	Rate (GHz/cm^2)	0.17	0.3	0.34	0.35	0.25	0.26	0.11	0.008
	Energy (MeV)	0.01-20				0.05-20	0.05-10	0.05-10	0.01-10
p	Rate (GHz/cm^2)	1.2 10^{-4}				2.3 10^{-4}	5 10^{-5}	2.7 10^{-5}	2 10^{-6}
	Energy (MeV)	2.5-500				5-2000	15-2800	10-650	
e^-	Rate (GHz/cm^2)	0.025				2.9	0.314	0.002	
	Energy (MeV)	0.01-20				0.01-1000	0.01-200	0.01-20	
γ	Rate (GHz/cm^2)	2.2				66	13.1	0.14	7 10^{-5}
	Energy (MeV)	0.05-10				0.05-100	0.05-50	0.06-20	0.2-15
λ	Rate (GHz/cm^2)	6.4 10^{-9} estimate				2.7 10^{-6}			
	Energy (MeV)					50-500			
Σ^-	Rate (GHz/cm^2)	1.5 10^{-9} estimate				5 10^{-7} estimate for 5 cm			
	Energy (MeV)								

Table 2. Rates and energy ranges for electron produced secondary particles for different lead thickness.

		Pions (0.1 10^{-3} GHz/cm^2)							
		Secondary Particles Backward				Secondary Particles Forward			
Lead Shielding:		5 cm	10 cm	20 cm	50 cm	5 cm	10 cm	20 cm	50 cm
π	Rate (GHz/cm^2)	5.6 10^{-6}				1.3 10^{-4}	1.3 10^{-4}	1.2 10^{-4}	4.3 10^{-5}
	Energy (MeV)	1-1000				77 %	58 %	33 %	7 %
μ	Rate (GHz/cm^2)	1.2 10^{-7}				1.7 10^{-7}	3 10^{-7}	5 10^{-7}	4 10^{-7}
	Energy (MeV)	2-500				5-8000			
n	Rate (GHz/cm^2)	1.1 10^{-3}	2.4 10^{-3}	4.1 10^{-3}	5.5 10^{-3}	1.4 10^{-4}	3 10^{-3}	5.2 10^{-3}	4 10^{-3}
	Energy (MeV)	0.1-400				0.1-400			
p	Rate (GHz/cm^2)	10^{-5}				4 10^{-5}	5 10^{-5}	5 10^{-5}	2.2 10^{-5}
	Energy (MeV)	2-800				5-7000			
e^-	Rate (GHz/cm^2)	1.5 10^{-5}				1.9 10^{-4}	2 10^{-4}	1.4 10^{-5}	3.8 10^{-5}
	Energy (MeV)	0.01-400				0.01-1000			
γ	Rate (GHz/cm^2)	4.2 10^{-4}	5 10^{-4}	5.6 10^{-4}	5.7 10^{-4}	3.4 10^{-3}	4.4 10^{-3}	3.1 10^{-3}	9 10^{-4}
	Energy (MeV)	0.05-100				0.05-100			
λ	Rate (GHz/cm^2)	2 10^{-8}				7.2 10^{-7}	10^{-6}	1.3 10^{-6}	4 10^{-7}
	Energy (MeV)	10-500				20-8000			3-5500
Σ^-	Rate (GHz/cm^2)	8.5 10^{-10}		3 10^{-9}		1.7 10^{-7}	2 10^{-7}	2.1 10^{-7}	6 10^{-8}
	Energy (MeV)					20-8000	20-8000	40-5000	20-5500

Table 3. Rates and energy ranges for pion produced secondary particles for different lead thickness.

VII Conclusion

In this report detailed studies of the shielding properties and the physical consequences of the shielding of the pion detector are performed for the highest electron and pion energies in the Moller experiment. Effects of the shielding on both, pion detector and the main detector system, are calculated for the lead shielding thicknesses of 5 cm, 10 cm, 20 cm, and 50 cm. The type, the energy distributions and the rates of the secondary particles are computed. In addition to help optimize the thickness of the shielding, the results will help to understand the consequences of the background produced by the shielding on both, pion detector and the main detector system, and, therefore, help in the design of the detectors. The result can be also used to estimate the secondary particles effects on the main detector system if one decides to put the shielding in front of main detectors.

Further simulation for lower electron and pion energies will improve the understanding of the background and the detector system.

References

[BATTISTONI 2007] G. Battistoni, S. Muraro, P.R. Sala, F. Cerutti, A. Ferrari, S. Roesler, A. Fasso`, J. Ranft, “The FLUKA code: Description and benchmarking”, Proceedings of the Hadronic Shower Simulation Workshop 2006, Fermilab 6--8 September 2006, M. Albrow, R. Raja eds., AIP Conference Proceeding 896, 31-49, (2007)

[FERRARI 2005] A. Ferrari, P.R. Sala, A. Fasso`, and J. Ranft, “FLUKA: a multi-particle transport code"” CERN-2005-10 (2005), INFN/TC_05/11, SLAC-R-773

[MOLLER2012] MOLLER: Jeferson Lab Experiment E12-09-005: http://hallaweb.jlab.org/12GeV/Moller/pubs/moller_proposal.pdf